

2013

## Total Synthesis of (+)-Malbrancheamide B Utilizing a Stereoselective Domino Reaction Sequence to Establish the Bicyclo[2.2]diazaoctane Core

Stephen William Laws  
*College of William & Mary - Arts & Sciences*

Follow this and additional works at: <https://scholarworks.wm.edu/etd>

 Part of the [Organic Chemistry Commons](#)

---

### Recommended Citation

Laws, Stephen William, "Total Synthesis of (+)-Malbrancheamide B Utilizing a Stereoselective Domino Reaction Sequence to Establish the Bicyclo[2.2]diazaoctane Core" (2013). *Dissertations, Theses, and Masters Projects*. Paper 1539626719.

<https://dx.doi.org/doi:10.21220/s2-rk6n-w245>

This Thesis is brought to you for free and open access by the Theses, Dissertations, & Master Projects at W&M ScholarWorks. It has been accepted for inclusion in Dissertations, Theses, and Masters Projects by an authorized administrator of W&M ScholarWorks. For more information, please contact [scholarworks@wm.edu](mailto:scholarworks@wm.edu).

Total synthesis of (+)-malbrancheamide B utilizing a stereoselective domino reaction sequence to establish the bicyclo[2.2.2]diazaoctane core

Stephen William Laws

Richmond, VA

Bachelor of Science, College of William and Mary, 2011

A Thesis presented to the Graduate Faculty  
of the College of William and Mary in Candidacy for the Degree of  
Master of Science

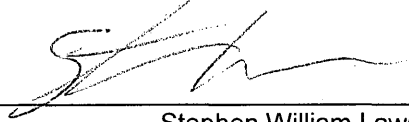
Chemistry Department

The College of William and Mary  
August, 2013

# APPROVAL PAGE

This Thesis is submitted in partial fulfillment of  
the requirements for the degree of

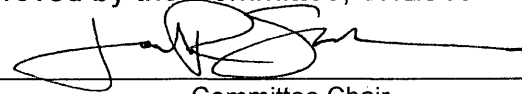
Master of Science



---

Stephen William Laws

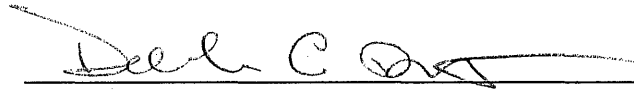
Approved by the Committee, 07/2013



---

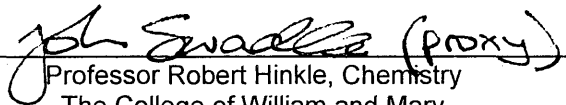
Committee Chair

Assistant Professor Jonathan Scheerer, Chemistry  
The College of William and Mary



---

Professor Deborah Bebout, Chemistry  
The College of William and Mary



---

Professor Robert Hinkle, Chemistry  
The College of William and Mary

## ABSTRACT

The total enantioselective and formal racemic syntheses of malbrancheamide B, a bicyclo[2.2.2]diazaoctane-containing fungal metabolite are described. Over seventy distinct [2.2.2]diazabicycles have been isolated from fungal sources spanning three genera. This class of molecules displays remarkable structural diversity and many members have demonstrated biological activity. Key to the successful syntheses of malbrancheamide B was a novel domino reaction sequence involving a 1-pot aldol condensation, alkene isomerization, and [4+2] cycloaddition. In the case of the enantioselective synthesis, a chiral, nonracemic aminal auxiliary on the diketopiperazine diene-precursor was used to direct facial selectivity in Diels–Alder reaction.

## TABLE OF CONTENTS

Acknowledgements	ii
Dedication	iii
List of Tables	iv
List of Figures	v
List of Schemes	vi
Chapter 1. The bicyclo[2.2.2]diazaoctane indole alkaloids	1
Chapter 2. Development of domino reaction sequence	35
Chapter 3. Synthesis of malbrancheamide B	46
Appendix	79
Vita	96

## ACKNOWLEDGEMENTS

I want to first give my thanks to Dr. Jonathan Scheerer for his guidance over these last few years. In hindsight I'm sure I was quite a project and I'm grateful for his patience in helping me develop as a chemist and as a professional. His impeccable insight was my greatest resource and truly an invaluable tool. Additionally, I give my thanks to Dr. Deborah Bebout, Dr. Robert Hinkle, and all my professors and advisers in the William and Mary chemistry faculty. This group of professors was unwaveringly patient, accessible, and respectful throughout my education at the College.

I also want to mention all my fellow Scheerer group members with whom I shared many successes and probably just as many failures. Special thanks to Todd Hovey whose infectious enthusiasm for chemistry I hope to take with me in the future. Thanks to Emily Eklund, Katherine Nenninger, Erin Morris, and Kaila Margrey who I could always rely on for a helping hand, and thanks to Alex Chinn and John Woo, good friends and good roommates. These people and the many others in the Scheerer group were an integral part of my lab experience.

Finally, I'd like to make one last shout out to my mentors and peers outside the Scheerer group. First I'd like to thank two fantastic laboratory teaching assistants, Alex Gade and Christina Davis, who inspired my interest in chemistry in the first place. Last but not least I'd like to mention Shane Lewis, Ajara Rahman, Justin Salvant, Emily Willard, and all my friends in the Hinkle lab..

To W. John and Lori Laws, my parents, to whom I owe my greatest thanks and without whose constant support and love I'm sure I could never have accomplished this task.

## LIST OF TABLES

1.1 Intramolecular SN2' cyclizations of precursor <b>9</b>	20
--	----



## LIST OF FIGURES

1.1 Bicyclo[2.2.2]diazaoctane core	1
1.2 Selected members of the brevianamide family	2
1.3 <i>Anti</i> - and <i>syn</i> -diastereomers of the diazabicyclic core	3
1.4 Marcfortines A-C	7
1.5 Selected members of the paraherquamide family of alkaloids	9
1.6 Sclerotiamide, stephacidins A and B, avrainvillamide, and notoamide B	11
1.7 The stephacidin-type alkaloids isolated from specific fungal sources	13
1.8 The asperparaline family of indole alkaloids	16
1.9 Chrysogenamide A	17
3.1 The malbrancheamide family of alkaloids	46

## LIST OF SCHEMES

1.1 Birch's early-stage biosynthesis of brevianamide A	5
1.2 Williams' alternative biosynthetic pathway proposals	6
1.3 <i>P. cf. canescens</i> incorporation study of preparaherquamide into paraherquamide A	10
1.4 Proposed biosynthesis of stephacidin A and notoamide B	14
1.5 Proposed unified synthesis of asperparaline A and paraherquamide A	17
1.6 Intramolecular S <sub>N</sub> 2' cyclization	18
1.7 Synthesis of a S <sub>N</sub> 2' precursor in the Williams synthesis of brevianamide B	19
1.8 Completion of the brevianamide B synthesis	21
1.9 S <sub>N</sub> 2' cyclizations toward paraherquamide B and the stephacidins	22
1.10 Intramolecular hetero Diels–Alder of a 5-hydroxypyrazine-2(1H)-one	23
1.11 Synthesis of an IMDA precursor	23
1.12 IMDA and endgame for brevianamide B synthesis	24
1.13 Liebscher's neutral conditions IMDA study	25
1.14 Model oxidative enolate coupling to form [2.2.2]diazaoctane bicycles	26
1.15 Completion of stephacidin A	27
1.16 Synthesis of avrainvillamide	29
1.17 Cation olefin cascade cyclization	30

1.18 Simpkins' synthesis of brevianamide B	31
2.1 Racemic IMDA in synthesis of stephacidin A	35
2.2 Diels–Alder cycloaddition of a chiral, non-racemic DKP diene	37
2.3 Directed IMDA of chiral DKP azadiene <b>5</b>	37
2.4 Model retrosynthesis for bicyclo[2.2.2]diazaoctane core	39
2.5 Synthesis of DKP azadiene-precursors <b>8</b> and <b>9</b>	39
2.6 Domino reaction sequence	40
3.1 A proposed unified biosynthesis of the malbrancheamides	48
3.2 Synthetic scheme of reverse prenylated tryptophan derivatives	49
3.3 Formation of [2.2.2]diazabicyclic	50
3.4 Synthetic preparation of [2.2.2]diazaoctane-precursor	51
3.5 Cation olefin cyclization	52
3.6 Retrosynthetic plan for enantioselective synthesis	53
3.7 Preparation of BOM-protected chloroindole <b>4</b>	54
3.8 Domino cyclization in the enantioselective synthesis of malbrancheamide B	55
3.9 Anticipated HWE, reduction and hydrogenation to (+)-malbrancheamide B	57
3.10 Observed hydrogenation of <b>11</b> to premalbrancheamide	58
3.11 Amended route for the completion of (+)-malbrancheamide B	59
3.12 Retrosynthetic plan for racemic synthesis	60

3.13 Racemic domino reaction sequence towards malbrancheamide B	62
3.14 Endgame of racemic synthesis	63

## CHAPTER I

### The BICYCLO[2.2.2]DIAZAOCTANE INDOLE ALKALOIDS

#### Introduction:

A number of prenylated indole alkaloids contain bicyclo[2.2.2]diazaoctane ring systems at their core (**Figure 1.1**).<sup>1</sup> This structural motif was originally identified in the brevianamides in 1969<sup>2</sup> and isolation of similarly bicyclic metabolites from various aquatic and terrestrial species of the *Aspergillus*, *Penicillium*, and *Malbranchea* genera continues today. Despite similar polycyclic skeletal structures, this family displays impressive structural diversity among its nearly 80 naturally occurring members (**Figure 1.2**).<sup>3</sup> Genetic evidence and commonalities in core structure and fungal source suggest that these metabolites share closely related biosynthetic pathways. While a great deal of insight into the biosynthetic relationships of the many subfamilies has been gained over the last four decades, many details remain elusive and thus, significant interest on the topic still exists. The core bicycle seen in all members of the family has also drawn attention from the community of synthetic chemists. Multiple methodologies for creating [2.2.2]diazabicycles have been developed and implemented in natural product total syntheses. Presented here is a discussion of this family's general structural themes, synopses of the isolation, bioactivities, and biosyntheses of each of the known subfamilies, and selected total syntheses that highlight the unique methods by which the diazabicyclic core has been

**Figure 1.1:** Bicyclo[2.2.2]diazaoctane core

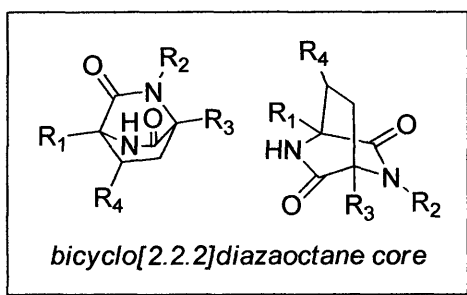
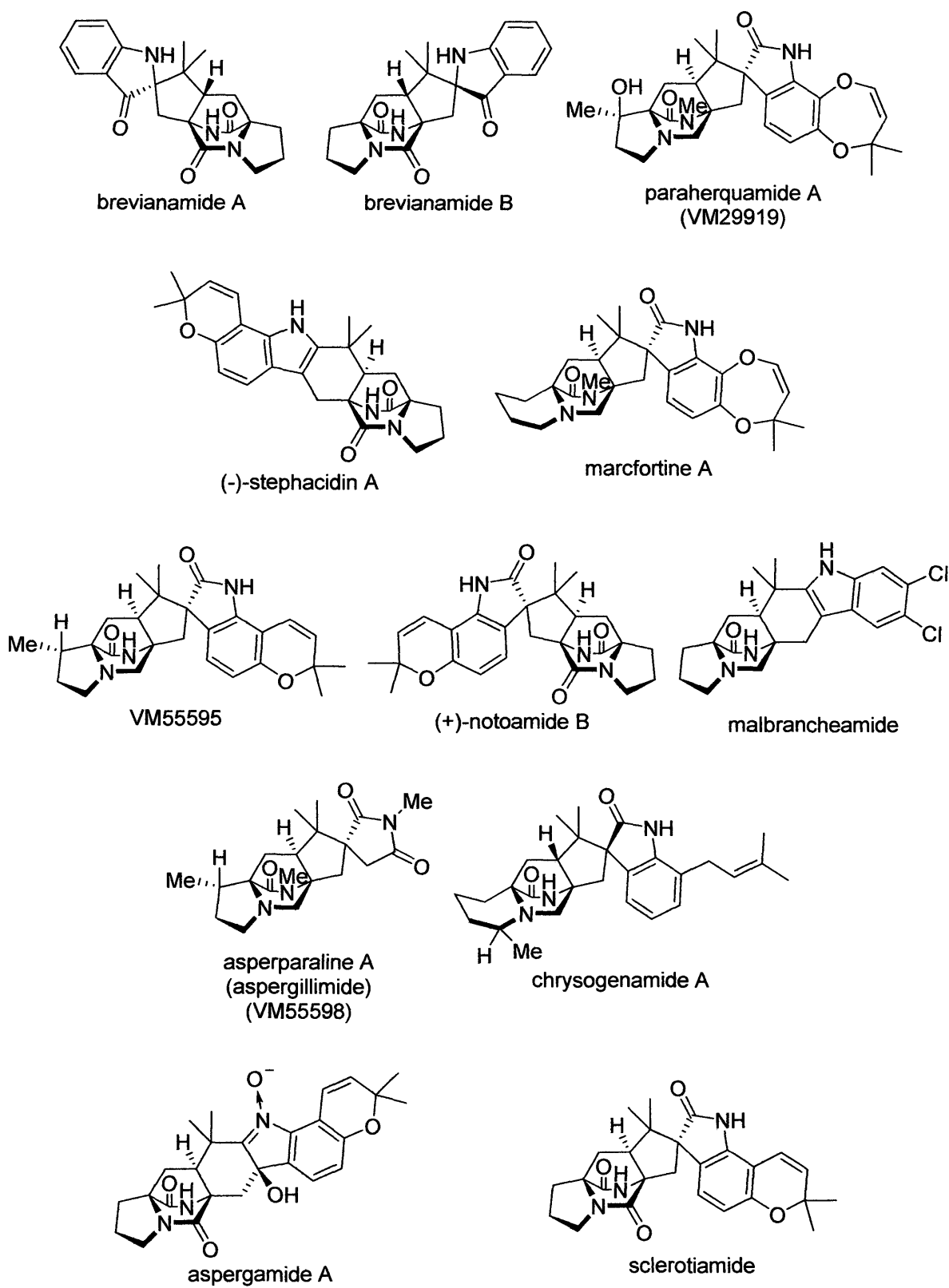


**Figure 1.2:** Selected members of the brevianamide family

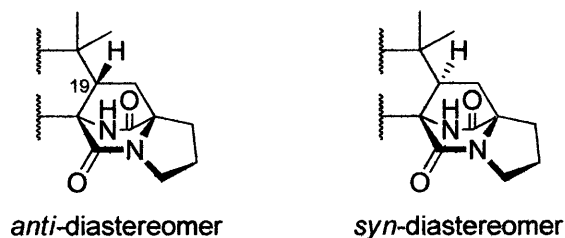


constructed. Introduction and discussion of the malbrancheamides will be presented in a later chapter.

#### Structural Themes:

This family of metabolites shares some key structural features in addition to the [2.2.2]-diazabicyclic core. Molecules of this family are biosynthetically derived from two amino acids, generally tryptophan and proline, and one or two isoprene units. Despite their common core feature and their similar biosynthetic origins, alkaloids of this family demonstrate remarkable structural variety. Members sharing the diazabicyclic core can differ in ring size, number, and fusion pattern, in oxidation state, substitution patterns, and in the *syn*- or *anti*-relationship of the diazaoctane bicyclic core (**Figure 1.3**). The numerous permutations coming from variations in all these criteria help account for the diversity of observed metabolites.

**Figure 1.3:** *Anti*- and *syn*-diastereomers of the diazabicyclic core



The most visible variation among members of the family occurs in their ring systems. Nearly all known examples contain 5-member pyrrolidine ring attached to the diazabicyclic core. Exceptions to this trend include the marcfortines which are biosynthetically related to pipercolic acid and therefore contain the amino-acid's 6-member ring. Other variations in ring size can be seen in differences between alkaloids with and without 7-member dioxepin rings in their structure. The number of rings in the bicycles' polycyclic systems range from five to seven and several ring fusion patterns are observed including spiro-oxindoles and spiro-indoxyls. Another major distinction between subfamilies is the oxidation state of the diazabicyclic core. Each

family of alkaloids exclusively contains either monoketopiperazine cores as in the paraherquamides or diketopiperazines as in the brevianamides.

While all members of this alkaloid family contain the geminal dimethyl substitution adjacent to the diazaoctane, other ring substitutions can occur. Brevianamides A and B, for example, contain the common gem-dimethyl groups and indole oxidation, but no further substituents. The most notable case of substitution in this family is seen in the malbrancheamides, which are unique in their indole halogenation.

The last noteworthy variable characteristic of this family is the stereochemical configuration of the diazabicyclic core (**Figure 1.3**). The majority of metabolites with this diazaoctane bicycle feature the amide bridge *syn* to the C-19 proton (brevianamide numbering). The relatively less common *anti*-configuration has so far been observed only in a few examples. From a synthetic perspective, this feature poses the most interesting challenge. Replicating the enantiomeric purity of such an unusual structure necessitates the development of stereoselective methodology.

#### The Brevianamides:

The brevianamide family of alkaloids was first isolated by Birch et al. from *Penicillium brevicompactum* in 1969.<sup>2</sup> Four of the six metabolites originally isolated in this study, brevianamides A-D, were found to contain the novel bicyclo[2.2.2]diazaoctane core structure. Eventually it was found that brevianamides C and D were artifacts of isolation resulting from exposure to light, leaving brevianamides A and B as the sole brevianamide natural products containing the unique core (**Figure 1.2**).<sup>4</sup> Brevianamide A gained particular interest after it demonstrated modest antifeedant and insecticidal effects.<sup>5</sup> Over time, *P. brevicompactum* has

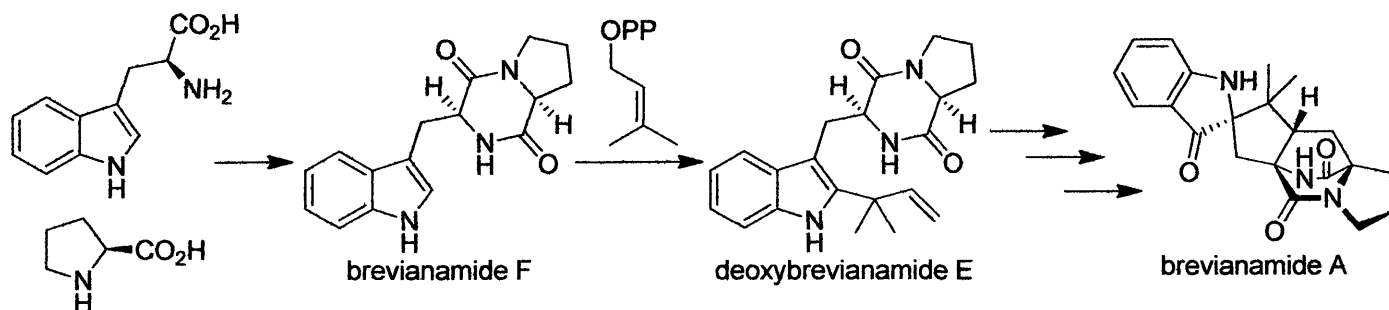


proven the most viable source for consistent isolation of brevianamides A and B, but *P. viridicatum* has also been established as a source for brevianamide A.<sup>6</sup>

Structural elucidation revealed that these naturally occurring [2.2.2]diazabicycles consist of diastereomeric hexacyclic ring systems. They display very little substitution on their polycyclic skeletal structures, lacking the proline or indole ring substituents observed on other indole alkaloids of the family. They contain *anti*-configured bicyclic cores, a conformation that has proven rare in the wake of subsequent isolation of numerous *syn*-configured diazabicycles. Additionally, they contain a spiro-indoxyl moiety not observed in any of the other subfamilies of alkaloids.

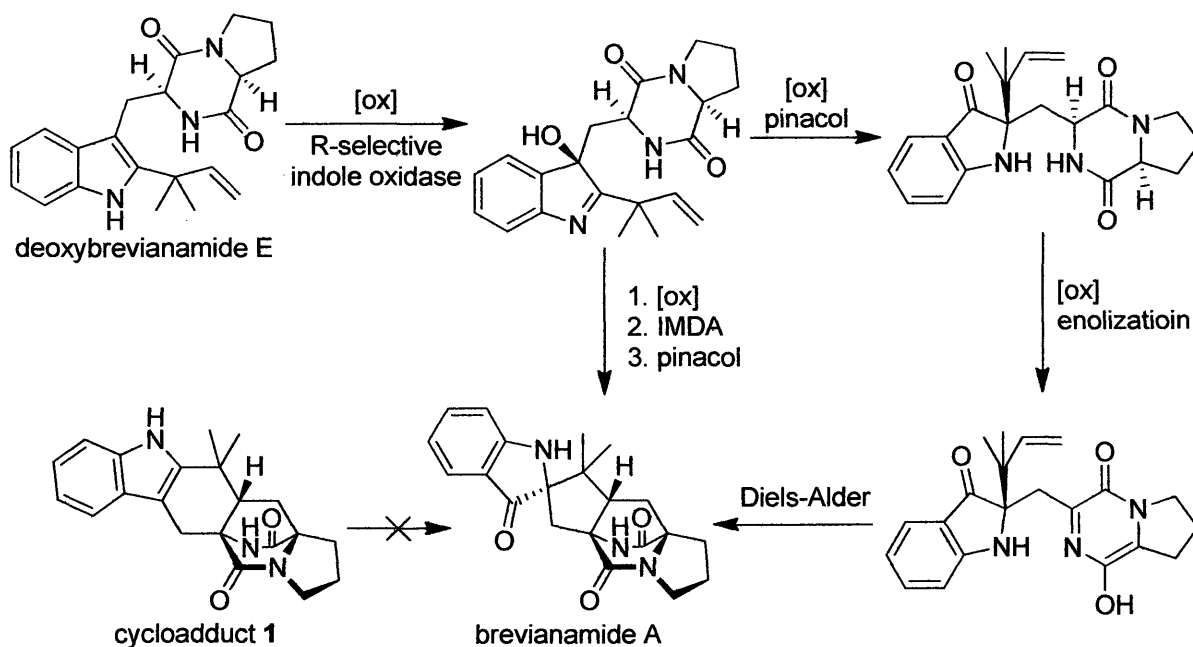
In order to probe the biosynthesis of these new alkaloids, Birch executed a series of radiolabeled precursor incorporation studies shortly after the molecules' initial isolation.<sup>2,4</sup> This work identified tryptophan, proline, and mevalonic acid as the basic precursors of the biosynthetic pathway in *P. brevicompactum*. Additionally, brevianamide F, the diketopiperazine product of condensation between tryptophan and proline, also incorporated into brevianamide A, suggesting that it was an intermediate along the biosynthetic pathway. These findings prompted Birch's proposal for the early biosynthesis of the brevianamides (**Scheme 1.1**).

**Scheme 1.1:** Birch's early-stage biosynthesis of brevianamide A



Continuing research into the biosynthesis of the brevianamides was conducted by Williams and coworkers who conducted incorporation studies with radiolabeled deoxybrevianamide E in *P. brevicompactum*.<sup>7</sup> In these studies it was determined that deoxybrevianamide E was indeed a brevianamide A precursor, but that the [2.2.2]cycloadduct **1** was not. These observations led to the proposal that the [2.2.2]diazabicycle must not form until after indole oxidation and pinacol shift, a conclusion that led to alternative biosynthetic pathway proposals (**Scheme 1.2**). Synthetic obstacles have prevented the verification of any part of these pathways at this time.

**Scheme 1.2:** Williams' alternative biosynthetic pathway proposals

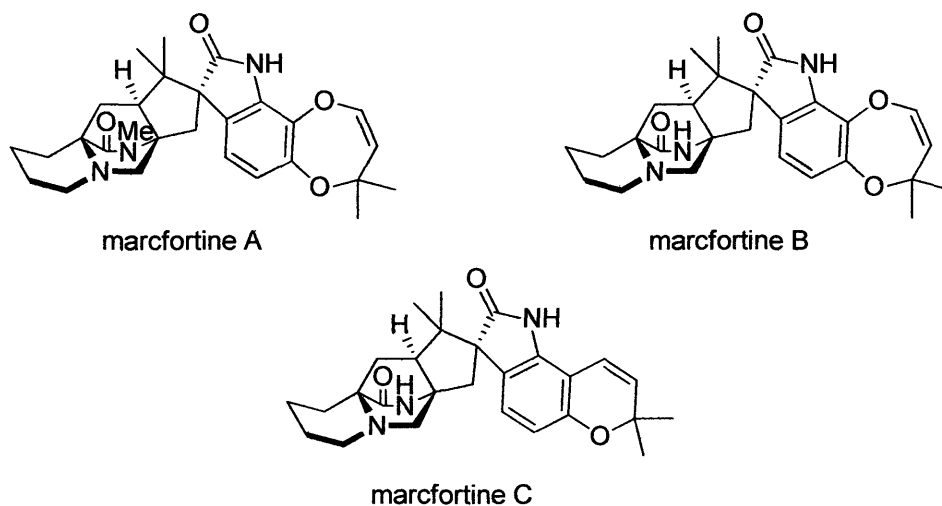


#### The Marafortines:

Eleven years after the original isolation of the brevianamides, Polonsky et al. introduced the next three [2.2.2]diazabicycles to the family of alkaloids, marafortines A, B, and C (**Figure 1.4**).<sup>8</sup> The marafortines were isolated from a fungus used in the production of blue cheeses

which was then called *Penicillium roqueforti*. Later this fungal species was reclassified and subdivided into three distinct species, at which point it was found that only one of these, *P. paneum*, produces the marcfortines.

**Figure 1.4:** Marcfortines A-C



While these metabolites share the family's defining core characteristic, their structural features distinguish them from the brevianamides. All three marcfortines contain heptacyclic ring systems with *syn*-configured, monoketopiperazine diazabicycles. Instead of the brevianamides' spiro-indoxyl moiety, the marcfortines contain spiro-oxindole skeletal fusion patterns with C-6 and C-7 substituted indole rings that connect either dioxepin or pyran moieties. The most unusual feature of these molecules is the six-membered, pipercolic acid-derived ring rather than the 5-member, proline-derived ring displayed in nearly all other [2.2.2]diazabicycles.

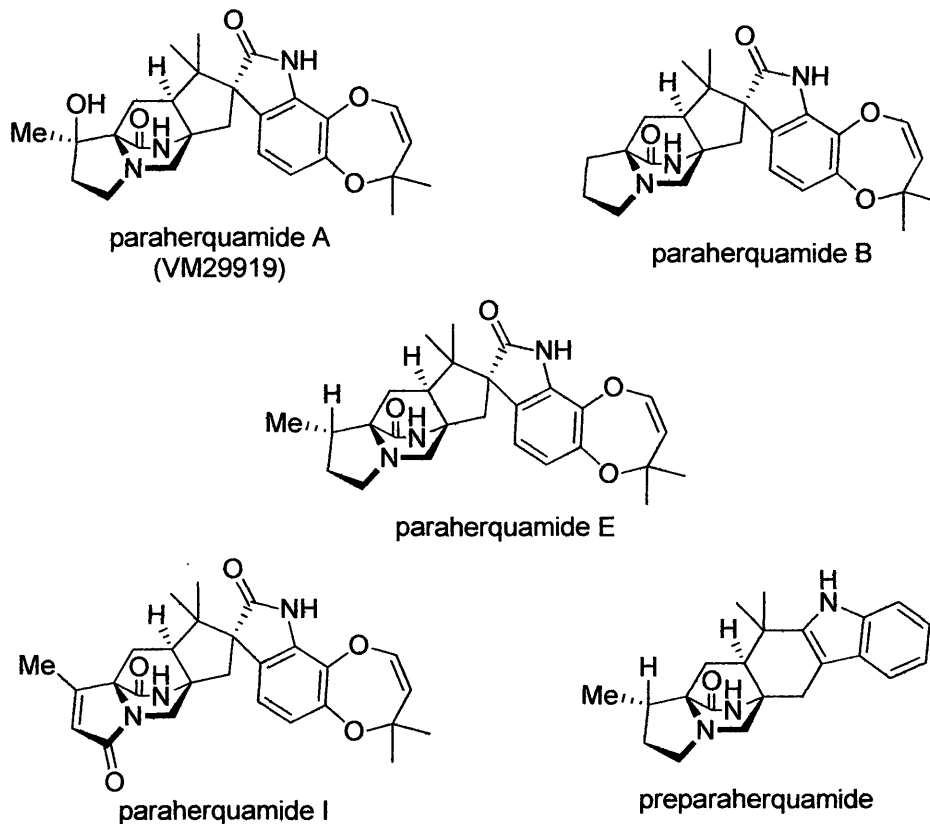
While the [2.2.2]diazaoctane bicycles that they share with the brevianamides suggest a similar biosynthesis, the distinct structural characteristics, especially that of the pipercolic acid ring, separate these alkaloids from those of the other subfamily. Biosynthetic investigation of

marcfortine A was first carried out by Kuo and coworkers.<sup>9</sup> Their work showed, L-tryptophan, L-methionine, L-lysine, and acetate as the biosynthetic precursors of the molecule, finding that tryptophan incorporated into the spiro-oxindole, methionine contributed via SAM methylation, lysine incorporated into the pipercolate, and acetate incorporated into the isoprene units.

#### The Paraherquamides:

The next major subfamily of [2.2.2]diazaoctane bicycles was discovered upon the isolation of paraherquamide A from *Penicillium paraherquei*, also known as *P. charlesii*, in 1981.<sup>10</sup> In the decades following the discovery of paraherquamide A, the paraherquamide subfamily of alkaloids experienced substantial growth with the discovery and characterization of some fifteen related molecules. Paraherquamides B-G were discovered next from *P. charlesii*, and paraherquamides H and I were found together with a variety of similar metabolites (**Figure 1.5**) in cultures of either *P. cluniae*, *Penicillium* sp. IMI 332995, *Aspergillus japonicus*, *P. charlesii*, or *Aspergillus* sp. IMI 337664.<sup>11</sup> Like brevianamide A, a number of the paraherquamides display biological activities. Paraherquamides A-G have demonstrated antinematodal properties, but paraherquamide A remains the most notable for its anthelmintic activity against drug-resistant parasites.<sup>12</sup> Early results indicated that paraherquamide A's anthelmintic effectiveness against nematodes with broad-spectrum drug resistance could lead to its use as a therapeutic, but it was subsequently determined that its unacceptable toxicity levels make it unsuitable for such use.<sup>13</sup> Development of semisynthetic paraherquamide derivatives<sup>14</sup> has successfully reduced toxicity in mammals while maintaining effectiveness and has seen some use in combination treatment in sheep.<sup>15</sup>

**Figure 1.5:** Selected members of the paraherquamide family of alkaloids

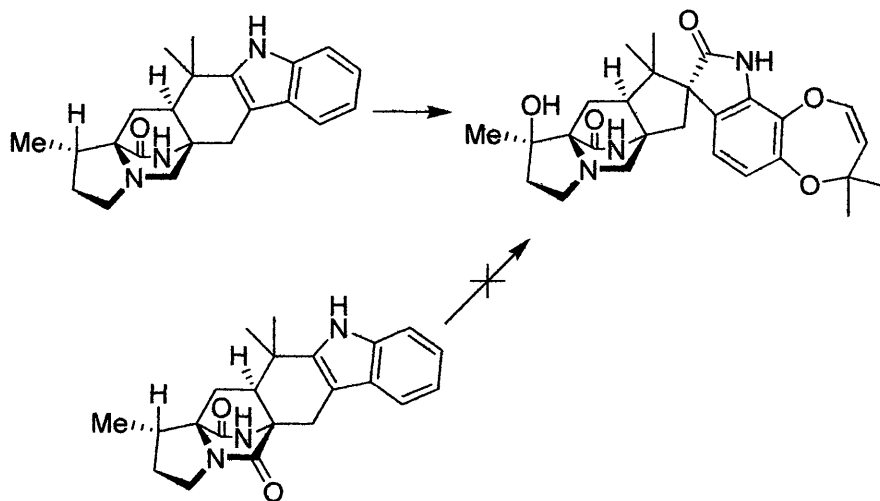


Given the number of known paraherquamide metabolites, the structural diversity evident in this subfamily of [2.2.2]diazabicycles is not surprising. Features conserved across this family include *syn*-configured [2.2.2]diazabicyclic cores at the monoketopiperazine oxidation state similar to those of the marcfortines. Most paraherquamides also possess the same tryptophan-derived spiro-oxindole and dioxepin rings seen in marcfortines A and B. Unlike the previously discussed family members however, the paraherquamides are distinguished by proline-derived rings, moieties upon which many different substitution patterns are observed, including several methylation and oxidation patterns.

As with previous subfamilies, biosynthetic interest has revealed the elementary components of these molecules. Through a series of feeding experiments with *P. cf. canescens*, the Williams group has found that the synthesis of paraherquamide A in this species

incorporates L-isoleucine,  $\beta$ -methyl-L-proline, L-methionine, and L-tryptophan.<sup>16</sup> Further feeding studies by this group went on to probe the incorporation of possible intermediates into paraherquamide A by *P. cf. canescens*.<sup>17</sup> This study also found that synthetic preparaherquamide **19** does incorporate into paraherquamide A, while the diketopiperazine analog of preparaherquamide **19** does not. These results suggest that the tryptophan-derived carbonyl is reduced to the monoketopiperazine before the [2.2.2]diazabicyclo is formed and that the key cyclization event must occur before dioxepin or spiro-oxindole formation (**Scheme 1.3**).

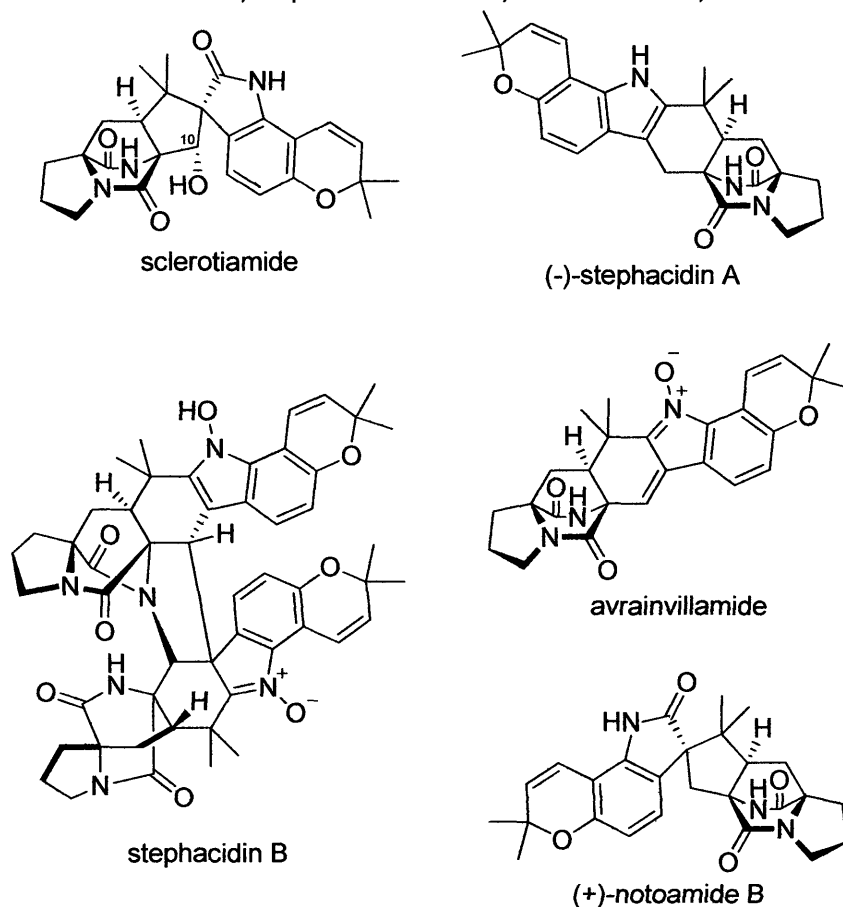
**Scheme 1.3:** *P. cf. canescens* incorporation study of preparaherquamide into paraherquamide A



#### The Stephacidins and Notoamides:

The first metabolite isolated from the next family of diazabicyclic indole alkaloids was discovered in 1996 by Gloer and White from *Aspergillus sclerotiorum* (**Figure 1.6**).<sup>18</sup> This molecule, sclerotiamide A, was originally misclassified as a member of the paraherquamides due to the skeletal features it shares with that family. It was determined, however, that sclerotiamide possesses a diketopiperazine core whereas all the paraherquamides contain monoketopiperazines. Thus, structurally distinct from the monoketopiperazine paraherquamides, the pipercolic acid-derived marcfortines, and the *anti*-configured

**Figure 1.6:** Sclerotiamide, stephacidins A and B, avrainvillamide, and notoamide B



brevianamides, sclerotiamide was correctly assessed as the first known member of a new family of indole alkaloids. This family saw several major expansions, first in 1999 with the discovery of the stephacidins A and B from *Aspergillus ochraceus* WC76466 by Bristol-Myers Squibb,<sup>19</sup> then with the isolation of avrainvillamide from *Aspergillus* sp. CNC358 by Fenical in the same year,<sup>20</sup> and again in 2007 when the Tsukamoto group isolated notoamides A-D from *Aspergillus* sp. MF297-2.<sup>21</sup>

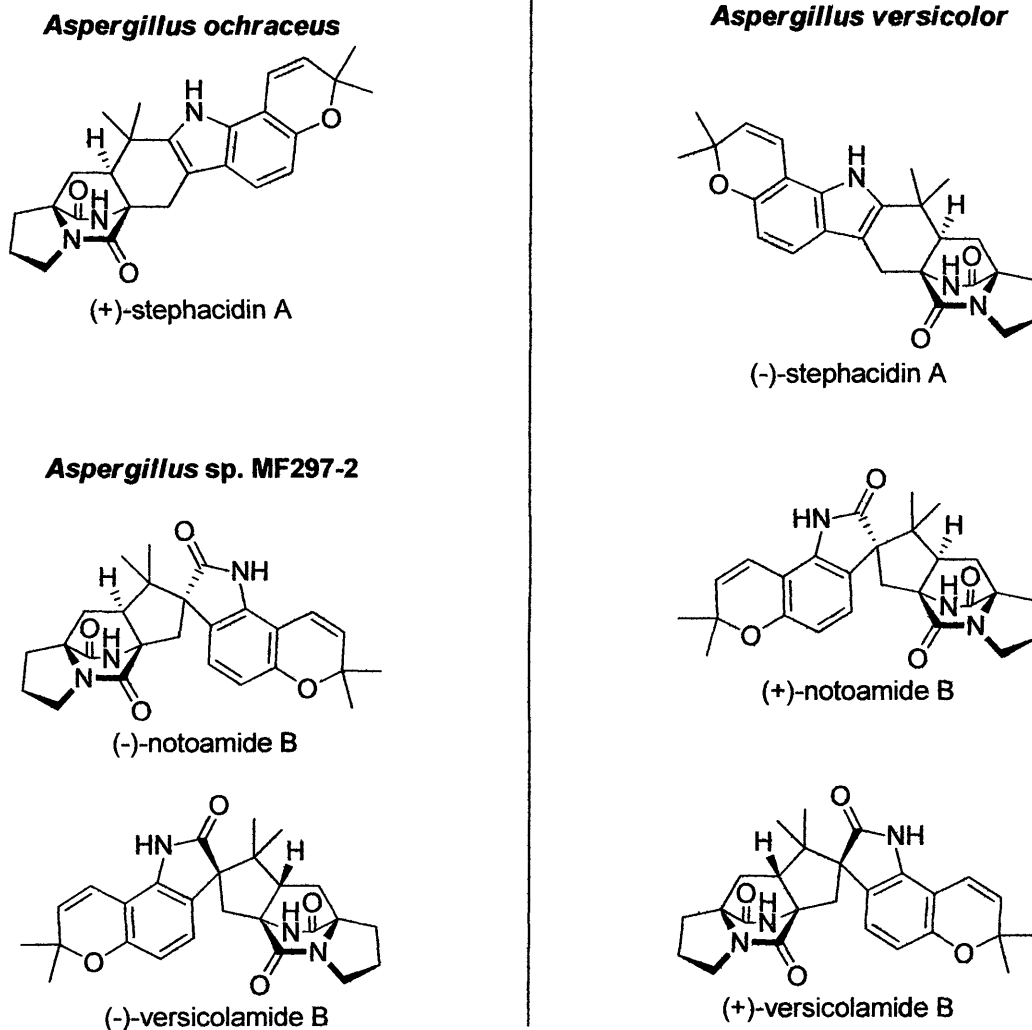
With the addition of so many novel isolates, there was a corresponding growth in the diversity of the family's structural characteristics (**Figure 1.6**). Sclerotiamide A, the first known family member, is structurally defined by its *syn*-configured core bicyclo[2.2.2]diazaoctane, a diketopiperazine core unit, spiro-oxindole and dioxepin rings, an unsubstituted proline ring, and

a unique C-10 hydroxyl substitution (paraherquamide numbering). Stephacidin A, B, and avrainvillamide in contrast, share these features, but lack the spiro-oxindole and hydroxyl substituent.

While the differences in substitution and ring fusion patterns provide interesting points of differentiation, it was not until the isolation of stephacidin A, notoamide B, and a novel isolate, versicolamide B from new fungal sources, *Aspergillus versicolor*<sup>22</sup> and *Aspergillus* sp. MF297-2<sup>23</sup> respectively (**Figure 1.7**), that the subfamily's most interesting feature became apparent. Characterization of these metabolites revealed that the stephacidin A and notoamide B isolates of *A. versicolor* were structurally identical to the *syn*-configured alkaloids previously seen and that versicolamide B displayed the comparatively rare *anti*-configuration which had only been previously observed in the brevianamides. These stereochemical conclusions did not, however, prove to be true for the isolates of *Aspergillus* sp. MF29702, which contained diazabicyclic rings of the configuration opposite of their *A. versicolor*-derived analogs. Members of this family do exhibit biological activities, although they are generally more moderate than the antinematodal properties of the paraherquamides. Sclerotiamide proved to be effective in killing *Helicoverpa zea* corn earworm larvae and inhibiting the growth of surviving larvae.<sup>18</sup> Stephacidins A and B both proved cytotoxic to various human cell culture lines, although it was proposed that the activity of the latter was the result of retrodimerization to form avrainvillamide *in vivo*.<sup>19</sup> Avrainvillamide was observed to inhibit the growth of multiple-antibiotic-resistant strains of *Staphylococcus aureus*, *Streptococcus pyogenes*, and *Enterococcus faecalis*<sup>21</sup> and was proved cytotoxic to a variety of human cancer cell lines.<sup>20</sup> Given the growing problem of antibiotic resistance, avrainvillamide and its dimer stephacidin B pose interesting candidates for further biological study.

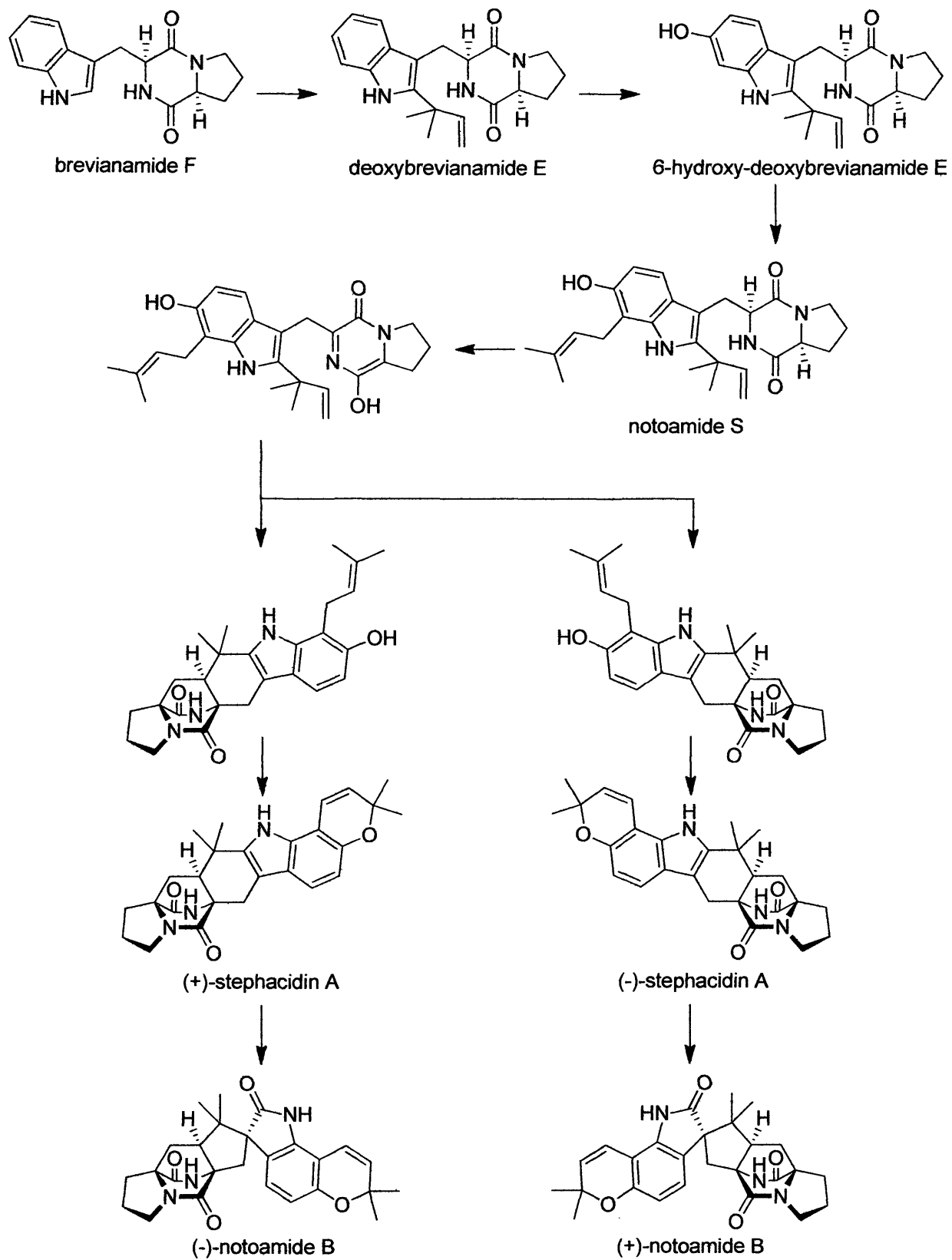


**Figure 1.7:** The stephacidin-type alkaloids isolated from specific fungal sources



Extensive research into the biosynthetic origins of the stephacidin and notoamide family of molecules has resulted in a proposal of a comprehensive biosynthesis of stephacidin A and notoamide B (Scheme 1.4).<sup>24</sup> The proposed biosynthesis of the stephacidin/notoamide family begins with a precursor that intersects the early stages of the brevianamide synthesis. The common precursor, brevianamide F, undergoes sequential prenylation, oxidation, and isomerization until it forms the requisite achiral azadiene precursor of both enantiomeric series of natural products. At this point, enantioselective intramolecular hetero-Diels-Alder

**Scheme 1.4:** Proposed biosynthesis of stephacidin A and notoamide B



establishes the bicyclo[2.2.2]diazaoctane. The absolute conformation of the resulting products depend upon the fungal species in question, with either the *syn*- or *anti*-conformation created exclusively in each organism. The resulting cycloadduct can then undergo oxidative cyclization to form stephacidin A, which can in turn undergo oxidative pinacol rearrangement to notoamide B.

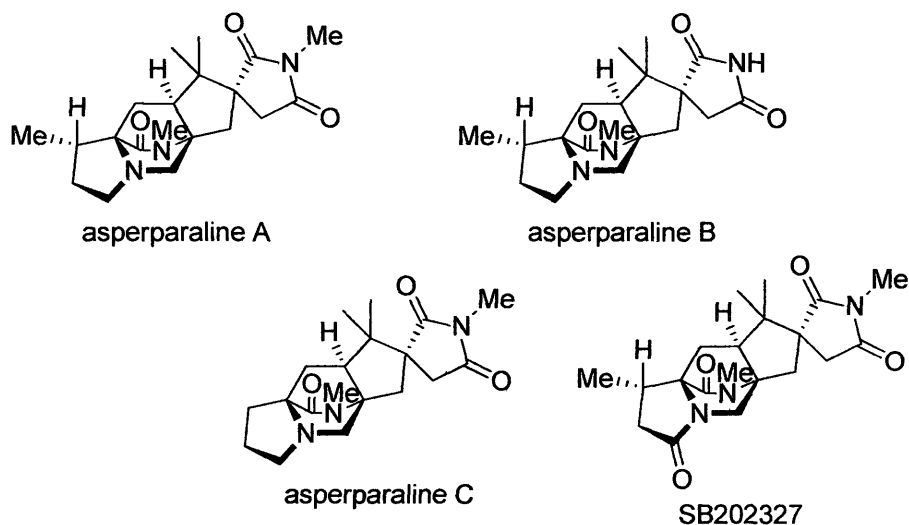
#### The Asperparalines:

Asperparaline A was first isolated one year after sclerotiamide by Hayashi and coworkers from what was then known as *Aspergillus japaconis* JV-23.<sup>25</sup> This species was later divided into seven species, only two of which, *A. aculeatinus* and *A. fijiensis*, were shown to be produce the diazabicyclic indole alkaloid.<sup>26</sup> In a 2000 journal entry, Hayashi et al. reported the isolation of asperparalines B and C from the same fungal source that yielded asperparaline A.<sup>27</sup> All of these alkaloids have demonstrated paralytic effects in silkworms and asperparaline A has also shown anthelmintic activity against *Trichostrongylus colubriformis* in gerbils.<sup>25,27,28</sup> The mechanism of silkworm paralysis by asperparaline A was further investigated by Hayashi et al. and was found to involve the molecules effect as a non-competitive antagonist of nicotinic acetylcholine receptors in silkworm neurons.<sup>29</sup> In a subsequent publication by Everett and coworkers, the isolation of asperparaline A and a new asperparaline A-derivative, SB202327 were reported from *Aspergillus fijiensis*.<sup>11e</sup>

Structurally, the four asperparalines are very similar (**Figure 1.8**). All four asperparalines contain *syn*-configured diazabicycles at the monoketopiperazine oxidation state. They each contain 5-member proline-derived rings which may unsubstituted, as in the case of asperparaline C, or display either methylation or oxidation. These molecules are distinguished

from other [2.2.2]diazaoctane alkaloid families by their 3-spiro-succinimide ring systems. This feature is unique to the asperparaline subfamily of alkaloids.

**Figure 1.8:** The asperparaline family of indole alkaloids

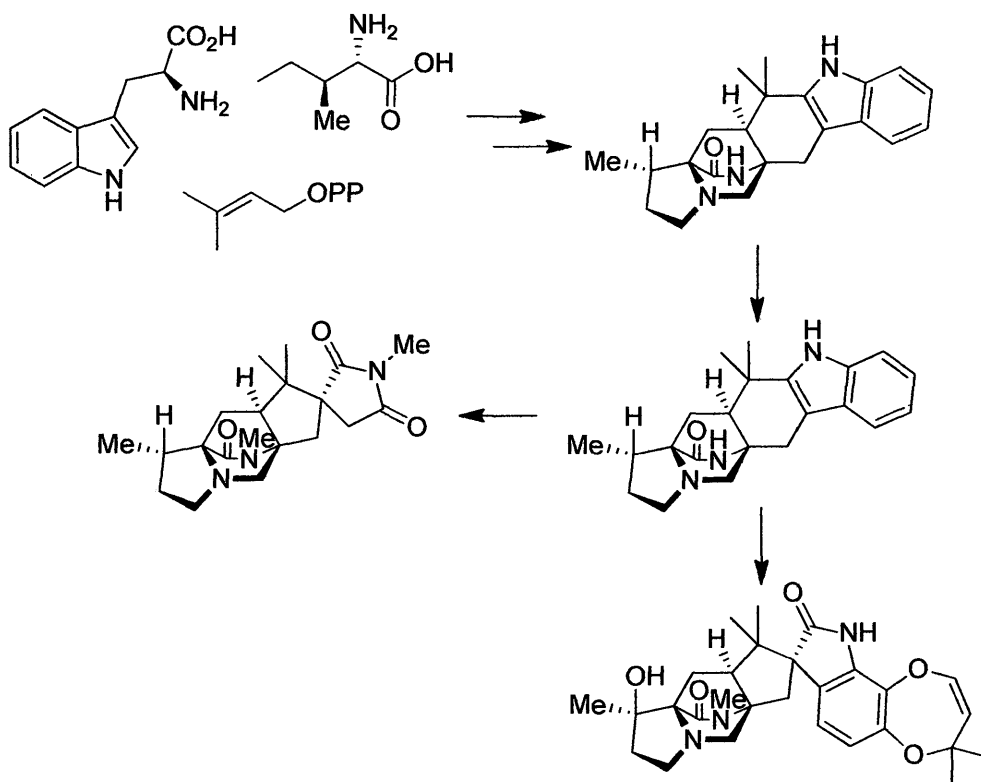


Given the skeletal similarities between the asperparalines and paraherquamides, the Williams group was motivated to perform precursor feeding studies aimed at elucidating the biosynthetic pathway of asperparaline A.<sup>30</sup> These results showed that despite its appearance to the contrary, asperparaline A incorporates not only tryptophan, but all the same basic units as paraherquamide A. This observation, together with the subsequent detection of preparaherquamide in *A. aculeatinus*, suggest that the biosynthesis of paraherquamide A and asperparaline A are unified at least up until preparaherquamide at which point the imide moiety of the asperparalines is likely the product of degradation of the paraherquamide indole nucleus (**Scheme 1.5**).<sup>11i</sup>

#### Chrysogenamide A:

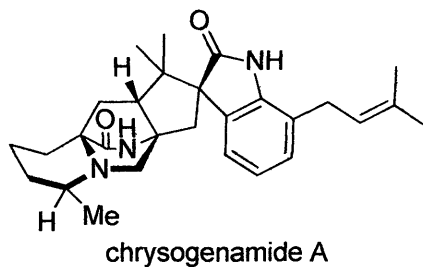
Chrysogenamide A, the only known member of the chrysogenamide family, was first isolated from *Penicillium chrysogenum* No. 005 by Zhu and coworkers in 2008 during screening for molecules with neuroprotective activity.<sup>31</sup> Structurally, this alkaloid very closely resembles

**Scheme 1.5:** Proposed unified synthesis of asperparaline A and paraherquamide A



the marcfortines. It contains an *anti*-configured [2.2.2]diazabicycle at the monoketopiperazine oxidation state, a methylated pipercolic acid ring much like that of the marcfortines, a spiro-oxindole ring fusion pattern, and a isoprene substitution at the indole's C-7 position. Little is known about the biosynthesis of this compound, while its structural similarities to the marcfortines suggest related biosynthesis, the *anti*-configured diazabicycle could indicate a distinct pathway.

**Figure 1.9:** Chrysogenamide A



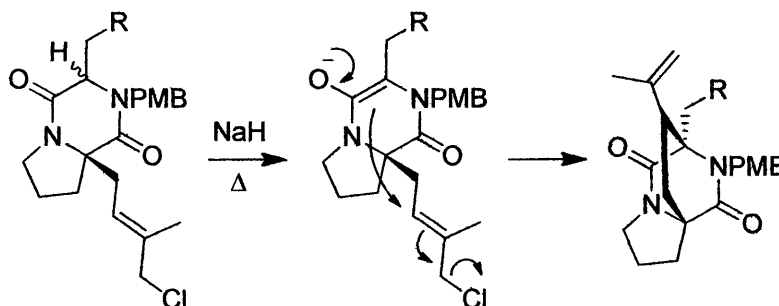
## Previous Synthetic Methods:

While not every indole alkaloid has been the target of a total synthesis, numerous syntheses of select diazabicycles have been completed. From these efforts have emerged five distinct methods for establishing the natural products' core structural feature. Syntheses representative of each method are presented here as an introduction to these strategies.

## Intramolecular $S_N2'$ Cyclization:

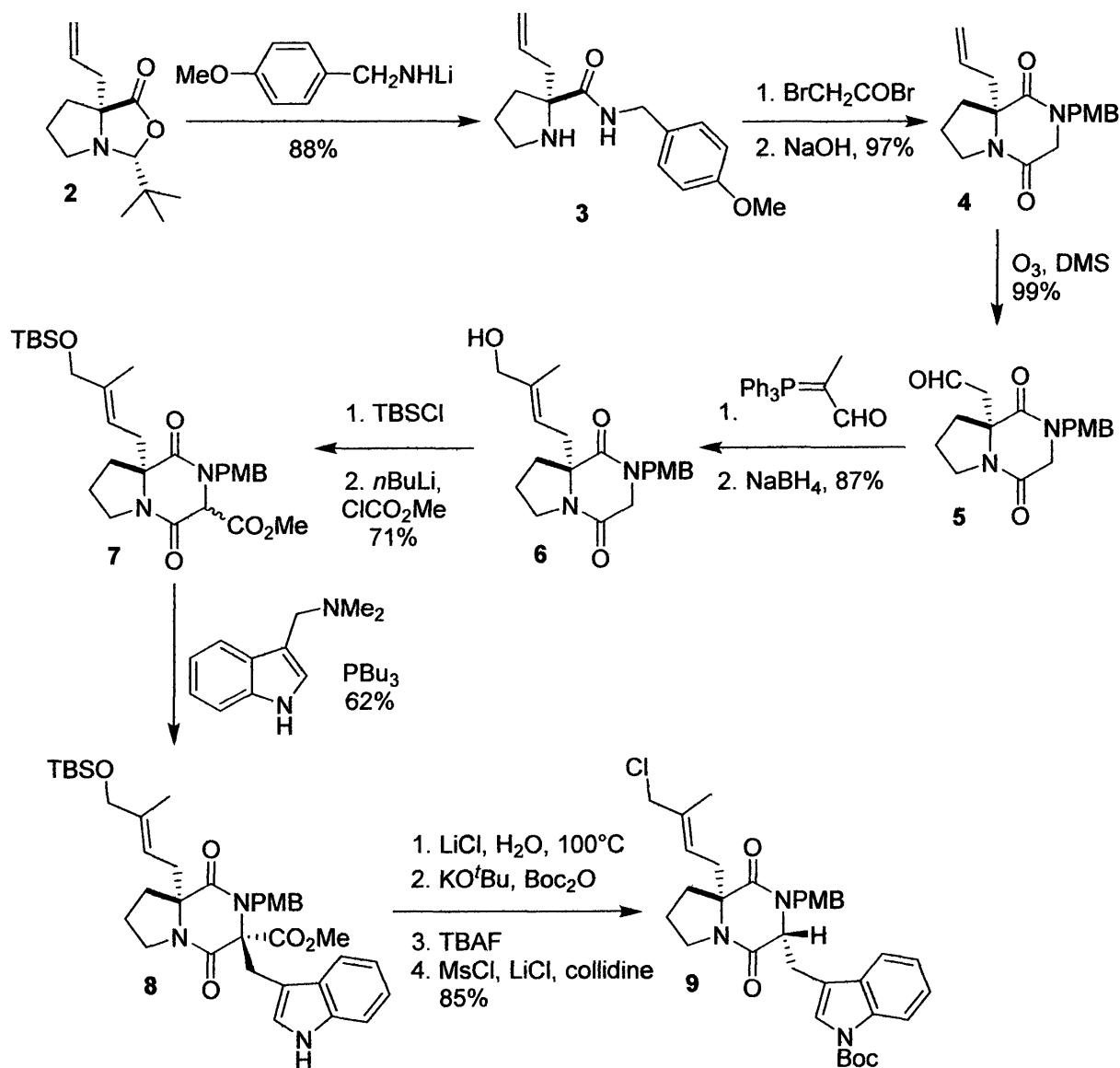
The first synthetic methodology used to establish the bicyclo[2.2.2]diazaoctane core was not performed in the context of a total synthesis until nearly two decades after the original isolation of the brevianamides. The Williams group developed an intramolecular  $S_N2'$  cyclization pathway in the synthesis of brevianamide B (**1**)<sup>32</sup>, but later adapted its use for the syntheses of several other indole alkaloids.<sup>33</sup> The key cyclization event of these syntheses involves a diketopiperazine precursor that undergoes enolization and intramolecular nucleophilic attack on its allylic halide in an  $S_N2'$  fashion (**Scheme 1.6**). This methodology was employed with great success in the Williams' brevianamide B synthesis which proved significant in that it represents the first synthesis of a diazabicyclic indole alkaloid.

**Scheme 1.6:** Intramolecular  $S_N2'$  cyclization



The Williams brevianamide synthesis began with allylated proline derivative **2** (Scheme 1.7).<sup>32</sup> Nucleophilic ring opening of this substrate with *p*-methoxybenzylamine yielded protected amide **3**. PMB-protected amide **3** was then converted to diketopiperazine **4** via secondary amine acylation and subsequent ring closure. Ozonolysis of **4** resulted in oxidative cleavage of the allylic olefin to aldehyde **5**. Wittig olefination of **5** followed by sodium borohydride

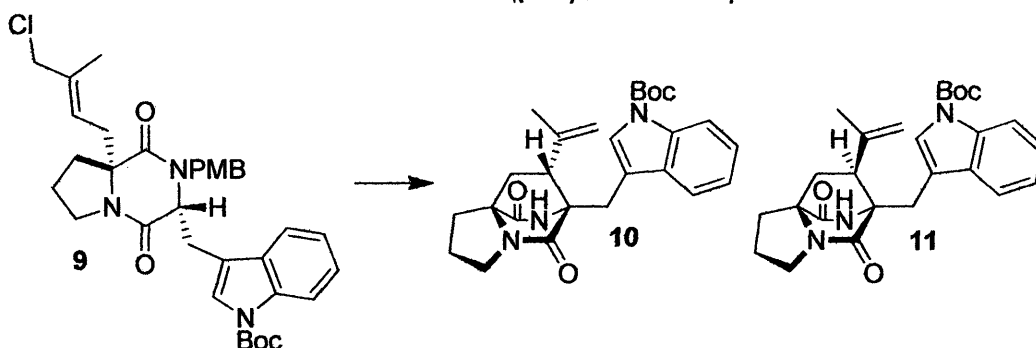
**Scheme 1.7:** Synthesis of a S<sub>N</sub>2' precursor in the Williams synthesis of brevianamide B



reduction of the resulting  $\alpha,\beta$ -unsaturated aldehyde gave primary alcohol **6**. Silyl protection of allylic alcohol **6** with TBSCl allowed for diketopiperazine deprotonation and formation of methyl ester **7** after quenching with methyl chloroformate. Coupling of the mixture of diastereomers in methyl ester **7** with gramine yielded **8**. A four step-sequence then removed the methyl ester group of **8**, converted its silyl-protected primary alcohol to an analogous primary halide, and Boc-protected the gramine to give **9**. The formation of this allylic halide precursor was crucial to the synthesis. The creation of this molecule allowed for the planned intramolecular  $S_N2'$  cyclization event that established the bicyclic core structure of the target alkaloid.

The key intramolecular  $S_N2'$  cyclization step of the brevianamide B synthesis was first attempted with the treatment of precursor **9** with NaH in DMF at room temperature (**Table 1.1**). This reaction gave bicycles **10** and **11** as a 2:1 mixture of diastereomers in 62% combined yield.

**Table 1.1:** Intramolecular  $S_N2'$  cyclizations of precursor **9**



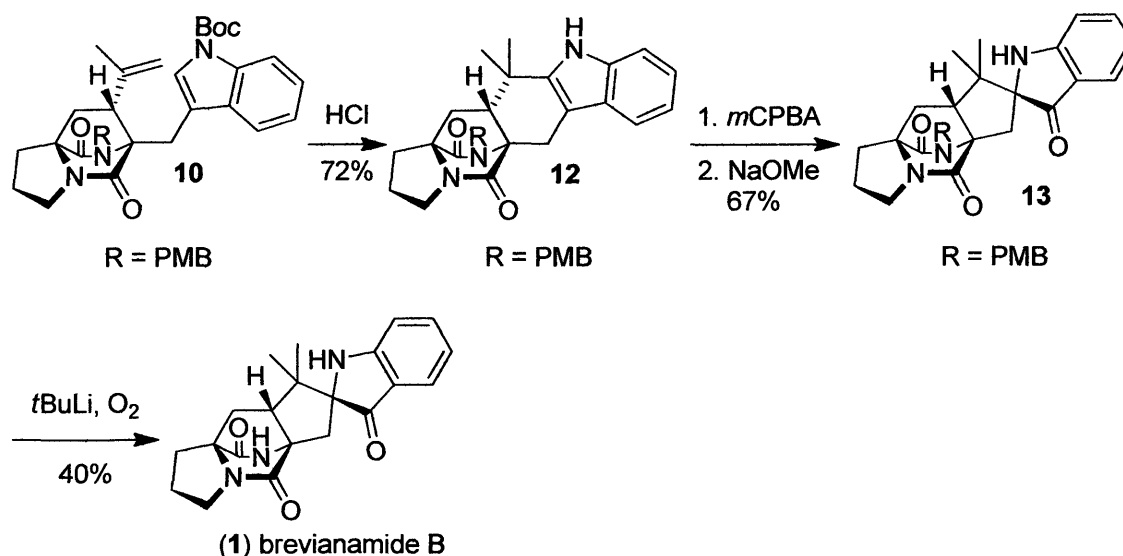
Entry	Conditions	Ratio 10:11	Combined Yield
1	NaH in DMF at rt	2:1	62%
2	NaH in DMF at 100°C	3:97	82%
3	NaH, 18-crown-6 in DMF at rt	4:1	56%



Interestingly, when the reaction was repeated in benzene at 100°C the epimeric ratio of **10:11** reversed its preference to 3:97 in 82% combined yield. Desiring an enhanced preference for the *anti*-configuration characteristic of the target alkaloid, further trials were conducted and it was found that exposing **9** to NaH and 18-crown-6 in DMF gives a 4:1 ratio of **10** to **11** in 56% combined yield.

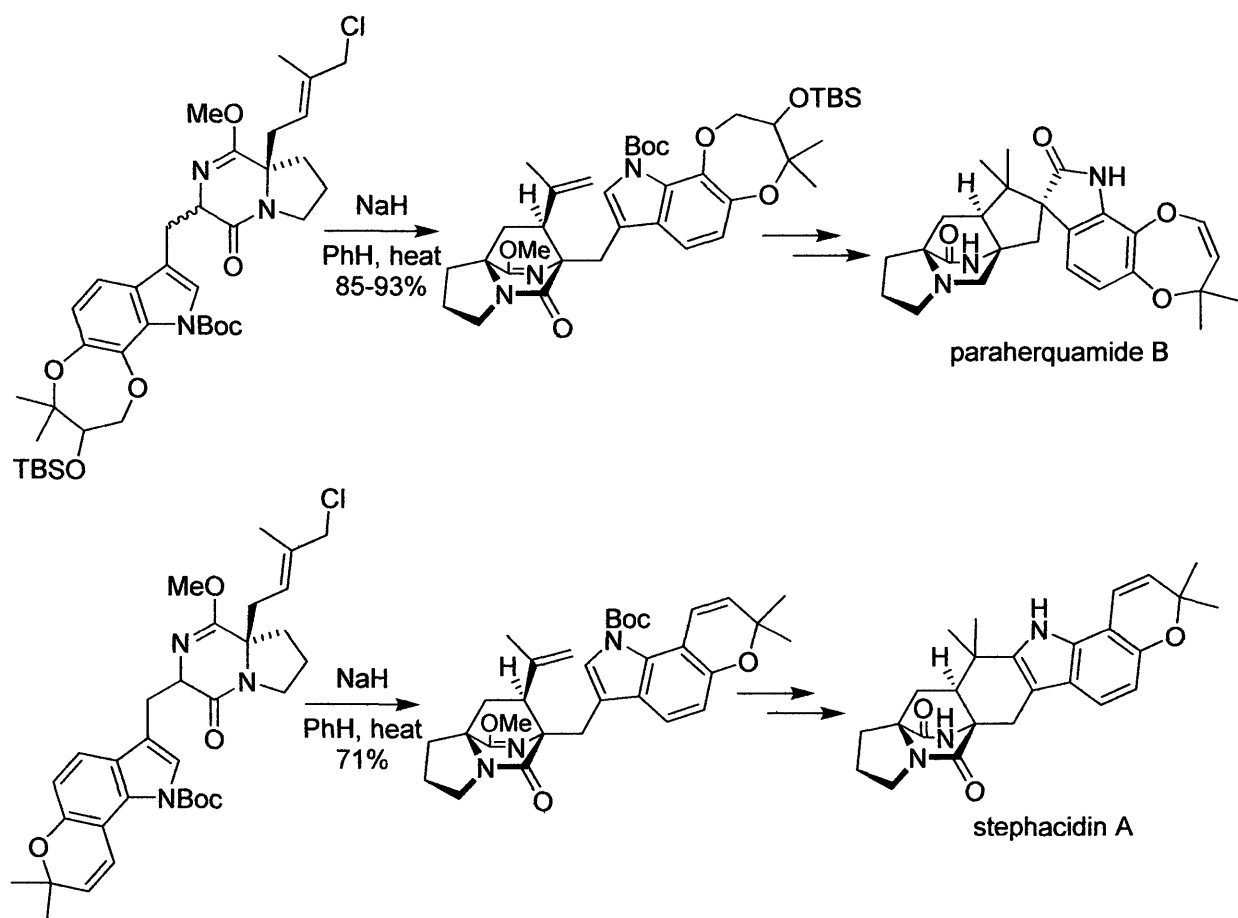
Satisfied with the selectivity and yield of the  $S_N2'$  cyclization for the *anti*-configured diazabicyclic, synthetic effort turned to forming the spiro-indoxyl moiety of the targeted metabolite. The *anti*-configured [2.2.2]diazabicyclic **10** was exposed to concentrated HCl affecting indole deprotection and olefin-cation cyclization (**Scheme 1.8**). Hexacyclic **12** was then converted to the corresponding indoxyl **13** via *m*CPBA treatment followed by exposure to NaOMe. After standard oxidative deprotection strategies failed to remove the PMB-group it was found that deprotonation with *t*BuLi followed by quenching and molecular oxygen respectively gave the final product, brevianamide B (**1**).

**Scheme 1.8:** Completion of the brevianamide B synthesis



The completion of the synthesis of this fungal metabolite proved interesting in multiple ways. The structural characterization of synthetic brevianamide B allowed for the confirmation of the proposed structure for the original isolate. The development of both *syn*- and *anti*-selective  $S_N2$  cyclization methodologies allowed access to structural cores of indole alkaloids of both configurations. The  $S_N2'$  cyclizations used in Williams' later [2.2.2]diazabicyclic syntheses also gave improved yields and were exclusively selective for the *syn*-diastereomer (**Scheme 1.9**).<sup>33</sup>

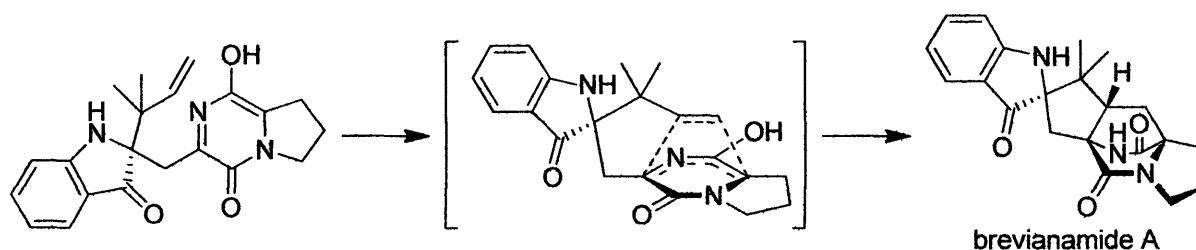
**Scheme 1.9:**  $S_N2'$  cyclizations toward paraherquamide B and the stephacidins



### Biomimetic Intramolecular Hetero Diels–Alder Reaction:

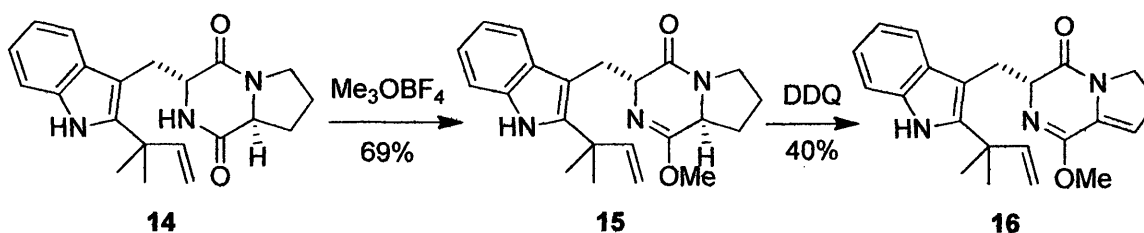
As originally proposed by Porter and Sammes one year after the first isolation of brevianamide B, the biosynthetic formation of the [2.2.2]diazabicyclic core in this family of indole alkaloids is believed to occur via intramolecular hetero Diels–Alder (IMDA) reaction.<sup>34</sup> The proposed IMDA of a 5-hydroxypyrazine-2(1*H*)-one would provide a powerful and elegant means of establishing the desired core structure with simultaneous formation of two bonds (Scheme 1.10). The Williams group executed a second synthesis of brevianamide B incorporating the IMDA cyclization instead of their previously developed intramolecular S<sub>N</sub>2' cyclization methodology.<sup>35</sup>

**Scheme 1.10:** Intramolecular hetero Diels–Alder of a 5-hydroxypyrazine-2(1*H*)-one



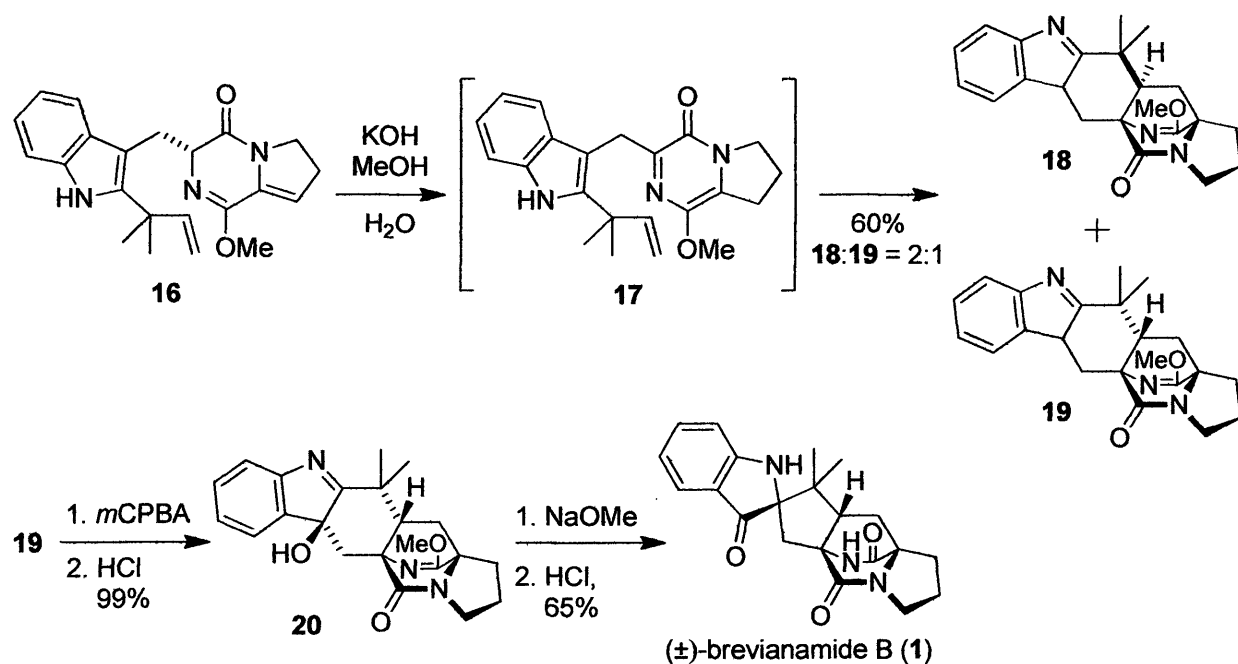
The Williams biomimetic IMDA brevianamide synthesis began with *epi*-deoxybrevianamide E (**14**) (Scheme 1.11). Conversion of **14** to its analogous diketopiperazine diene precursor proceeded in only two steps. First the diketopiperazine secondary amide was

**Scheme 1.11:** Synthesis of an IMDA precursor



converted to its lactim ether **15**. Lactim ether **15** was then oxidized with DDQ to IMDA precursor **16**. Exposure of precursor **16** to aqueous KOH resulted in olefin isomerization to intermediate azadiene **17** which immediately underwent [4+2] cycloaddition with the readily accessible exocyclic alkene (**Scheme 1.12**). In this system, IMDA led to a 2:1 mixture of the undesired *syn*-diastereomer **18** and the *anti*-diastereomer **19** with a combined yield of 60%. The desired minor product of this cyclization (**19**) was then quantitatively oxidized to its corresponding hydroxyindolenine **20**. Finally, pinacol rearrangement and lactim ether deprotection affected the desired transformation of **20** to ( $\pm$ )-brevianamide B (**1**).

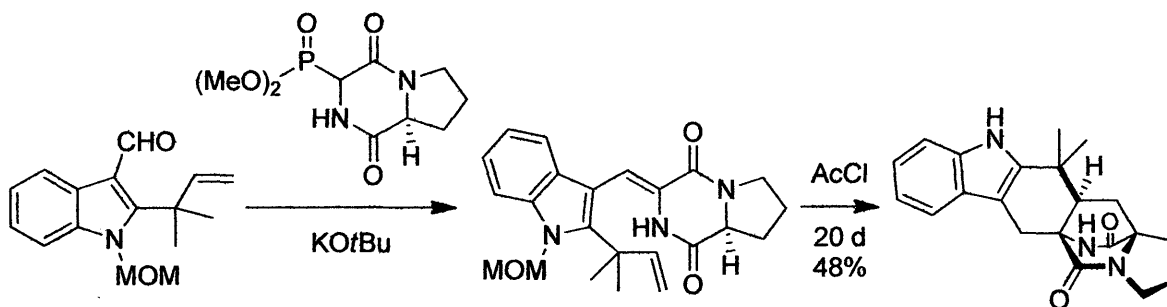
**Scheme 1.12:** IMDA and endgame for brevianamide B synthesis



The incorporation of an IMDA in the synthesis of brevianamide B marked the first use of the biomimetic reaction in the total synthesis of a natural product. While a complete total synthesis supported the possibility for a biosynthetic IMDA, the poor stereoselectivity during the cycloaddition and the necessarily racemic reaction products posed an obvious drawback of the

approach. One noteworthy variation on this methodology was developed as an alternative to the basic conditions used by Williams in the brevianamide synthesis. Liebscher and coworkers pioneered alternative reaction conditions for accessing the [2.2.2]diazabicyclic that involved neutral conditions (**Scheme 1.13**).<sup>36</sup> Basic and neutral IMDA reactions have since been used in a number of natural product total syntheses.<sup>37</sup>

**Scheme 1.13:** Liebscher's IMDA study

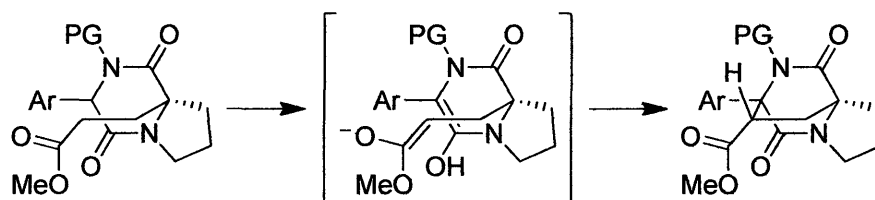


#### Oxidative Enolate Coupling Reaction:

After a successful series of investigations into the reactivity of enolated carbonyl functionalities with heterocyclic aromatic rings exposed to metal oxidants like Cu(II), the Baran group demonstrated the potential utility of these developments in the syntheses of [2.2.2]diazabicyclic alkaloids.<sup>38</sup> In 2006, the Baran group reported the most recent total synthesis of stephacidin A (**21**) that incorporated their new oxidative enolate coupling method for creating [2.2.2]diazabicycles.<sup>39</sup> This enantioselective ring formation effectively applied their oxidative coupling while providing improved synthetic yield of the diazabicyclic target and involved the intramolecular oxidative coupling of ester and amide enolates (**Scheme 1.14**). They predicted that the close proximity of  $sp^2$ -hybridized  $\alpha$ -carbons in the metal-bound transition state would drive reactivity and that the quaternary stereocenter of the proline ring would

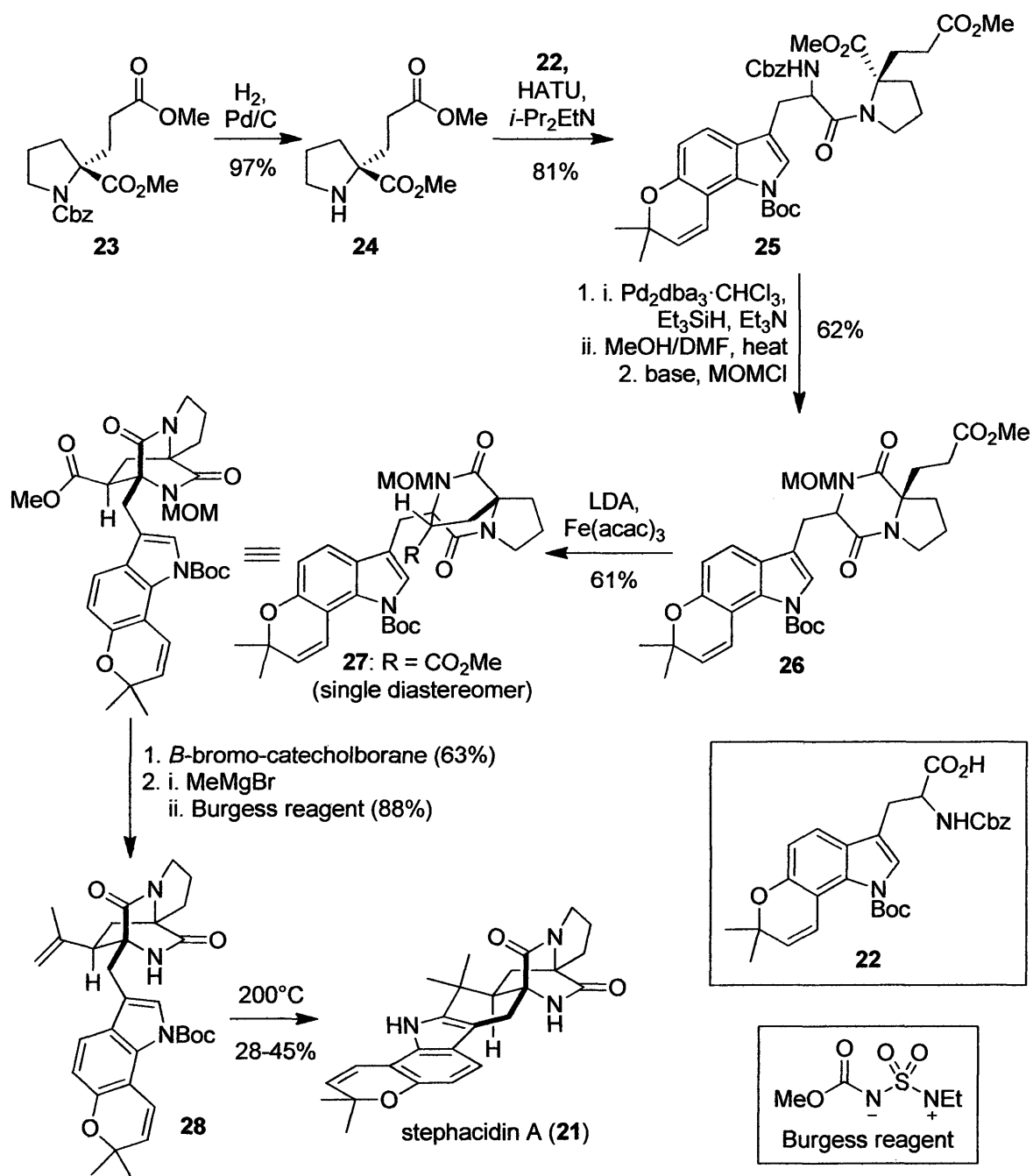
contribute to facial selectivity of bond formation. In this manner, they achieved a highly selective synthesis of the natural product.

**Scheme 1.14:** Model oxidative enolate coupling to form [2.2.2]diazaoctane bicycles



Extensive effort led to the preparation of tryptophan and proline derived starting materials, **22** and **23** (Scheme 1.15). With both amino acid-derived components necessary for the stephacidin synthesis on-hand, reductive deprotection of the carboxybenzyl (Cbz) protecting group in **23** with palladium on carbon revealed proline methyl ester **24**. Immediate exposure of **24** to **22** with HATU allowed peptide coupling and prevented formation of the  $\gamma$ -lactam corresponding to **24**. Resulting amide **25** then underwent chemoselective Cbz deprotection, diketopiperazine ring closure, and *N*-methoxymethyl (MOM) protection of the ring-closed secondary amide functionality. MOM-protected amide **26** was deemed an appropriate starting material for the key synthetic step and screening revealed  $\text{Fe}(\text{acac})_3$  as the most effective metal oxidant for the reaction. Enolation of **26** with LDA and exposure to  $\text{Fe}(\text{acac})_3$  provided **27** as a single diastereomer in 61% yield. Having successfully executed the stereoselective intramolecular oxidative enolate coupling to form the alkaloid's core [2.2.2]diazabicyclic, the synthesis of stephacidin A only required a few more transformations. Coupling product **27** was MOM-deprotected, excess methyl Grignard converted the exocyclic methyl ester to a tertiary alcohol, and the alcohol intermediate was dehydrated to the corresponding alkene. Because instability of **28** under acidic conditions precluded Friedel-Crafts alkylation, sulfolane was used to facilitate thermolytic Boc deprotection and ring closure to form **21** in modest yield.

**Scheme 1.15: Completion of stephacidin A**



### Aminoacyl Radical Cyclization:

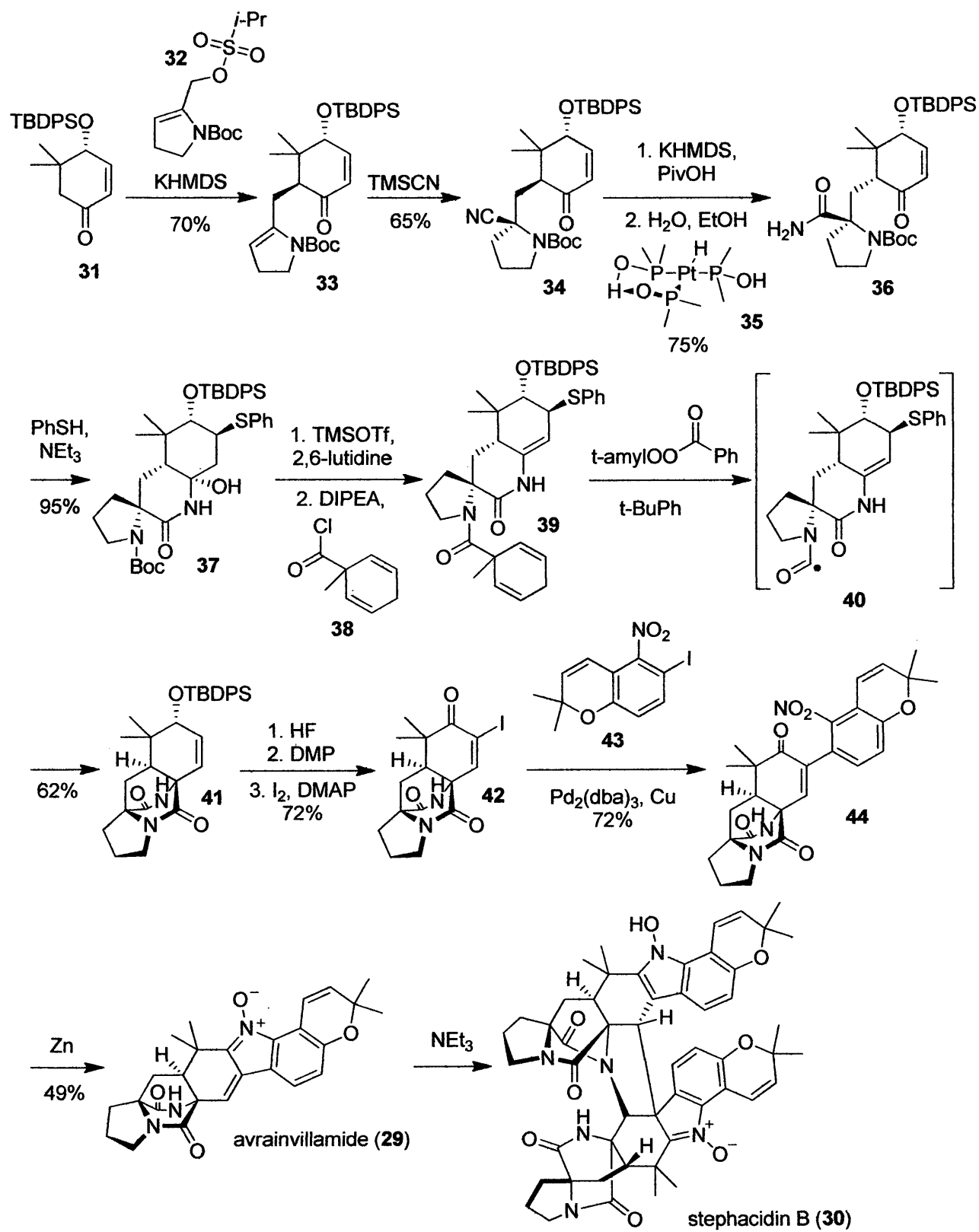
In their synthesis of avrainvillamide (**29**) and stephacidin B (**30**) the Myers group applied an aminoacyl radical cyclization to form the alkaloid core structure.<sup>40</sup> The application of this

new approach marked the use of the fourth unique method for forming [2.2.2]diazabicycles in total syntheses. In synthesizing monomeric avrainvillamide, they also showed the ease with which **29** dimerizes to stephacidin B (**30**) in mild conditions.

The Myers synthesis began with cyclohexanone **31**, a structure synthesized in two steps from commercially available materials (**Scheme 1.16**). Cyclohexanone **31** was deprotonated, facilitating the diastereoselective addition of novel electrophile **32** to the resulting enolate. Coupling product **33** was then converted to *N*-Boc amino nitrile **34** through Strecker-like addition of hydrogen cyanide with reasonable diastereoselectivity. The  $\alpha$ -carbon of ketone **34** was epimerized by deprotonation with KHMDS in order to install the necessary stereochemistry of the target alkaloids and platinum catalyst **35** was used to convert **34**'s nitrile moiety to a primary amide. Thiophenol and triethylamine treatment of resulting primary amide **36** led to conjugate thiophenol addition as well as cyclic hemiaminal formation. Spirocyclic **37** was then dehydrated and its *N*-Boc protecting group was cleaved. Subsequent acylation of the deprotected pyrrolidinyl amino group with radical precursor **38** produced amide **39**. At this point amide **39** featured both a radical initiator and terminator in such a way that it could undergo the envisioned radical cyclization. Heating of amide **39** with *tert*-amyl peroxybenzoate in *tert*-butyl benzene resulted in homolytic bond cleavage to form aminoacyl radical intermediate **40**. The radical formed in this homolytic cleavage quickly attacks the more substituted constituent of the enamide C-C double bond before it is finally trapped with the expulsion of the thiophenol radical acceptor. Radical cyclization gives [2.2.2]diazabicyclic avrainvillamide-precursor **41**, for which transformation to the natural product proved relatively simple. **41** was converted to  $\alpha$ -



Scheme 1.16: Synthesis of avrainvillamide

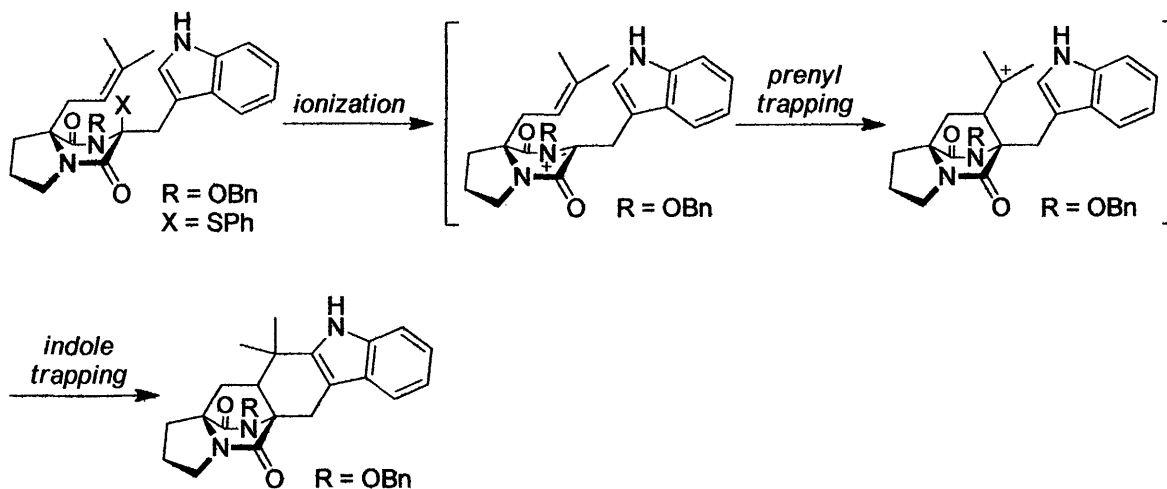


iodoenone **42** in three steps. Following these manipulations,  $\alpha$ -iodoenone **42** underwent Ullman-like coupling with aryl iodide **43** to give nitroarene product **44**. Reduction of **44** with activated zinc powder yielded the first synthetic target (-)-**29**, which could be easily converted to (+)-stephacidin B (**30**) in the presence of triethylamine.

#### Cation Olefin Cyclization:

The Simpkins lab employed a novel method for establishing [2.2.2]diazabicycles in a series of total syntheses including that of brevianamide B.<sup>41</sup> The Simpkins' cation cascade sequence for creating the alkaloids' bridged diketopiperazine cores was envisioned to initiate via cation formation of an appropriately substituted DKP (**Scheme 1.17**). Prenyl trapping of the cation would result in bicyclo[2.2.2]diazaoctane core formation and would allow a second cyclization with the indole ring. This method promised a succinct means for accessing two rings of the indole alkaloids' core structure in a single operation.

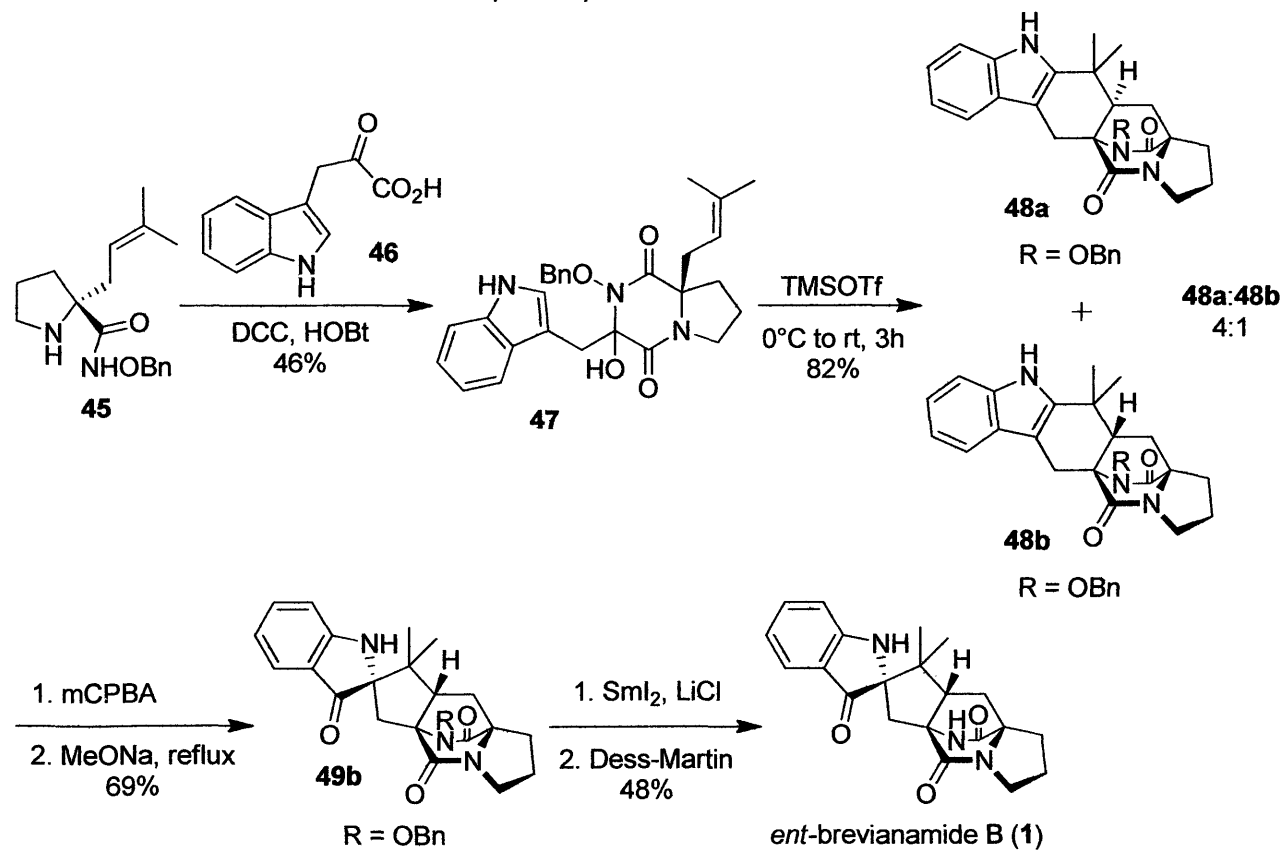
**Scheme 1.17:** Cation olefin cascade cyclization



The Simpkins synthesis of brevianamide B began with the coupling of prenylated proline **45** to indole pyruvic acid **46** (**Scheme 1.18**). Hydroxy-DKP **47** then underwent cation olefin

cyclization to establish both the bridged DKP core and adjacent gem-dimethyl 6-member ring of the diastereomeric products **48a** and **48b**. This reaction was observed with only moderate selectivity, giving a 4:1 ratio of epimers. It was hypothesized, but never investigated in this system, that more sterically bulky amide protecting groups would impart a stronger facial bias. The minor diastereomer, **48b**, which corresponded to the bicyclic core of brevianamide B was then isolated and underwent a two-step sequence of peracid oxidation and base-catalyzed rearrangement to spiro-indoxyl bridged DKP **49b**. Deprotection of **49b** via reductive cleavage with  $\text{SmI}_2/\text{LiCl}$  led to problematic over-reduction of the indoxyl moiety, which then required oxidation with Dess-Martin periodinane to establish the target, brevianamide B (**1**). While the selectivity in this synthesis was moderate and favored the undesired diastereomeric bicycle, it did demonstrate a strong step-wise efficiency.

**Scheme 1.18:** Simpkins' synthesis of brevianamide B



## REFERENCES

1. Williams, R. M.; Cox, R, J. *Acc. Chem. Res.* **2003**, *36*, 127–139.
2. Birch, A. J.; Wright, J. J. *J. Chem. Soc., Chem. Commun.* **1969**, 644–645.
3. Finefield, J. M.; Frisvad, J. C.; Sherman, D. H.; Williams, R. M. *J. Nat. Prod.* **2012**, *75*, 812–833.
4. (a) Birch, A. J.; Wright, J. J. *Tetrahedron* **1970**, *26*, 2329–2344. (b) Birch, A. J.; Russel, R. A. *Tetrahedron* **1972**, *28*, 2999–3008. (c) Robbers, J. E.; Straus, J. W.; Tuite, J. J. *Nat. Prod.* **1975**, *38*, 355–356. (d) Wilson, B. J.; Yang, D. T. C.; Harris, T. M. *Appl. Microbiol.* **1973**, *26*, 633–635.
5. (a) Paterson, R. R. M.; Simmonds, M. S. J.; Blaney, W. M. *J. Invertebr. Pathol.* **1987**, *50*, 124–133. (b) Paterson, R. R. M.; Simmonds, M. S. J.; Kimmelmeier, C.; Blaney, W. M. *Mycol. Res.* **1990**, *94*, 538–542.
6. Frisvad, J. C.; Filtenborg, O. *Mycologia* **1989**, *81*, 836–851.
7. Sanz-Cervera, J. F.; Glinka, T.; Williams, R. M. *Tetrahedron*, **1993**, *49*, 8471–8482.
8. (a) Polonsky, J.; Merrien, M.-A.; Prange, T.; Pascard, C.; Moreau, S. *J. Chem. Soc., Chem. Commun.* **1980**, 601–602. (b) Prange, T.; Billion, M.-A.; Vuilhorgen, M.; Pascard, C.; Polonsky, J. *Tetrahedron Lett.* **1981**, *22*, 1977–1980.)
9. (a) Kuo, M. S.; Wiley, V. H.; Cialdella, J. L.; Yurek, D. A.; Whaley, H. A.; Marshall, V. P. *J. Antibiot.* **1996**, *49*, 1006–1013. (b) Kuo, M. S.; Yurek, D. A.; Mizsak, S. A.; Cialdella, J. L.; Baczynskyj, L.; Marshall, V. P. *J. Am. Chem. Soc.* **1999**, *121*, 1763–1767.
10. Yamazaki, M.; Okuyama, E.; Kobayashi, M.; Inoue, H. *Tetrahedron Lett.* **1981**, *22*, 135–136
11. (a) Ondeyka, J. G.; Goegelman, R. T.; Schaeffer, J. M.; Kelemen, L.; Zitano, L. *J. Antibiot.* **1990**, *43*, 1375–1379. (b) Goegelman, R.; Ondeyka, J. U.S. Patent 4,873,247, **1987**. (c) Lopez-Gresa, M. P.; Gonzalez, M. C.; Ciavatta, L.; Ayala, I.; Moya, P.; Primo, J. *J. Agric. Food Chem.* **2006**, *54*, 2921–2925. (d) Blanchflower, S. E.; Banks, R. M.; Everett, J. R.; Reading, C. *J. Antibiot.* **1993**, *46*, 1355–1363. (e) Banks, R. M.; Blanchflower, S. E.; Everett, J. R.; Manger, B. R.; Reading, C. *J. Antibiot.* **1997**, *50*, 840–846. (f) Blanchflower, S. E.; Banks, R. M.; Everett, J. R.; Manger, B. R.; Reading, C. *J. Antibiot.* **1991**, *44*, 492–497. (g) Liesch, J. M.; Wichmann, C. F. *J. Antibiot.* **1990**, *43*, 1380–1386. (h) Nielsen, K. F.; Sumarah, M. W.; Frisvad, J. C.; Miller, J. D. *J. Agric. Food Chem.* **2006**, *54*, 3756–3763. (i) Ding, Y.; Gruschow, S.; Greshock, T. J.; Finefield, J. M.; Sherman, D. H.; Williams, R. M. *J. Nat. Prod.* **2008**, *71*, 1574–1578. (j) Antia, B. S.; Aree, T.; Kasetrathat, C.; Wiyakrutta, S.; Ekpa, O. P.; Ekpe, U. J.; Mahindol, C.; Ruchirawat, S.; Kittakop, P. *Phytochemistry* **2011**, *72*, 816–820.
12. Zinser, E. W.; Wolfe, M. L.; Alexander-Bowman, S. J.; Thomas, E. M.; Davis, J. P.; Groppi, V. E.; Lee, B. H.; Thomphson, D. P.; Geary, T. G. *J. Vet. Pharmacol. Ther.* **2002**, *25*, 241–250.
13. Shoop, W. L.; Haines, H. W.; Eary, C. H.; Michael, B. F. *Am. J. Vet. Res.* **1992**, *53*, 2032–2034.
14. (a) Byung, H. L.; Clothier, M. F.; Dutton, F. E.; Nelson, S. J.; Johnson, S. S.; Thompson, D. P.; Geary, T. G.; Whaley, H. D.; Haber, C. L.; Marshall, V. P.; Kornis, G. I.; McNally, P. L.; Ciadella, J. I.; Martin, D. G.; Bowman, J. W.; Baker, C. A.; Coscarelli, E. M.; Alexander-Bowman, S. J.; Davis, J. P.; Zinser, E. W.; Wiley, V.; Lipton, M. F.; Mauragis, M. A. *Curr. Top. Med. Chem.* **2002**, *2*, 779–793. (b) Lee, B. H.; Clothier, M. F.; Johnson, S. S. *Bioorg. Med. Chem. Lett.* **2001**, *11*, 553–554.

15. (a) Kaminsky, R.; Bapst, B.; Stein, P. A.; Strehlau, G. A.; Allan, B. A.; Hosking, B. C.; Rolfe, P. F.; Sager, H. *Parasitol. Res.* **2011**, *109*, 19–23. (b) Love, S. *AFBM J.* **2010**, *7*, 45–52. (c) Little, P. R.; Hodges, A.; Watson, T. G.; Seed, J. A.; Maeder, S. J. *N. Z. Vet. J.* **2010**, *58*, 121–129.
16. (a) Stocking, E. M.; Sanz-Cervera, J. F.; Unkefer, C. J.; Williams, R. M. *Tetrahedron* **2001**, *57*, 5303–5320. (b) Kellenberger, J. L. The Stereochemical Course of the C-methylation Steps in the Biosynthesis of Botromycin. Ph.D. Thesis, ETH Zurich, Zurich, Switzerland, 1997. (c) Stocking, E. M.; Sanz-Cervera, J. F.; Williams, R. M.; Unkefer, C. J. *J. Am. Chem. Soc.* **1996**, *118*, 7008–7009. (d) Stocking, E. M.; Martinez, R. A.; Silks, L. A.; Sanz-Cervera, J. F.; Williams, R. M. *J. Am. Chem. Soc.* **2001**, *123*, 3391–3392.
17. Stocking, E. M.; Sanz-Cervera, J. F.; Williams, R. M. *Angew. Chem., Int. Ed.* **2001**, *40*, 1296–1298.
18. Whyte, A. C.; Gloer, J. B.; Wicklow, D. T.; Dowd, P. F. *J. Nat. Prod.* **1996**, *59*, 1093–1095.
19. (a) Qian-Cutrone, J.; Krampitz, K. D.; Shu, Y.-Z.; Chang, L.-P.; Lowe, S. E. U.S. Patent 6,291,461, 2001. (b) Qian-Cutrone, J.; Huang, S.; Shu, Y.-Z.; Vydas, D.; Fairchild, C.; Menendez, A.; Krampitz, K.; Dalterio, R.; Klohr, S. E.; Gao, Q. *J. Am. Chem. Soc.* **2002**, *124*, 14556–14557.
20. Fenical, W.; Jensen, P. R.; Cheng, X. C. U.S. Patent 6,066,635, 2000.
21. Sugie, Y.; Hirai, H.; Inagaki, T.; Ishiguro, M.; Kim, Y.-J.; Kojima, Y.; Sakakibara, T.; Sakemi, S.; Sugiura, A.; Suzuki, Y.; Brennan, L.; Duignan, J.; Huang, L. H.; Sutcliffe, J.; Kojima, N. *J. Antibiot.* **2001**, *54*, 911–916.
22. Greshock, T. J.; Grubbs, A. W.; Jiao, P.; Wicklow, D. T.; Gloer, J. B.; Williams, R. M. *Angew. Chem., Int. Ed.* **2008**, *47*, 3573–3577.
23. Tsukamoto, S.; Kawabata, T.; Kato, H.; Greshock, T. J.; Hirota, H.; Ohta, T.; Williams, R. M. *Org. Lett.* **2009**, *11*, 1297–1300.
24. Ding, Y.; de Wet, J. R.; Cavalcoli, J.; Li, S.; Greshock, T. J.; Miller, K. A.; Finefield, J. M.; Sunderhaus, J. D.; McAfoos, T. J.; Tsukamoto, S.; Williams, R. M.; Sherman, D. H. *J. Am. Chem. Soc.* **2010**, *132*, 12733–12740.
25. Hayashi, H.; Nishimoto, Y.; Nozaki, H. *Tetrahedron Lett.* **1997**, *38*, 5655–5658.
26. (a) Pareniková, L.; Skouboe, P.; Frisvad, J. C.; Samson, R. A.; Rossen, L.; Hoor Suykerbuyk, M.; Visser, J. *Appl. Environ. Microbiol.* **2001**, *67*, 521–527. (b) Samson, R. A.; Houbraeken, J. A. M. P.; Kuijpers, A. F. A.; Frank, J. M.; Frisvad, J. C. *Stud. Mycol.* **2004**, *50*, 45–61. (c) Samson, R. A.; Noonim, P.; Meijer, M.; Houbraeken, J.; Frisvad, J. C.; Varga, J. *Stud. Mycol.* **2007**, *59*, 129–145. (d) Perrone, G.; Varga, J.; Susca, A.; Frisvad, J. C.; Stea, G.; Kocsubé, S.; Tóth, B.; Kozakiewicz, Z. *Int. J. Syst. Evol. Microbiol.* **2008**, *58*, 1032–1039. (e) Sørensen, A.; Lübeck, P. S.; Lübeck, M.; Nielsen, K. F.; Ahring, B. K.; Teller, P. J.; Frisvad, J. C. *Int. J. Syst. Evol. Microbiol.* **2011**, *61*, 3077–3083. (f) Varga, J.; Frisvad, J. C.; Kocsubé, S.; Brancovics, B.; Tóth, B.; Szigeti, G.; Samson, R. A. *Stud. Mycol.* **2011**, *69*, 1–17.
27. Hayashi, H.; Nishimoto, Y.; Akiyama, K.; Nozaki, H. *Biosci. Biotechnol. Biochem.* **2000**, *64*, 111–115.
28. Banks, R. M.; Blanchflower, S. E.; Everett, J. R.; Manger, B. R.; Reading, C. *J. Antibiot.* **1997**, *50*, 840–846.
29. Hirata, K.; Kataoka, S.; Furutani, S.; Hayashi, H.; Matsuda, K. *PLoS ONE* **2011**, *6*, e18354.
30. Gray, C. R.; Sanz-Cervera, J. F.; Silks, L. A.; Williams, R. M. *J. Am. Chem. Soc.* **2003**, *125*, 14692–14693.
31. Lin, Z.; Wen, J.; Zhu, T.; Fang, Y.; Gu, Q.; Zhu, W. *J. Antibiot.* **2008**, *61*, 81–85.
32. Williams, R. M.; Glinka, T.; Kwast, E. *J. Am. Chem. Soc.* **1988**, *110*, 5927–5929.

33. (a) Cushing, T. D.; Sanz-Cervera, J. F.; Williams, R. M. *J. Am. Chem. Soc.* **1993**, *115*, 9323–9324. (b) Artman, G. D.; Grubbs, A. W.; Williams, R. M. *J. Am. Chem. Soc.* **2007**, *129*, 6336–6342.
34. Porter, A. E. A.; Sammes, P. G. *Chem. Commun.* **1970**, 1103.
35. Williams, R. M.; Sanz-Cervera, J. F.; Sancenon, F.; Marco, J. A.; Halligan, K. J. *Am. Chem. Soc.* **1998**, *120*, 1090–1091.
36. Jin, S.; Wessig, P.; Liebscher, J. *J. Org. Chem.* **2001**, *66*, 3984–3997.
37. (a) Stocking, E. M.; Sanz-Cervera, J. F.; Williams, R. M. *J. Am. Chem. Soc.* **2000**, *122*, 1675–1683. (b) Sanz-Cervera, J. F.; Williams, R. M. *J. Am. Chem. Soc.* **2002**, *124*, 2556–2559. (c) Adams, L. A.; Valente, M. W. N.; Williams, R. M. *Tetrahedron* **2006**, *62*, 5195–5200. (d) Greshock, T. J.; Grubbs, A. W.; Tsukamoto, S.; Williams, R. M. *Angew. Chem., Int. Ed.* **2007**, *46*, 2262–2265. (e) Greshock, T. J.; Williams, R. M. *Org. Lett.* **2007**, *9*, 4255–4258. (f) Greshock, T. J.; Grubbs, A. W.; Williams, R. M. *Tetrahedron* **2007**, *63*, 6124–6130. (g) Miller, K. A.; Welch, T. R.; Greshock, T. J.; Ding, Y.; Sherman, D. H.; Williams, R. M. *J. Org. Chem.* **2008**, *73*, 3116–3119. (h) Miller, K. A.; Tsukamoto, S.; Williams, R. M. *Nature Chem.* **2009**, *1*, 63–68.
38. (a) Baran, P. S.; Richter, J. M. *J. Am. Chem. Soc.* **2004**, *126*, 7450–7451. (b) Baran, P. S.; Richter, J. M. *J. Am. Chem. Soc.* **2005**, *127*, 15394–15396.
39. Baran, P. S.; Hafensteiner, B. D.; Ambhaikar, N. B.; Guerrero, C. A.; Gallagher, J. D. *J. Am. Chem. Soc.* **2006**, *128*, 8678–8693.
40. Herzon, S. B.; Myers, A. G. *J. Am. Chem. Soc.* **2005**, *127*, 5342–5344.
41. Frebault, F. C.; Simpkins, N. S. *Tetrahedron* **2010**, *66*, 6585–6596.

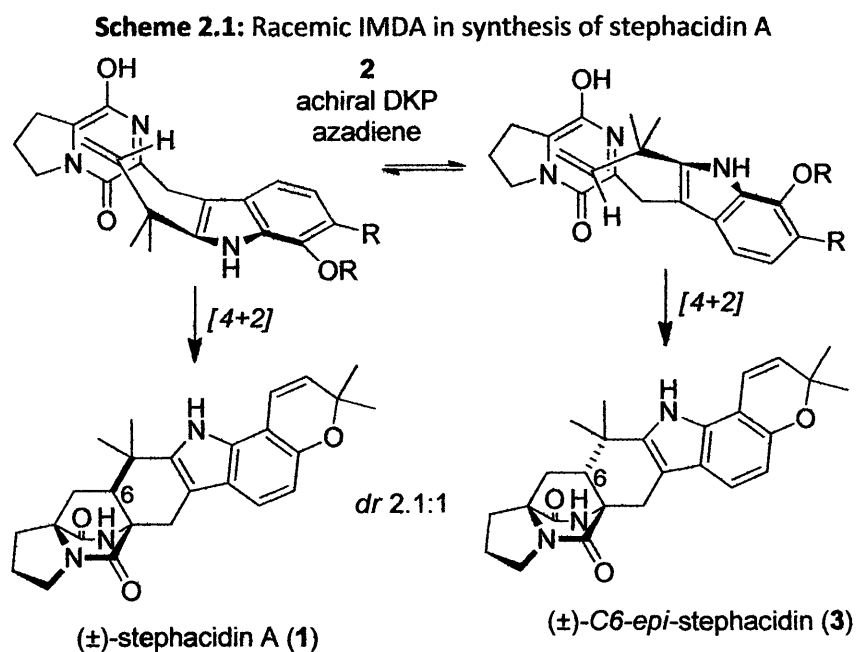
## CHAPTER II

### DEVELOPMENT OF DOMINO REACTION SEQUENCE

#### Introduction and Retrosynthesis:

The primary goal of our initial studies was to develop a general and stereoselective method for establishing bicyclo[2.2.2]diazaoctane cores that could be applied to multiple targets. We chose to pursue a diastereoselective intramolecular hetero-Diels–Alder (IMDA) because of the existing methods for forming the core structure, we were most impressed by Williams' IMDA.<sup>1</sup> The Williams' IMDA had proven elegant in its powerful, concerted bond formation and so our main challenge would be to devise a method with which to execute the reaction stereoselectively.

As demonstrated in both the previously discussed brevianamide synthesis<sup>1a</sup> and a subsequent synthesis of stephacidin A (**1**),<sup>2f</sup> the reactive diketopiperazine (DKP) azadienes involved in the key [4+2] cycloadditions of these syntheses and nearly all of Williams' other syntheses are achiral (**Scheme 2.1**). Achirality in the intramolecular reaction of prestephacidin **2** necessarily leads to a racemic mixture of cycloadducts ( $\pm$ )-stephacidin A (**1**) and its epimer, ( $\pm$ )-



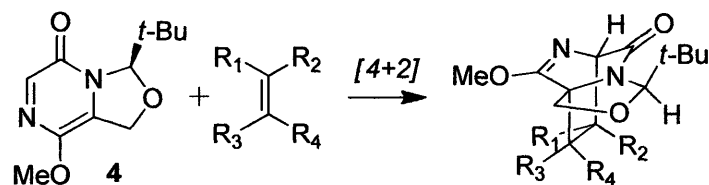
C6-*epi*-stephacidin (**3**). These epimeric cycloadducts were isolated in a 2.1:1 diastereomeric ratio representative of similar achiral IMDA reactions. While biosynthetic studies suggest that achiral precursors are consistent with natural alkaloid biosyntheses, a weak diastereomeric ratio is not representative of the single enantiomeric series with which these metabolites are produced in nature. From a synthetic perspective, this suggests that by adhering closely to the presumed biosynthetic pathway, we may limit the potential to make [2.2.2]diazabicycles stereoselectively.

In contrast to the numerous racemic syntheses which involved achiral intermediates, Williams and coworkers also conducted asymmetric biomimetic IMDA syntheses of VM55599<sup>1c</sup> and versicolamide B.<sup>1i</sup> Unlike the precursors of related alkaloids, the reactive azadiene intermediates of the VM55599 and versicolamide B syntheses possess chiral centers at their spiro-oxindole and proline ring moieties respectively. The IMDA of versicolamide B precursor gave a racemic mixture of cycloadducts with a diastereomeric ratio of 1.4:1, suggesting that chirality at the spiro-oxindole functionality exerts little effect on facial preference of the IMDA. In contrast, the IMDA of VM55599 did demonstrate more reasonable facial preference with a diastereomeric ratio of 7.3:2.0, supporting the idea that chiral proline substituents could restrict access of a single azadiene face:

Previous work in the Scheerer research group has also probed the effect of chiral azadienes on the diastereoselectivity of the IMDA. In this investigation researchers characterized the thermal, intermolecular Diels–Alder cycloadditions of a readily prepared chiral, nonracemic DKP diene (**4**) with a variety of dieneophiles (**Scheme 2.2**).<sup>2</sup> Azadiene **4** was synthesized in five steps from L-serine and featured a chiral *t*-butyl aminal. This sterically bulky aminal proved very effective in exerting diastereofacial control over the cycloaddition and could be removed following cyclization. In addition to the clear facial bias, cycloadditions of **4**



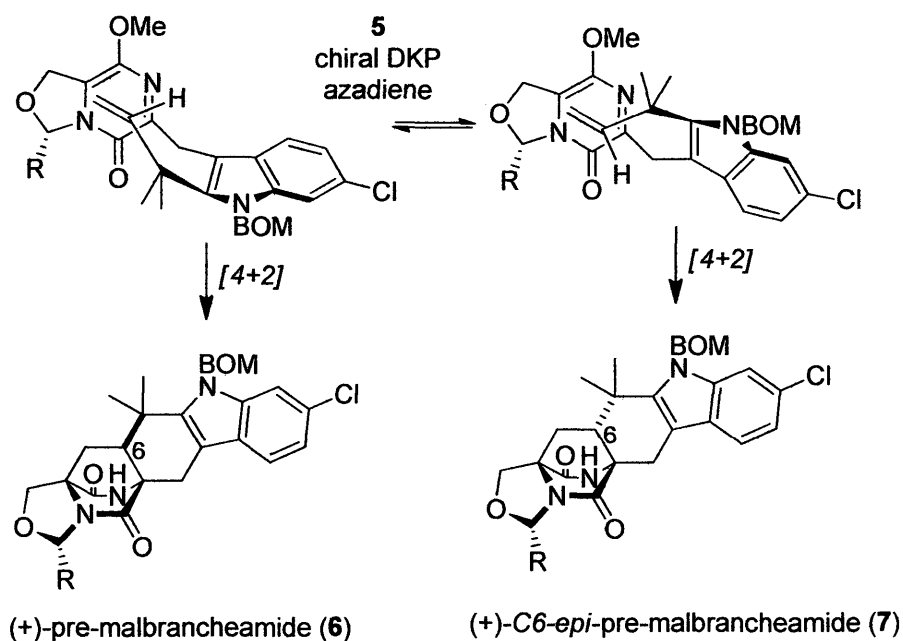
**Scheme 2.2:** Diels–Alder cycloaddition of a chiral, non-racemic DKP diene



revealed a modest preference for the *endo* transition state and predictable regiochemistry with electron-rich or electron-deficient dienophiles, despite the dissonant charge affinity pattern of the azadiene. This predictable direction and subsequent cleavage encouraged the use of similarly bulky, removable substrates in our synthetic endeavors.

Interested in adapting our methodology to a targeted synthesis, we envisioned the IMDA of a possible malbrancheamide precursor **5** (Scheme 2.3).<sup>3</sup> As in the previous intermolecular, chiral DKP Diels–Alder cycloadditions, we anticipated that the chiral aminal could effectively hinder one face of the diketopiperazine and drive dienophile to approach exclusively to the opposite ring face during [4+2] cycloaddition. Although we still expected the

**Scheme 2.3:** Directed IMDA of chiral DKP azadiene **5**



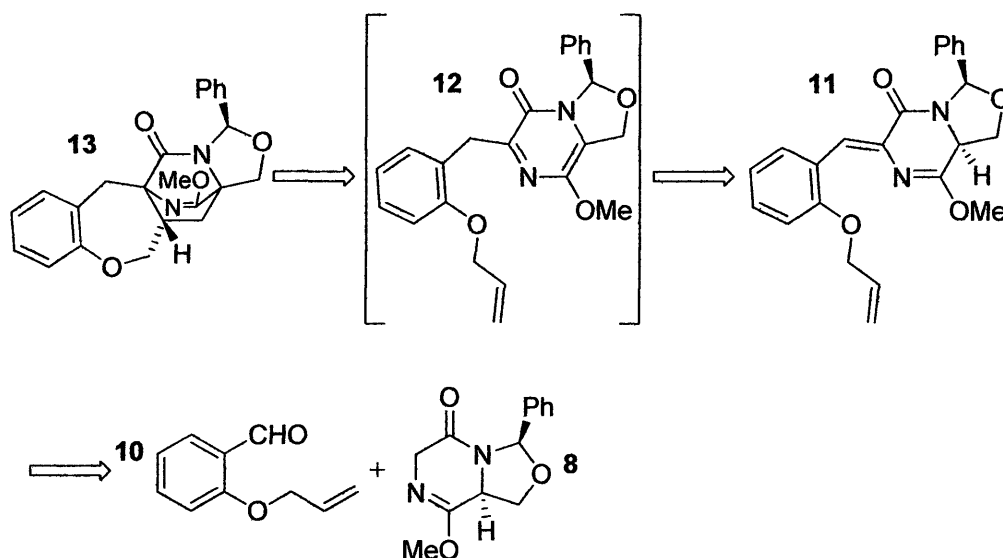
formation of a C6-epimer (**7**) of our desired cycloadduct (**6**), we were curious to see which, how many, and in what diastereomeric ratio this reaction's cycloadducts would form.

Our initial model study focused on exploring the possibility of directed intramolecular hetero-Diels–Alder reactions of DKP-derived azadienes not necessarily related to natural products. Based on the numerous examples of syntheses and biosynthesis of [2.2.2]diazabicycles, we recognized that the model IMDA precursor analogue of **5** must contain a chiral, non-racemic DKP azadiene coupled to an aromatic ring substituted with an alkene dieneophile. Fortunately, DKPs **8** and **9**, formed in the same process as DKP-derived azadiene **4**, and aromatic aldehyde **10** were easily prepared. While the *t*-butyl analog of **8** had been synthesized previously as a precursor to **4** and could have been used in this model reaction, difficulty in removal of the *t*-butyl group via acidic aminal hydrolysis in previous studies motivated the use of an alternative directing functionality. We anticipated the steric hindrance exerted by DKP diene-precursor **8**'s phenyl aminal to be comparable to that of the *t*-butyl aminal and valued the option to remove the phenyl directing group from our IMDA cycloadduct via reductive methods. We envisioned that the aldol condensation of **8** and **10** would afford coupling product **11** (Scheme 2.4). The isomerization of **11** under basic conditions would generate the azadiene intermediate **12**, which would rapidly undergo IMDA. We hoped this synthetic sequence would generate model target [2.2.2]diazabicycle **13** with good diastereofacial selectivity and yield. We chose to conduct our model study with DKP **8** due to the abundance of this material over its epimer **9**.

#### Methods and Results:

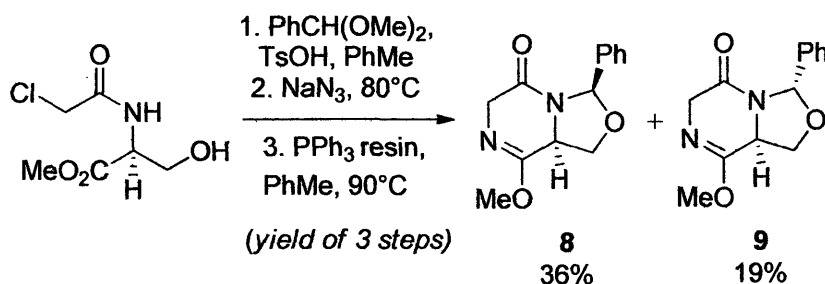
We began our model study with the preparation of DKP-lactim ether **8** in an analogous fashion to the synthesis of azadiene **4** (Scheme 2.5). *N*-chloroacetyl L-serine methyl ester was added to benzaldehyde dimethyl acetal with *p*-toluenesulfonic acid monohydrate to install the

**Scheme 2.4: Model Retrosynthesis for bicyclo[2.2.2]diazaoctane core**



phenyl aminal auxiliary. Subsequent treatment with sodium azide led to halide displacement and the resulting intermediate azide underwent Staudinger reduction with resin-bound phosphine to afford diastereomeric cyclized products **8** and **9** in 36% and 19% yield, respectively.

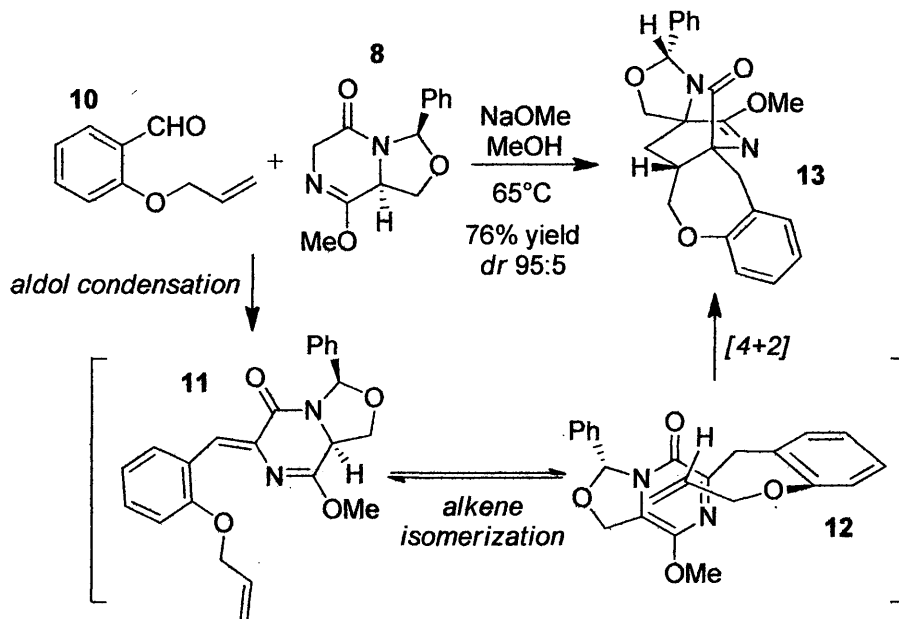
**Scheme 2.5: Synthesis of DKP azadiene-precursors **8** and **9****



The aromatic aldehyde **10** was easily prepared upon completion of **8**. It was quickly recognized that a so called “domino” sequence of the desired transformations was occurring under a single set of conditions (**Scheme 2.6**). When left to reflux under basic conditions for 24 hours, DKP **8** and salicylic aldehyde **10** yielded [2.2.2]diazabicyclo **13** in good yield (76%) and with excellent diastereoselectivity (*dr* 95:5). X-ray crystallographic analysis revealed the

absolute configuration of this molecule, confirming the facial preference of the azadiene to engage the ring face opposite the phenyl aminal in cycloaddition.

**Scheme 2.6:** Domino reaction sequence



To achieve this domino reaction sequence, basic conditions first affected enolization of the amide functionality of DKP **8**, allowing aldol addition and condensation to intermediate **11**. The same basic conditions then caused alkene isomerization to reactive azadiene **12** which underwent thermal IMDA cycloaddition. Satisfied with the yield, diastereomeric ratio, and ease of operation of our model synthesis, we shifted our synthetic efforts toward the natural product, malbrancheamide B.

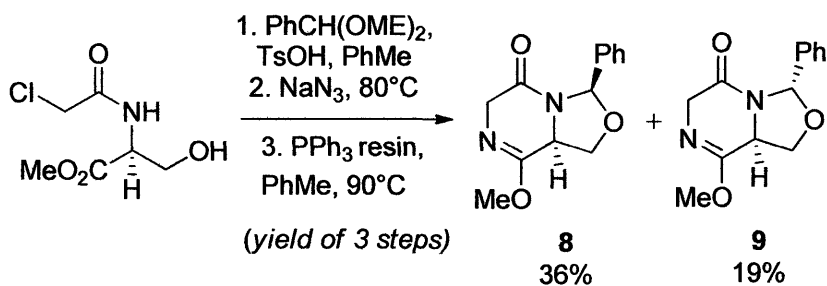
In summary, we successfully employed a novel diastereofacially selective IMDA cycloaddition in the synthesis of a model [2.2.2]diazaoctane bicycle. The originally envisioned two-step, three-transformation model sequence was found to instead occur in a single pot with good yield (76%) and excellent diastereoselectivity (95:5). We attribute the observed diastereofacial bias to a non-racemic, chiral phenyl aminal auxiliary on the DKP-derived azadiene

component of the [4+2]. Pleased with the reliable reactivity and selectivity, we next set out to adapt this reaction sequence to the total synthesis of malbrancheamide B.

#### Experimental Section:

**General Information.** All reactions were carried out under an atmosphere of nitrogen in flame-dried or oven-dried glassware with magnetic stirring unless otherwise indicated. Acetonitrile, THF, toluene, and Et<sub>2</sub>O were degassed with argon and purified by passage through a column of molecular sieves and a bed of activated alumina.<sup>4</sup> Dichloromethane was distilled from CaH<sub>2</sub> prior to use. All reagents were used as received unless otherwise noted. Flash column chromatography<sup>5</sup> was performed using SiliCycle siliaflash P60 silica gel (230-400 mesh). Analytical thin layer chromatography was performed on SiliCycle 60Å glass plates. Visualization was accomplished with UV light, anisaldehyde, ceric ammonium molybdate (CAM), potassium permanganate, or ninhydrin, followed by heating. Film (or KBr pellet) infrared spectra were recorded using FTIR spectrophotometer. Optical rotations were determined by digital polarimeter at 25 °C. <sup>1</sup>H NMR spectra were recorded on a 400 MHz spectrometer and are reported in ppm using solvent as an internal standard (CDCl<sub>3</sub> at 7.26 ppm) or tetramethylsilane (0.00 ppm). Proton-decoupled <sup>13</sup>C-NMR spectra were recorded at 100 MHz spectrometer and are reported in ppm using solvent as an internal standard (CDCl<sub>3</sub> at 77.00 ppm). All compounds were judged to be homogeneous (>95% purity) by <sup>1</sup>H and <sup>13</sup>C NMR spectroscopy unless otherwise noted as mixtures. Mass spectra data analysis was obtained through positive electrospray ionization (ICR-MS w/ NaCl). HPLC was performed using a binary gradient (acetonitrile, water with 0.1% TFA) and peak detection was accomplished with photodiode array.

## Experimental Procedures.

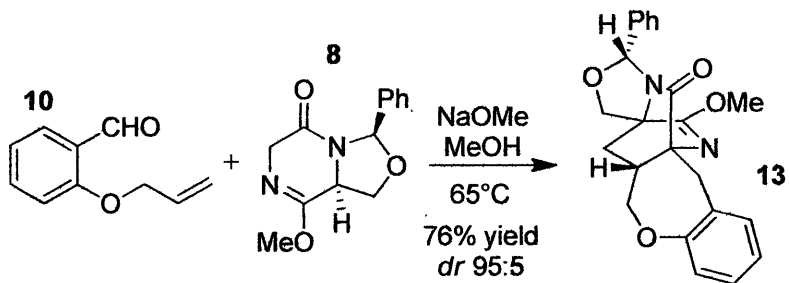


**Diketopiperazine lactim methyl ether 8, 9.** To *N*-chloroacetyl L-serine methyl ester<sup>6</sup> (4.5 g, 22.8 mmol) in toluene (220 mL) at rt was added benzaldehyde dimethyl acetal (2.9 ml, 27.4 mmol) and *p*-toluenesulfonic acid monohydrate (108 mg, 0.57 mmol). The solution was heated at reflux for 16 h with a Dean-Stark trap. After cooling to rt, the solution was diluted with saturated aqueous NaHCO<sub>3</sub> (2 x 50 ml). The organic layer was removed and the aqueous portion extracted with Et<sub>2</sub>O (75 ml). The combined organic layers were washed with brine (50 ml), dried with Na<sub>2</sub>SO<sub>4</sub>, and concentrated *in vacuo*. The viscous product was purified by flash column chromatography on silica gel (elution: 10% to 60% EtOAc in hexane) to afford a yellow oil (5.48 g, 19.23 mmol, dr *ca.* 2:1). This intermediate product was dissolved in butanone (110 ml), sodium azide (2.50 g, 38.5 mmol) was added, and the heterogenous mixture was heated to 80 °C for 15 h. After cooling to rt, the mixture was concentrated to a syrup and diluted with a half-saturated NaCl solution (100 ml) and extracted with Et<sub>2</sub>O (3 x 50 ml). The combined organic phases were dried with Na<sub>2</sub>SO<sub>4</sub>, and concentrated to afford a reddish-brown oil (5.34 g, 18.3 mmol). This intermediate azide product was used without purification in the subsequent Staudinger reduction. After dissolving the intermediate azide product (2.3 g, 7.9 mmol) in toluene (45 ml), resin-bound triphenyl phosphine (3.3 g, ~10.0 mmol) was added at rt. The mixture was stirred for 10 min at rt until gas evolution steadied and was heated to 90 °C for 20 h. Additional resin-bound triphenyl phosphine was added (0.5 g), until consumption of the starting material was apparent by TLC. After cooling to rt, the phosphine resin was removed by

vacuum filtration. The filtrate was concentrated and purified by flash column chromatography on silica (elution: 30% to 100% EtOAc in hexane) to afford product **8** (0.88 g, 36% yield, 3 steps) as a colorless solid and **9** (0.44 g, 19% yield, 3 steps) as a light yellow oil:

**8**: mp 133 °C; TLC (60% EtOAc in hexane), R<sub>f</sub>: 0.15 (KMnO<sub>4</sub>); [α]<sub>D</sub><sup>25</sup> = -63.2° (c = 2.02, CH<sub>2</sub>Cl<sub>2</sub>); IR (film) 3022, 2948, 2872, 1684, 1559, 1361, 1265, 1185, 1048, 934, 760 cm<sup>-1</sup>; <sup>1</sup>H NMR (400MHz, CDCl<sub>3</sub>) 7.37 (m, 3H), 7.29 (m, 2H), 6.25 (s, 1H, C<sub>8</sub>H), 4.49 (m, 1H), 4.31 (m, 1H), 4.28 (d, J = 19.5 Hz, 1H), 4.12 (dd, J = 19.9, 3.9 Hz, 1H), 4.04 (t, J = 9.0, 1H, C<sub>6</sub>H), 3.83 (s, 3H); <sup>13</sup>C NMR (100 MHz, CDCl<sub>3</sub>) δ 166.0, 161.3, 136.9, 129.6, 128.9, 126.8, 90.2, 65.7, 55.1, 54.1, 53.6; Exact mass calcd for C<sub>13</sub>H<sub>14</sub>N<sub>2</sub>O<sub>3</sub>Na [M+Na]<sup>+</sup>, 269.0897. Found 269.0892.

**9**: TLC (60% EtOAc in hexane), R<sub>f</sub>: 0.20 (KMnO<sub>4</sub>); [α]<sub>D</sub><sup>25</sup> = -107° (c = 2.30, CH<sub>2</sub>Cl<sub>2</sub>); IR (film) 2993, 2950, 2892, 1704, 1438, 1338, 1315, 1224, 1113, 1011, 850, 769 cm<sup>-1</sup>; <sup>1</sup>H NMR (400 MHz, CDCl<sub>3</sub>) 7.50 (m, 3H), 7.40 (m, 2H), 6.50 (s, 1H, C<sub>8</sub>H), 4.49 (dd, obs triplet, J = 6.6 Hz, 1H), 4.37 (m, 1H), 4.23 (s, 2H), 3.88 (t, J = 9.0 Hz, 1H, C<sub>6</sub>H), 3.76 (s, 3H); <sup>13</sup>C NMR (100 MHz, CDCl<sub>3</sub>) δ 165.4, 158.6, 138.2, 129.3, 128.8, 126.5, 88.9, 69.4, 54.3, 53.8, 52.2; Exact mass calcd for C<sub>13</sub>H<sub>14</sub>N<sub>2</sub>O<sub>3</sub>Na [M+Na]<sup>+</sup>, 269.0897. Found 269.0901.



**Cycloadduct 13.** To a solution of compound **8** (40.4 mg, 0.25 mmol) in methanol (2.00 mL) under nitrogen was added salicaldehyde **10** (57.1 mg, 0.23 mmol) and sodium methoxide (0.37 mL, 2M, 0.75 mmol). The reaction vessel was fitted with a reflux condenser and heated to 65 °C. After stirring at reflux for 21 h, the mixture was cooled to 23 °C, diluted with sat. aqueous NH<sub>4</sub>Cl and extracted with EtOAc (4 x 15 mL). The combined organic layers were washed with brine,

dried with sodium sulfate, and concentrated *in vacuo*. The unpurified product was a single diastereomer as judged by  $^1\text{H}$  NMR spectroscopy. Purification by flash chromatography on silica gel (elution: 20% to 60% EtOAc in hexane) afforded product **13** (68.7 mg, 76% yield) as a colorless amorphous solid: TLC (40% EtOAc in hexane), Rf: 0.40 (CAM);  $[\alpha]_{\text{D}}^{25} = -75.3^\circ$  ( $c = 0.77$ , MeOH); IR (film) 2948, 2865, 1691, 1633, 1490, 1289  $\text{cm}^{-1}$ ;  $^1\text{H}$  NMR (400 MHz,  $\text{CDCl}_3$ ) 7.38–7.35 (m, 3H), 7.32–7.28 (m, 3H), 7.18 (t,  $J = 7.4$  Hz, 1H), 7.05 (t,  $J = 7.4$  Hz, 1H), 6.97 (d,  $J = 7.8$  Hz, 1H), 6.26 (s, 1H), 4.51 (d,  $J = 9.3$  Hz), 4.06 (dd,  $J = 11.7, 3.9$  Hz, 1H), 4.02 (d,  $J = 9.4$  Hz, 1H), 3.63 (s, 3H), 3.49 (d,  $J = 14.9$  Hz, 1H), 3.42 (d,  $J = 14.9$  Hz, 1H), 3.28 (t,  $J = 11.7$  Hz, 1H), 2.77 (m, 1H), 2.35 (dd,  $J = 12.9, 9.8$  Hz, 1H), 1.00 (dd,  $J = 12.9, 4.7$  Hz, 1H);  $^{13}\text{C}$  NMR (100 MHz,  $\text{CDCl}_3$ )  $\delta$  170.5, 168.9, 159.0, 136.4, 132.5, 131.3, 129.2, 128.5, 127.5, 126.3, 123.9, 120.2, 88.4, 70.7, 67.2, 66.0, 62.5, 54.5, 43.0, 36.6, 32.9); HRMS (ES<sup>+</sup>): Exact mass calcd for  $\text{C}_{23}\text{H}_{22}\text{N}_2\text{O}_4\text{Na}$   $[\text{M}+\text{Na}]^+$ , 413.1472. Found 413.1470.



## REFERENCES

1. (a) Williams, R. M.; Sanz-Cervera, J. F.; Sancenon, F.; Marco, J. A.; Halligan, K. *J. Am. Chem. Soc.* **1998**, *120*, 1090–1091. (b) Stocking, E. M.; Sanz-Cervera, J. F.; Williams, R. M. *J. Am. Chem. Soc.* **2000**, *122*, 1675–1683. (c) Sanz-Cervera, J. F.; Williams, R. M. *J. Am. Chem. Soc.* **2002**, *124*, 2556–2559. (d) Adams, L. A.; Valente, M. W. N.; Williams, R. M. *Tetrahedron* **2006**, *62*, 5195–5200. (e) Greshock, T. J.; Grubbs, A. W.; Tsukamoto, S.; Williams, R. M. *Angew. Chem., Int. Ed.* **2007**, *46*, 2262–2265. (f) Greshock, T. J.; Williams, R. M. *Org. Lett.* **2007**, *9*, 4255–4258. (g) Greshock, T. J.; Grubbs, A. W.; Williams, R. M. *Tetrahedron* **2007**, *63*, 6124–6130. (h) Miller, K. A.; Welch, T. R.; Greshock, T. J.; Ding, Y.; Sherman, D. H.; Williams, R. M. *J. Org. Chem.* **2008**, *73*, 3116–3119. (i) Miller, K. A.; Tsukamoto, S.; Williams, R. M. *Nature Chem.* **2009**, *1*, 63–68.
2. Morris, E. N.; Nenninger, E. K.; Pike, R. D.; Scheerer, J. R. *Org. Lett.* **2011**, *13*, 4430–4433.
3. Margrey, K. A.; Chinn, A. J.; Laws, S. W.; Pike, R. D.; Scheerer, J. R. *Org. Lett.* **2012**, *14*, 2458–2461.
4. Pangborn, A. B.; Giardello, M. A.; Grubbs, R. H.; Rosen, R. K.; Timmers, F. J., *Organometal.* **1996**, *15*, 1518–1520.
5. Still, W. C.; Kahn, M.; Mitra, A. *J. Org. Chem.* **1978**, *43*, 2923–2925.
6. Bedürftig, S.; Wunsch, B. *Bioorg. Med. Chem.* **2004**, *12*, 3299–3311.

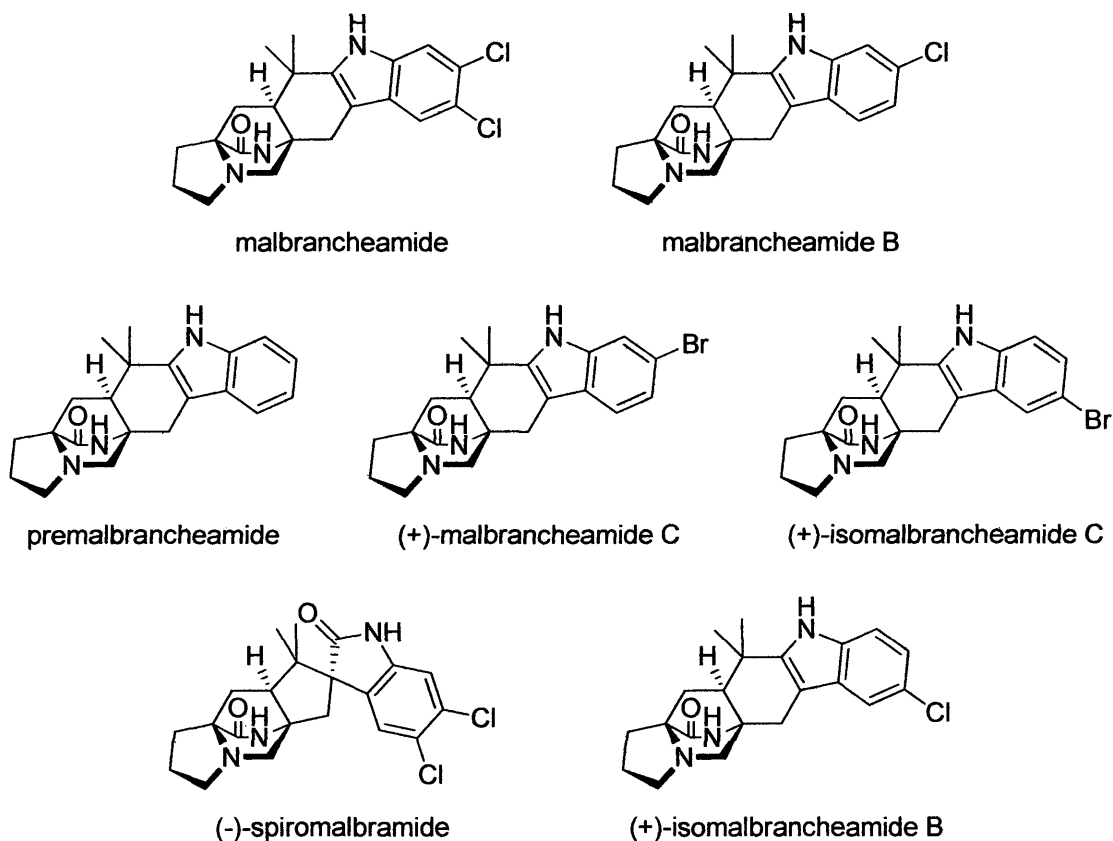
## CHAPTER III

### SYNTHESIS OF MALBRANCHEAMIDE B

#### Introduction to Malbrancheamides:

The malbrancheamide family of diazabicyclic alkaloids was one of the most recently discovered groups containing a [2.2.2]diazabicyclic core. Malbrancheamide and malbrancheamide B were originally isolated together from *Malbranchea aurantiaca* RRC1813 by the Mata group in 2006 (Figure 3.1).<sup>1</sup> These molecules represented the first members of the alkaloid family to be isolated from a species not belonging to the *genii* of *Aspergillus* or *Penicillium* and were the first to contain halogenation. Both of these molecules demonstrate moderate biological activity as concentration-dependent calmodulin inhibitors of CaM-

Figure 3.1: The malbrancheamide family of alkaloids



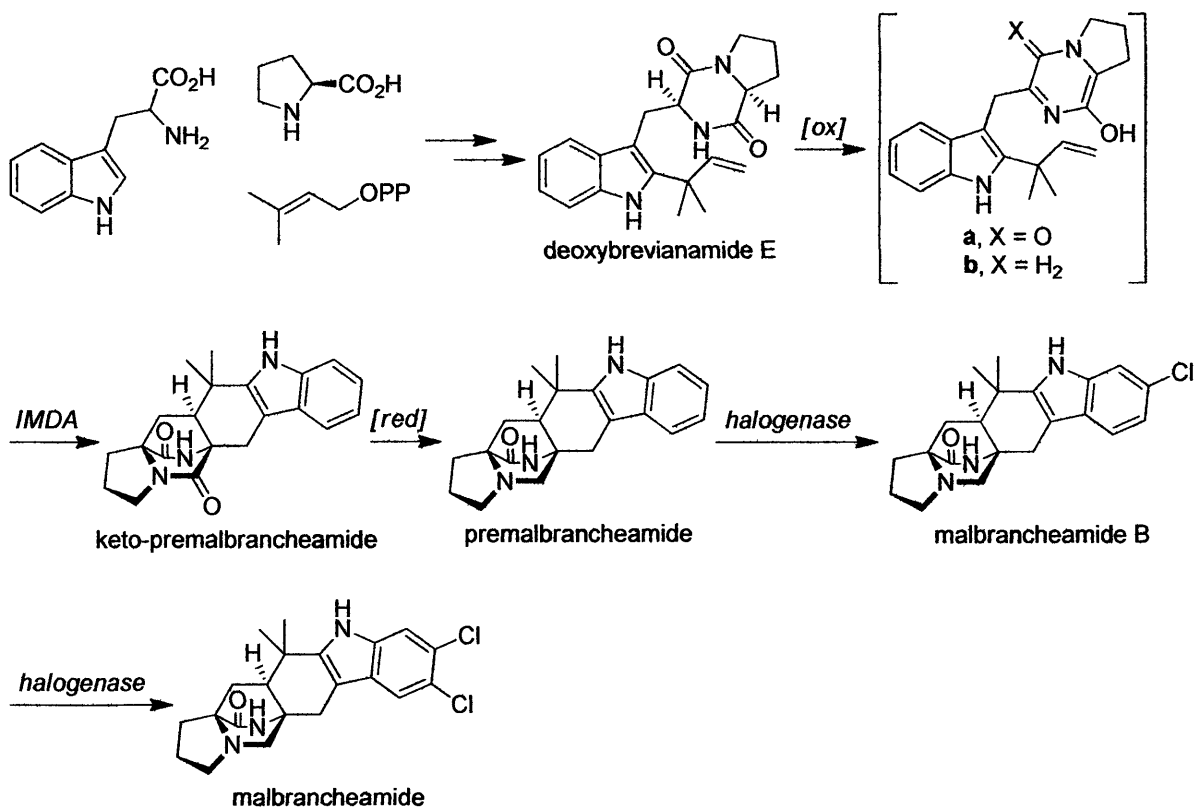
dependent phosphodiesterase (PDE1).<sup>2</sup> The Mata group later isolated an additional family member, the nonhalogenated premalbrancheamide, from the same fungal species of *Malbranchea*. In 2011, Crews and coworkers identified (–)-spiromalbramide and (+)-isomalbrancheamide B, two novel chlorinated [2.2.2]diazabicycles from *Malbranchea graminicola* UCSC 086937A.<sup>3</sup> The Crews group also isolated brominated analogues of malbrancheamide B and (+)-isomalbrancheamide B upon fungal growth on bromine-enriched medium. These brominated bicycles were named (+)-malbrancheamide C and (+)-isomalbrancheamide C.

Compared to related alkaloids like the stephacidins, the malbrancheamides demonstrate little structural diversity. Structural features include a monoketopiperazine core, bicycles of the more prevalent *syn*-conformation, and unsubstituted proline-derived rings. Only spiromalbramide contains a spirocyclic ring fusion pattern resembling the spiro-oxindoles of the marcfortines, paraherquamides, and notoamides. Structural variations between the malbrancheamides occur mainly in their indole halogenation patterns. All the malbrancheamides except premalbrancheamide exhibit either indole monohalogenation at the C-5 or C-6 position or indole dihalogenation at both C-5 and C-6. This halogen substitution feature is unique among the family of [2.2.2]diazabicycles and suggests a biogenic halogenation pathway exclusive to the *Malbranchea* genus.

Investigation into the biosyntheses of the malbrancheamides has largely focused on the timing of the indole halogenation and the sequence of diketopiperazine reduction to monoketopiperazine core and intramolecular hetero-Diels–Alder (IMDA).<sup>4</sup> The first proposal for a biosynthesis of the malbrancheamides began with the condensation of L-tryptophan, L-proline, and dimethylallyl pyrophosphate (DMAPP) to deoxybrevianamide E (**Scheme 3.1**). At

this point oxidation to either the reactive azadiene intermediate 5-hydroxypyrazin-2(1*H*)-one or its carbonyl-reduced analog would allow the IMDA to keto-premalbrancheamide or premalbrancheamide respectively. In the event that IMDA occurs prior to carbonyl reduction, keto-premalbrancheamide would then be reduced to premalbrancheamide, which would in turn lead to two successive halogenations, first to malbrancheamide B, then to malbrancheamide. Precursor incorporation studies with doubly  $^{13}\text{C}$ -labeled premalbrancheamide and keto-premalbrancheamide by the Williams group showed that of the two potential precursors, only  $^{13}\text{C}$ -labeled premalbrancheamide is incorporated into malbrancheamide B by *Malbranchea aurantiaca*. This observation suggests that carbonyl reduction precedes [4+2] cycloaddition which is followed by indole chlorination to malbrancheamide B and malbrancheamide.

**Scheme 3.1:** A proposed unified biosynthesis of the malbrancheamides

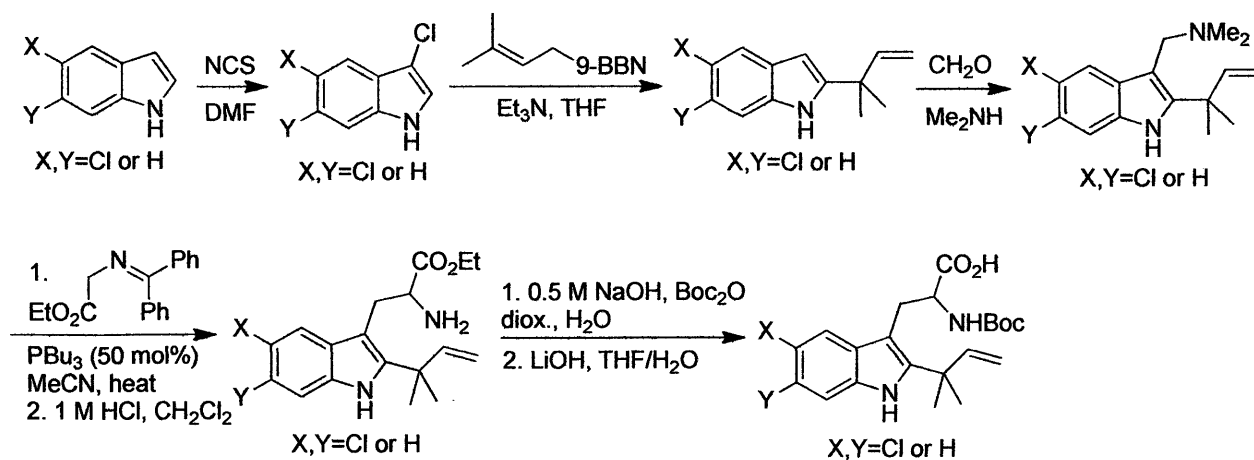


## Previous Syntheses:

In a 2008 report, Williams and coworkers reported the first synthesis of malbrancheamide.<sup>5</sup> At the time, the absolute structural configuration of malbrancheamide B was unknown and as a result the authors chose to target three molecules through parallel syntheses. The first target for synthesis was the known dihalogenated malbrancheamide. The authors recognized that malbrancheamide B was halogenated at either the indole 5- or 6-position. To establish the configuration of the monohalogenated malbrancheamide B, the authors chose to synthesize both 5- and 6-chloroindoles for comparison with natural samples.

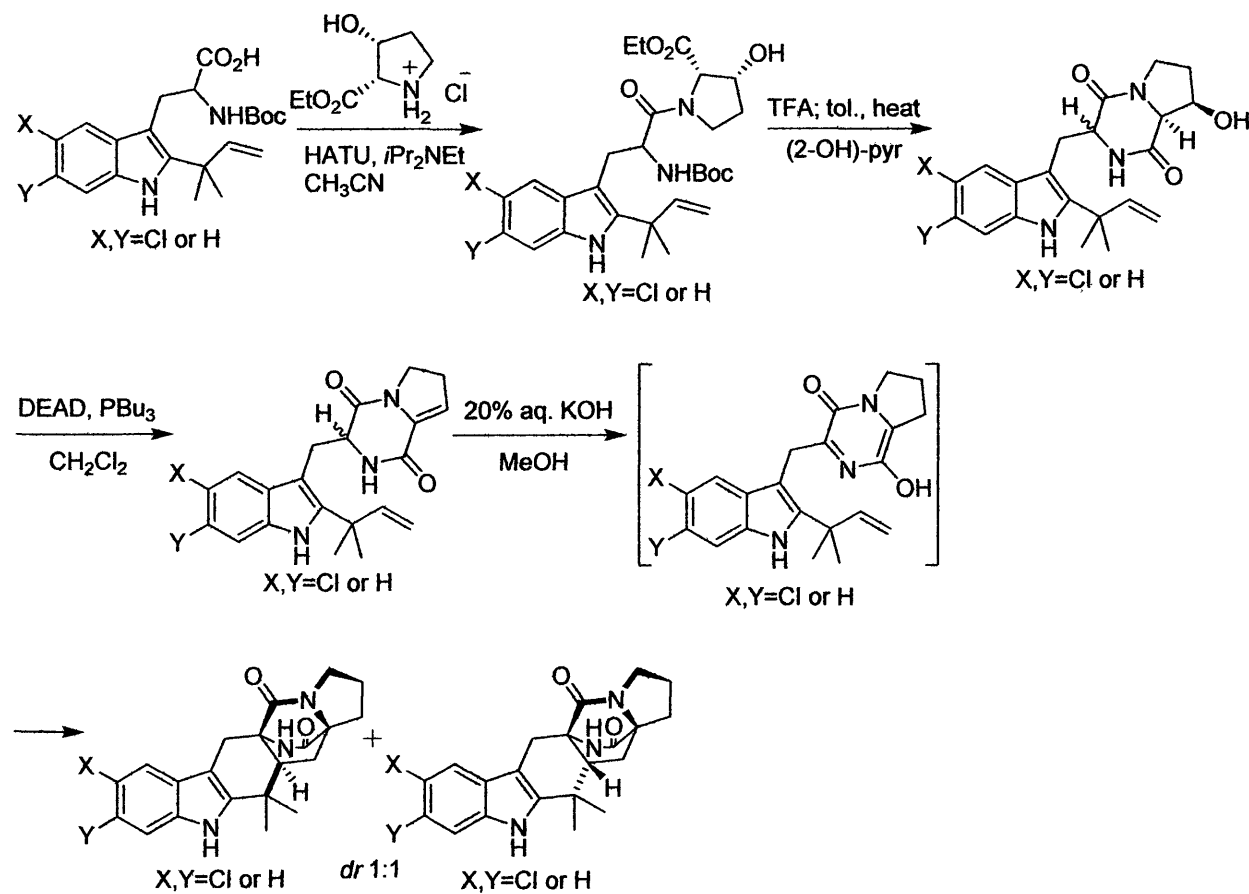
These syntheses began by building around indoles which could be easily halogenated in the 5- or 6-position. The three varieties of chlorinated indoles were functionalized with reverse prenyl groups at the 2-position of the ring system (**Scheme 3.2**). These reverse-prenylated indoles were then converted to gramines, which in turn were converted into their corresponding tryptophan derivatives and Boc-protected at the free amine moiety. Ester hydrolysis led to the formation of tryptophan-derived acids (**Scheme 3.3**). Having already incorporated tryptophan and isoprene-derived units into the hetero-Diels–Alder precursor, the sole remaining component required for a biomimetic approach was a proline-derived unit. To

**Scheme 3.2:** Synthetic scheme of reverse prenylated tryptophan derivatives



this end, the tryptophan-derived acids were coupled with *cis*-3-hydroxyproline ethyl ester and deprotected, allowing immediate cyclization to the corresponding diketopiperazines. Dehydration of these products yielded the appropriate IMDA substrates, cyclization of which gave a separable mixture of [2.2.2]diazaoctane bicycle diastereomers. Selective reduction of these [2.2.2]bicycles with Dibal-H produced the three desired targets at which point the absolute structure of malbrancheamide B was verified by comparison to synthetic material. These biomimetic syntheses are elegant and concise, but possess the obvious drawback of intercepting an achiral azadiene IMDA substrate resulting in a racemic mixture of [2.2.2]diazaoctane bicyclic adducts.

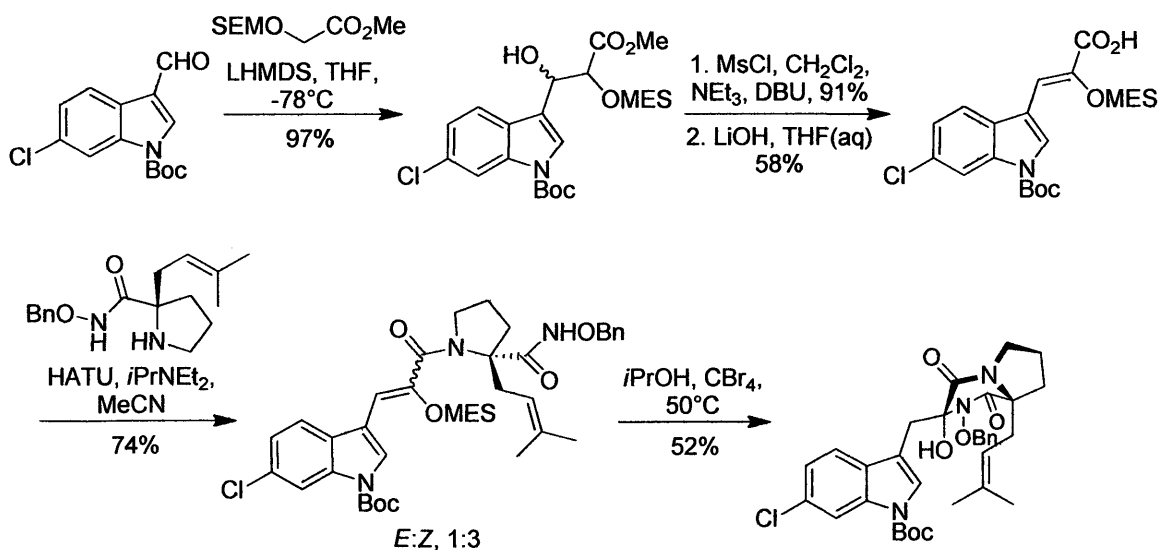
**Scheme 3.3:** Formation of [2.2.2]diazabicycle



Simpkins and coworkers reported the enantioselective total synthesis of *ent*-malbrancheamide B in 2009.<sup>6</sup> Model studies from the Simpkins lab revealed that the [2.2.2]-diazabicyclic core could be accessed with desired stereoselectivity by cation olefin cyclization from a suitable diketopiperazine precursor via  $\alpha$ -amido *N*-acyliminium species intermediate.<sup>7</sup> To apply this novel cyclization methodology, Simpkins elected to initially target (-)-*ent*-malbrancheamide B, the unnatural stereoisomer, primarily because of the low cost of the corresponding L-proline.

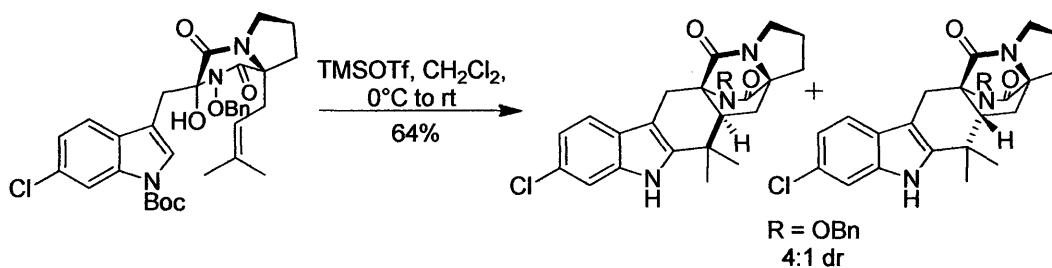
The Simpkins synthesis, much like the Williams synthesis, began from an indole nucleus; the illustrated Boc-protected 6-chlorocarboxaldehyde was easily prepared from commercially available materials (**Scheme 3.4**).<sup>6</sup> Aldol addition of this formylated indole nucleus to a methyl ester led to an alcoholic aldol adduct. Dehydration and saponification of this aldol product led to the corresponding carboxylic acid which was then bonded to a prenylated proline derivative via standard amino acid coupling. At this point, all three essential components of the natural product, tryptophan, proline, and an isoprene unit, have been incorporated. Deprotection of

**Scheme 3.4:** Synthetic preparation of [2.2.2]diazaoctane-precursor



the remaining protected enol with  $\text{CBr}_4$  in warm isopropyl alcohol delivered the key diketopiperazine cyclization precursor necessary for the planned cation olefin cyclization. Upon treatment with trimethylsilyl triflate, both the indole *N*-Boc protecting group was cleaved and the [2.2.2]diazaoctane bicycle was formed in 4:1 mixture of epimers favoring the desired product in 64% yield (**Scheme 3.5**). The product of reductive cleavage of the remaining BOM protecting group was the same diketopiperazine bicycle made in Williams' malbrancheamide synthesis. Following Williams' precedent, Simpkins employed a Dibal-H reduction to form (-)-*ent*-malbrancheamide B.

**Scheme 3.5:** Cation olefin cyclization



Previous research into [2.2.2]diazaoctane bicycles proved very useful in our pursuit of malbrancheamide B. Having five strategies for installing the core structural motif at our disposal and comparing the strengths and weaknesses of two excellent existing syntheses of our target provided great insight. Inspired by the elegance of the biomimetic approach to establishing the core structure, we chose to pursue a modified version of Williams' biomimetic approach in which the incorporation of a chiral, nonracemic DKP-derived azadiene into the key IMDA would impart diastereofacial bias.

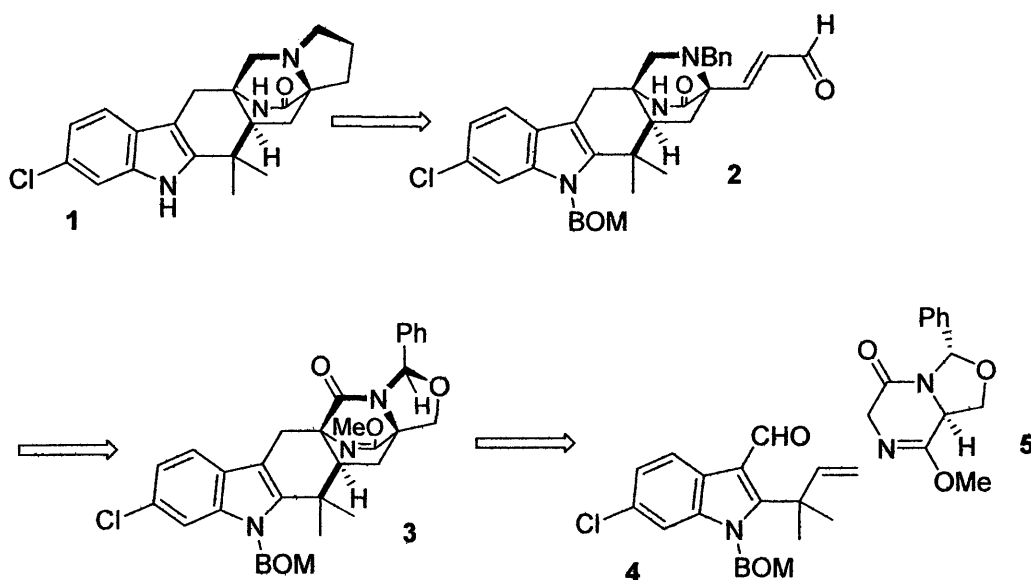
#### Enantioselective Retrosynthesis:

We constructed the retrosynthesis of our enantioselective route to (+)-malbrancheamide B upon the effective demonstration of the directed domino reaction sequence in a model system (**Scheme 3.6**). We anticipated that malbrancheamide B (**1**) could be



accessed directly through palladium-catalyzed reduction of  $\alpha,\beta$ -unsaturated aldehyde (**2**), an intermediate which could be synthesized from domino reaction product **3** in a series of functional group transformations aimed at removing the aminal directing group essential to the domino sequence, but not present in the natural product. The domino sequence itself would be the crux of our synthetic plan, establishing the core structure as previously discussed through the one-pot aldol condensation, alkene isomerization, and intramolecular hetero-Diels–Alder cyclization. Finally, we knew that the domino reaction substrates **4** and **5** could also be easily prepared as the necessary preparatory precedent had almost entirely been established already.

**Scheme 3.6:** Retrosynthetic plan for enantioselective synthesis

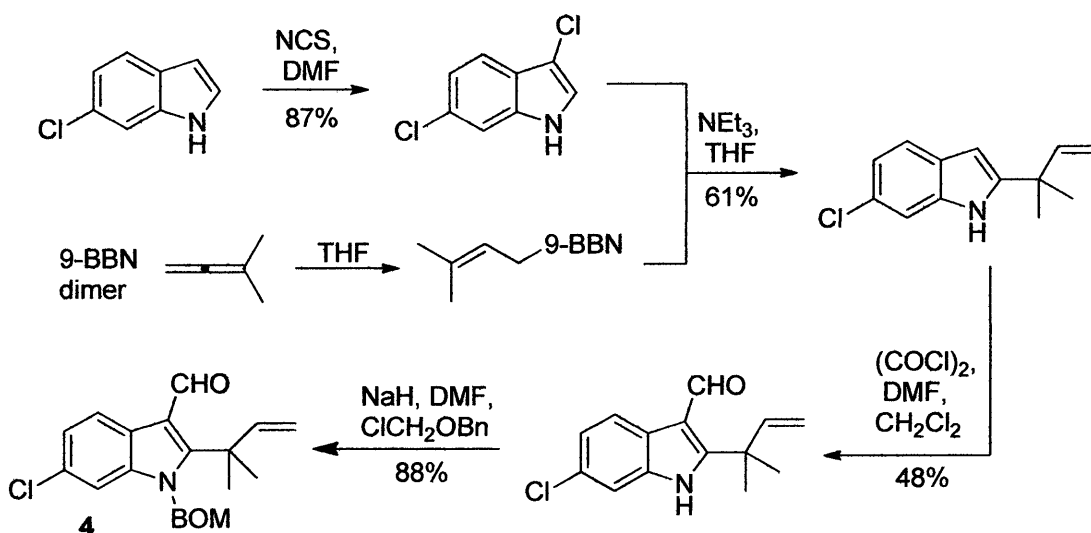


#### Methods, Results, and Total Enantioselective Synthesis:

In the forward sense, the first phase of the enantioselective synthesis was the preparation of appropriate indole carboxaldehyde and DKP azadiene-precursor components necessary for a domino reaction sequence. This necessitated a 4-step synthesis of the modified chloroindole **4**. These transformations mainly followed the procedures developed by Williams in his biomimetic malbrancheamide synthesis and converted the commercially-available 6-

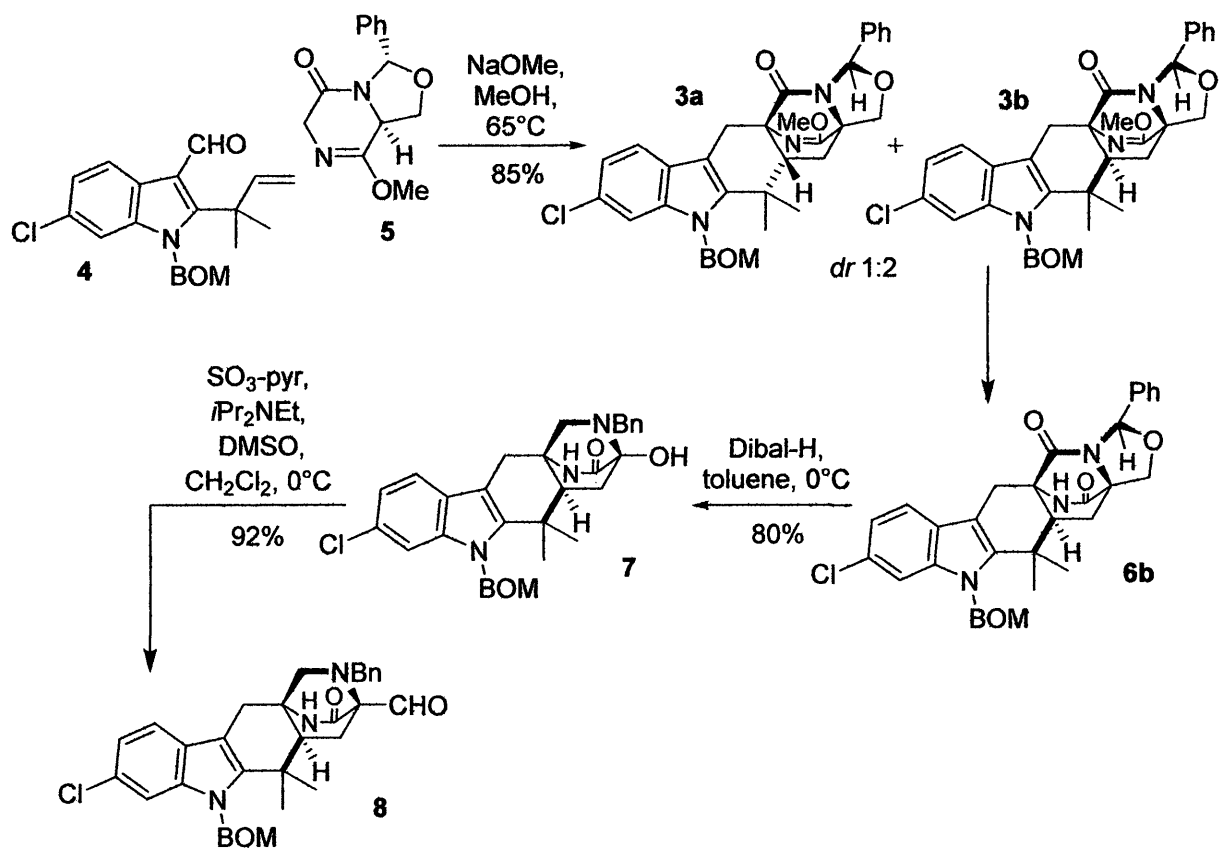
chloroindole to our desired product (**Scheme 3.7**).<sup>5</sup> No additional synthetic effort was necessary in the preparation of an appropriate diketopiperazine since chiral, nonracemic phenyl-substituted DKP-precursor **5** was available in appreciable quantities following our model study (**Chapter II**).

**Scheme 3.7:** Preparation of BOM-protected chloroindole **4**



The union of BOM-protected indole **4** and phenyl-functionalized DKP **5** was achieved on exposure to basic conditions at reflux overnight (**Scheme 3.8**). The resulting domino reaction sequence yielded an inseparable mixture of two diazabicyclic cycloadducts, **3a** and **3b**, in a 1:2 ratio as estimated by <sup>1</sup>H NMR spectroscopy with a combined yield of 85%. Not only did this result confirm that the conditions employed were sufficient in affecting enolization in the DKP substrate and isomerization in the aldol condensate, but it also suggested that the chiral phenyl aminal on the DKP azadiene-precursor was effective in controlling facial accessibility in the intermediate azadiene. At this time it was unclear whether the phenyl aminal exerted any control over the facial accessibility of the alkene, but the 2:1 ratio of diastereomers observed from this reaction was consistent with those of multiple racemic syntheses of the Williams

**Scheme 3.8:** Domino cyclization in the enantioselective synthesis of malbrancheamide B



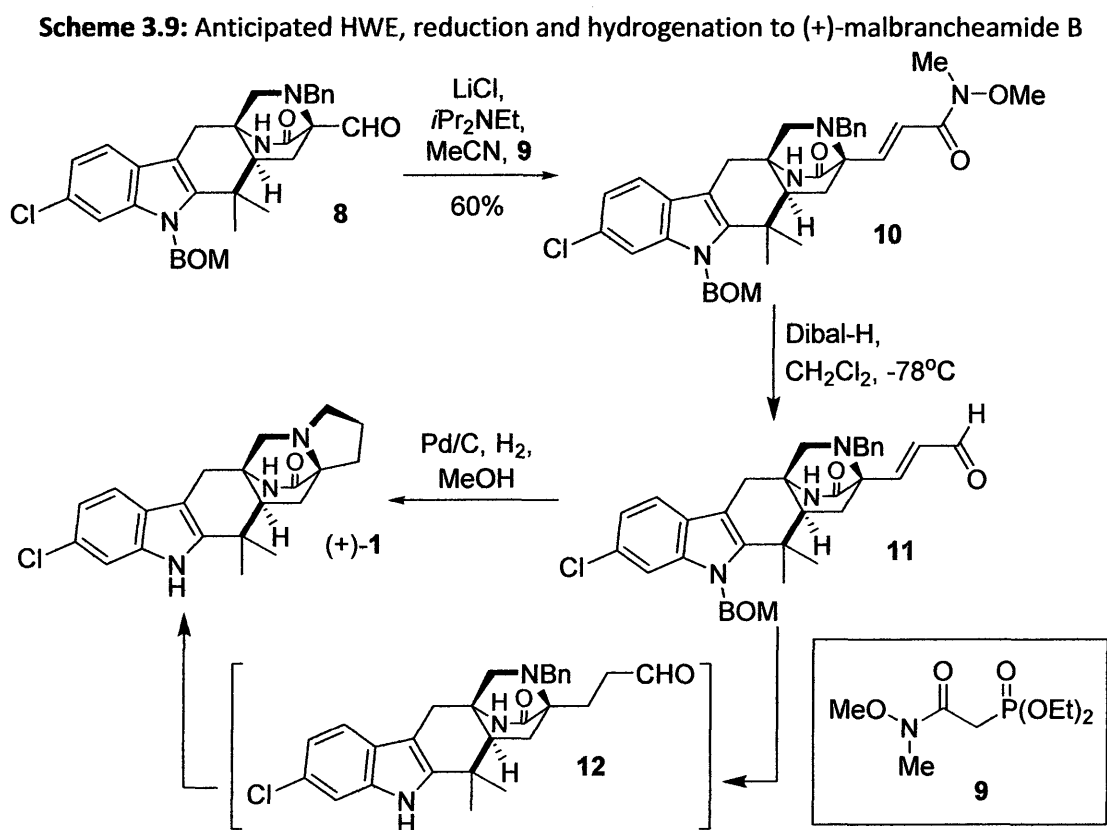
group.<sup>2</sup> The question of the aminal's role in facial preference would eventually be further illuminated upon the completion of an analogous racemic domino reaction sequence. In spite of the successful coupling of BOM-protected indole **4** and DKP **5** into a [2.2.2]diazabicyclo, the challenge of separating these cycloadducts proved overly difficult. Failure to isolate the major diastereomeric product of the cycloaddition following multiple attempts at separation by chromatography on silica gel forced the progression of the synthesis with the existing 1:2 mixture of diastereomers. Conversion of the diastereomeric mixture to a separable mixture of diketopiperazines required one additional step. Initially, reaction with TMSI was employed as the preferred method of cleaving the cycloadducts' lactim methyl ether. Although this method proved successful in derivatizing the lactim methyl ether with acceptable yields at first pass, the

success of this method was inconsistent. As an alternative, exposing the diastereomers to mild acidic conditions with equimolar quantities of TsOH·H<sub>2</sub>O in CH<sub>2</sub>Cl<sub>2</sub> followed by basification allowed for an identical conversion. These acidic conditions affected the desired imine hydrolysis more consistently than TMSI. It was also observed through repetitions at room temperature and 0°C that imine hydrolysis at higher temperature led to hydrolysis of the indolic BOM group. This additional hydrolytic cleavage was avoided in the total synthesis as eventual experience with both protected and unprotected materials revealed that preservation of the BOM group led to improved solubility of later malbrancheamide precursors in most organic solvents. The mixture of BOM-protected diketopiperazines **6a** and **6b** could be easily separated by flash column chromatography on silica gel, but was achieved more efficiently by selective precipitation of **6b** through recrystallization of the mixture (60% yield).

The focus of our synthetic effort after establishing the diketopiperazine bicycle of **6b** was to establish the monoketopiperazine characteristic of the targeted natural product through selective reduction of the tertiary amide. Treatment with Dibal-H realized the desired transformation and also revealed the benzyl amine and primary alcohol functionalities of **7** as a result of the decomposition of the aminal auxiliary. At this point, we anticipated that four remaining transformations would be required to complete the synthesis of malbrancheamide B. As we envisioned utilizing the Horner-Wadsworth-Emmons olefination to affect a two carbon extension of the chain opened upon Dibal-H treatment, it was necessary to oxidize (SO<sub>3</sub>·pyr, DMSO, Hünig's base) alcohol **7** to the corresponding aldehyde **8**.

The newly formed aldehyde **8** was an appropriate substrate for Horner-Wadsworth-Emmons olefination under soft enolization conditions<sup>8</sup> and was coupled with phosphoramidate **9** to form Weinreb amide **10** (Scheme 3.9). This reaction proved sufficient in extending the C1

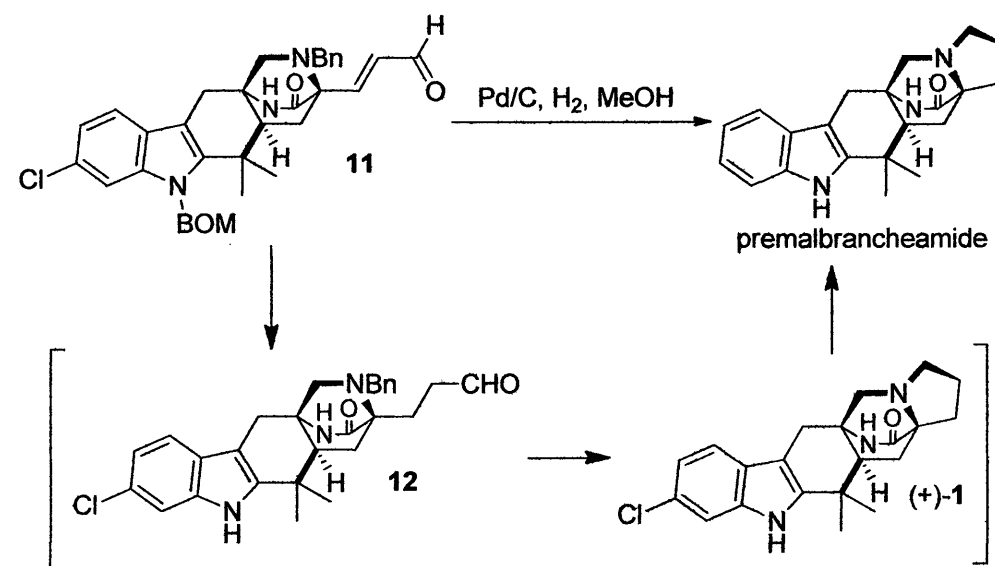
chain by the two carbons required to form the target's pyrrolidine ring. With the requisite chain length installed, we next performed the reduction of amide **10** to corresponding  $\alpha,\beta$ -unsaturated aldehyde **11** in order to set the stage for the planned cyclization strategy via palladium-catalyzed reduction cascade.



We hoped that upon exposure to  $\text{H}_2$  and  $\text{Pd/C}$ , aldehyde **11** would undergo several transformations, ultimately resulting in the formation of malbrancheamide B. We anticipated that BOM cleavage and hydrogenation of the  $\alpha,\beta$ -unsaturation would occur rapidly to form intermediate **12**. Saturated aldehyde **12** would itself undergo benzyl cleavage followed quickly by cyclization to form (+)-malbrancheamide B (**1**). Initially, a small amount of the unsaturated aldehyde **11** was used to probe the palladium reduction cascade. The crude  $^1\text{H}$  NMR spectral data collected on this reaction product suggested that while the cascade was executing the desired transformations, it was also effecting the removal of the C6-indole chlorination (**Scheme**

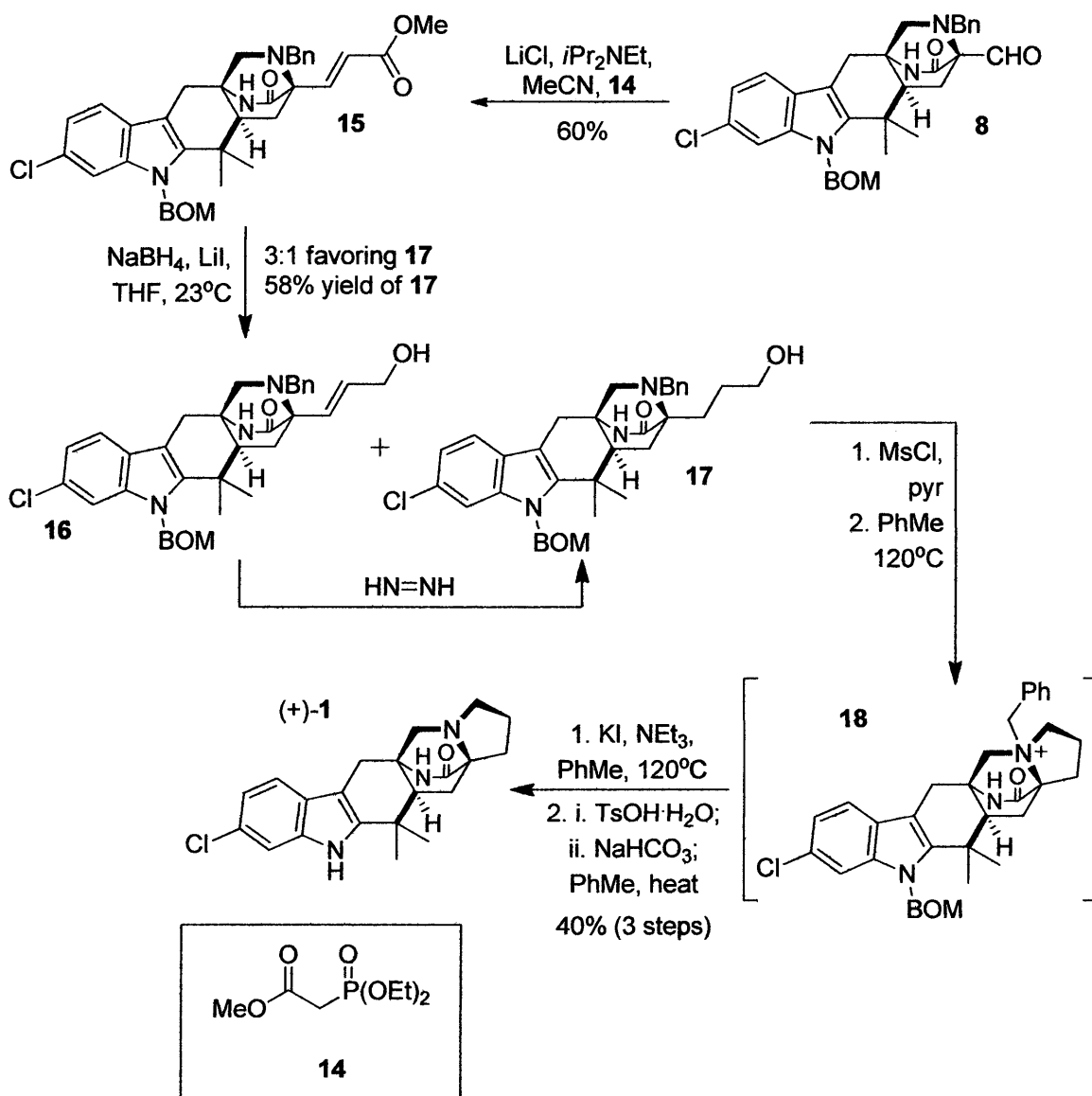
**3.10).** Manipulations of the reaction conditions yielded no success in preserving the halogen. While ineffective in completing the synthesis, these reactions did yield high resolution mass spectrometry hits which supported our identification of the product as a des-chloro analog of the targeted natural product. Since loss of halogen proved unavoidable with catalytic hydrogenation, we returned to aldehyde **8** and pursued an alternative reductive strategy for completing the synthesis.

**Scheme 3.10:** Observed hydrogenation of **11** to premalbrancheamide



Our experience working through the first attempted endgame informed us that aldehyde **8** was suitable for extension through Horner-Wadsworth-Emmons. Since the main advantage of Weinreb amide was the ease with which it could be converted to the  $\alpha,\beta$ -unsaturated aldehyde, we chose to replace phosphonamide **9** for phosphonacetate **14**. This revised Horner-Wadsworth-Emmons led to the formation of  $\alpha,\beta$ -unsaturated methyl ester **15** (Scheme 3.11). We anticipated that reduction of the  $\alpha,\beta$ -unsaturation in **15** would allow subsequent cyclization to a pyrrolidine ring. Sodium borohydride was selected to perform this 1,4-hydride reduction and proved competent, but at first attempt led to a 2:1 formation of

**Scheme 3.11:** Amended route for the completion of (+)-malbrancheamide B

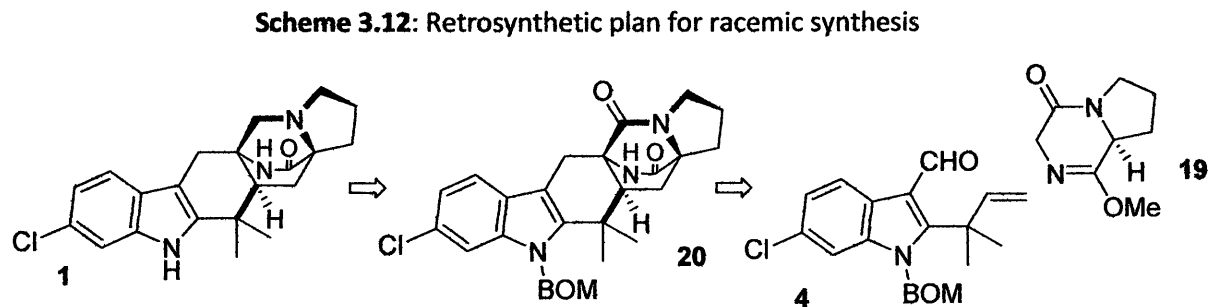


allylic alcohol **16** over the desired saturated alcohol **17**. Unsatisfied with this ratio of products, further effort was devoted to finding preferable conditions and eventually the formation of allylic alcohol was minimized. Under these optimized conditions, saturated alcohol **17** could be isolated in 58% yield. Our supply of the desired alcohol was supplemented by a diimide reduction of the allylic alcohol converted undesired byproduct **16** to **17**.

With an extended C1 chain in hand, our synthetic focus transitioned to achieving the cyclization forming the pyrrolidine ring. To complete this transformation, the primary saturated alcohol **17** was first activated through mesylation. We had anticipated that the displacement of this mesylate by the non-bonding pair of electrons of the benzyl amine in an intramolecular *N*-alkylation would happen at room temperature, but it turned out that the ambient temperature was insufficient to drive this change. The mesylate was heated to 120 °C in a sealed tube with toluene in order to achieve *N*-alkylation and form the desired quaternary salt **18**. After formation of **18** was completed, KI and triethylamine were added to mixture, the tube was returned to heat (120°C) for 20 hours, completing the dealkylation of the benzyl functionality. Finally, (+)-malbrancheamide B (**1**) was formed through the deprotection of the indole using the mild TsOH-H<sub>2</sub>O developed previously.

#### Racemic Retrosynthesis:

Having completed the total enantioselective synthesis of (+)-malbrancheamide B, we were pleased with the facial selectivity of our IMDA cyclization and wanted to demonstrate the brevity with which a racemic synthesis using the domino reaction sequence could be achieved. The retrosynthesis built around this racemic domino reaction sequence involved only four transformations (**Scheme 3.12**). In the forward sense we planned to couple the indole





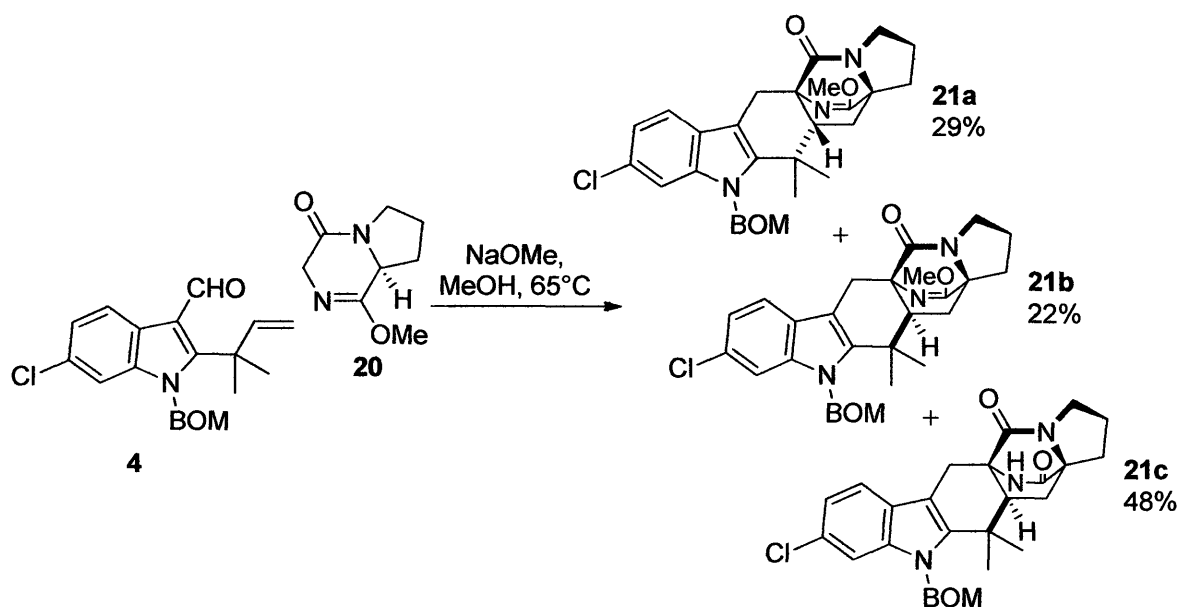
dieneophile **4** to an achiral diketopiperazine diene-precursor **19**, then convert the resulting cycloadduct to the diketopiperazine analog **19**, which could be deprotected and, following removal of the BOM-group, directly reduced using published precedent to the racemic natural product.

#### Methods, Results, and Formal Racemic Synthesis:

The BOM-protected chloroindole **4** was prepared in previous synthetic work leaving only the synthesis of the achiral diketopiperazine demanded by the planned domino sequence. This simplified alternative to the diene-precursor used in our enantioselective synthesis was prepared in only 3 steps from proline methyl ester with a single chromatographic separation in 80% yield. This DKP substrate **20** was then coupled to chloroindole **4** under the same basic conditions employed in all our other domino reactions.

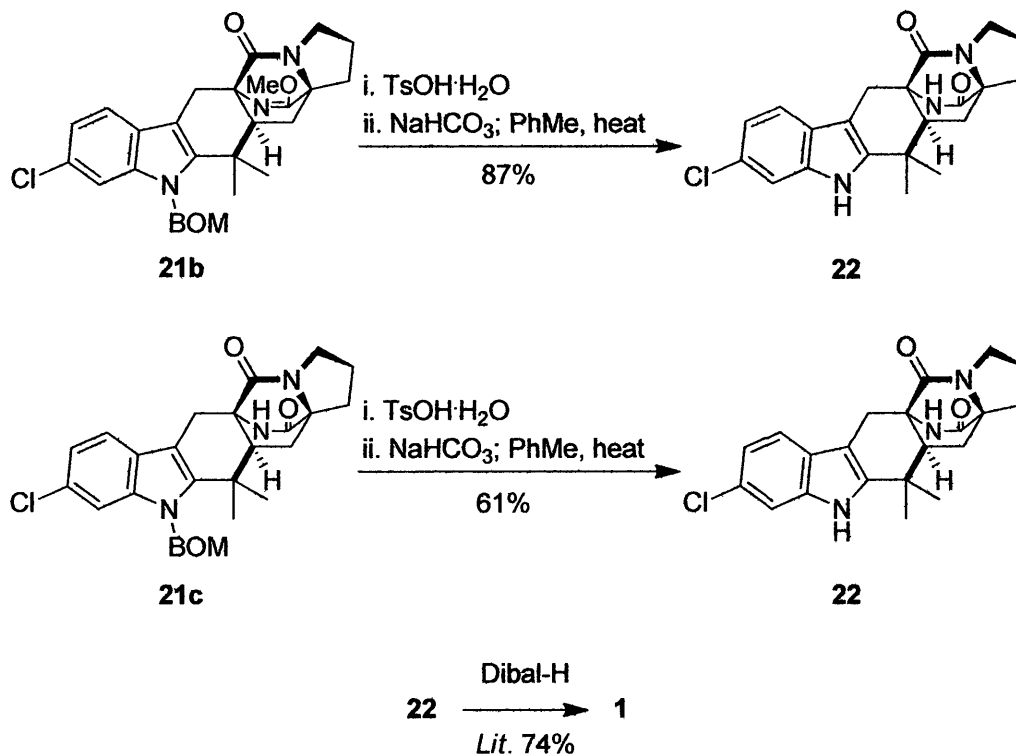
The anticipated result of the racemic domino reaction sequence were IMDA cycloadducts **21a** and **21b**, racemic cycloadducts resulting from the achiral nature of the intermediate formed (**Scheme 3.13**). Unlike in any other domino reaction sequence however, the diketopiperazine **21c** was also consistently observed as a product of this reaction. The presence of this third, unexpected product suggests that in addition to the envisioned domino pathway, the lactim functionality of **21b** was consistently and selectively hydrolyzing to the diketopiperazine. The yield of these three products was nearly quantitative and the ratio of *syn*-configured cycloadducts **21b** and the derived DKP **21c** to *anti*-configured product cycloadduct **21a**, was 2.3:1 as judged by <sup>1</sup>H NMR spectroscopy. This result meant that since the *syn*-configured cycloadduct was hydrolyzing exclusively, both **21b** and **21c** could be advanced toward the similarly *syn*-configured malbrancheamide B.

**Scheme 3.13:** Racemic domino reaction sequence towards malbrancheamide B



Satisfied that the results of the domino sequence had been thoroughly accounted for, we used the chemistry established in our enantioselective synthesis of malbrancheamide B to convert both racemic *syn*-configured cycloadducts to *oxo*-malbrancheamide B (**22**) under mild acidic conditions (**Figure 3.14**). In **21b**, this involved the deprotection of both the lactim *O*-methyl ether and the BOM-group on the indole, and in **21c**, which had already been converted from lactim ether to DKP, the acidic conditions only served to cleave the BOM functionality. These two reactions proved reliable in synthesizing *oxo*-malbrancheamide B (87% from **21b**; 61% from **21c**), and given that this product was the penultimate precursor to the monoketopiperazine natural product in Williams' synthesis, we felt content with the completion of a formal synthesis.<sup>5</sup>

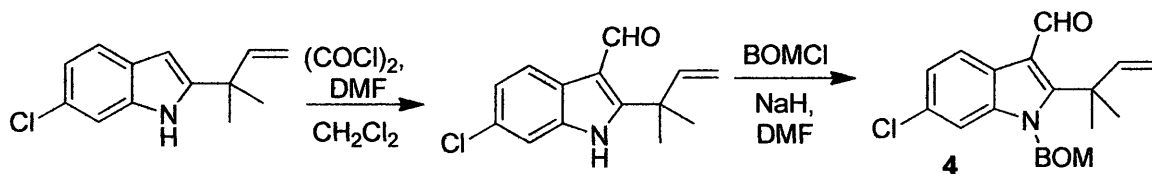
Figure 3.14: Endgame of racemic synthesis



### Conclusions:

The total enantioselective of (+)-malbrancheamide B and an analogous racemic synthesis are reported. In both cases, the core [2.2.2]diazabicyclo of the natural product was established via domino reaction sequence involving aldol condensation, isomerization, and IMDA. In the case of the enantioselective synthesis, a chiral aminal auxiliary on the IMDA-precursor introduced via a chiral, non-racemic DKP diene-precursor enforced complete diastereofacial control over the cycloaddition.

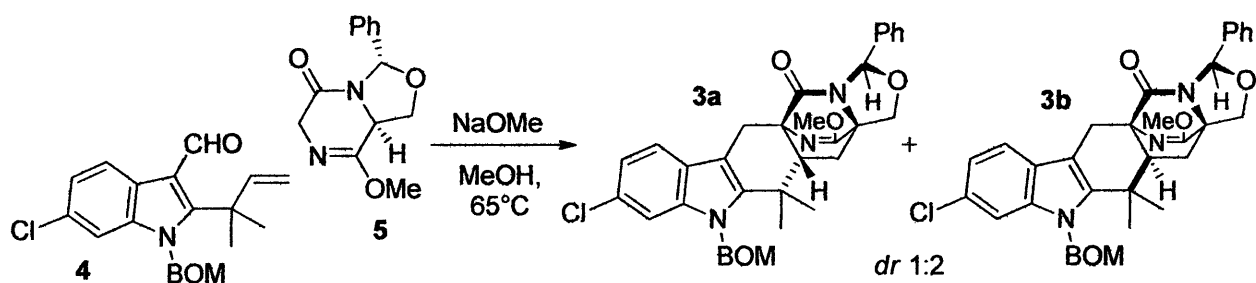
## Experimental Section:



**Chloroindole 4.** Oxalyl chloride (1.00 mL) was added to DMF (0.95 mL) and CH<sub>2</sub>Cl<sub>2</sub> (31 mL) at 0 °C and the solution was allowed to stir for 15 minutes at 0 °C. 6-Chloro-2-(2-methylbut-3-en-2-yl)-1H-indole-3-carbaldehyde<sup>5</sup> (1.641 g, 7.47 mmol) was dissolved in CH<sub>2</sub>Cl<sub>2</sub> (21 mL) and transferred to the oxalyl chloride solution over 2 min via syringe. The reaction mixture was allowed to stir at 0 °C for 5 min and the cooling bath was removed. After stirring 1.5 h at rt, the mixture was concentrated to a volume of ~5 mL and THF (10 mL), NaOH (10 mL), and H<sub>2</sub>O (10 mL) were added. The biphasic mixture was stirred rapidly for 2 h, Et<sub>2</sub>O was added (15 mL) and the organic layer removed. The aqueous layer was extracted with additional Et<sub>2</sub>O (3 x 15 mL). The combined organic layers were washed with brine, dried (Na<sub>2</sub>SO<sub>4</sub>), and concentrated *in vacuo*. Recrystallization (MeOH/toluene) of the white powder afforded 1-((benzyloxy)methyl)-6-chloro-2-(2-methylbut-3-en-2-yl)-1H-indole-3-carbaldehyde (910 mg, 49% yield) as colorless needles: mp 227 °C; TLC (10% EtOAc in hexane), R<sub>f</sub>: 0.40 (CAM); IR (KBr pellet) 1628, 1577, 1457, 1378, 1352, 1294, 1179, 1147, 1102, 1061, 1104, 964, 922 cm<sup>-1</sup>; <sup>1</sup>H NMR (400 MHz, CDCl<sub>3</sub>) 10.45 (s, 1H), 8.34 (s, 1H), 8.28 (d, J = 8.6 Hz, 1H), 7.35 (d, J = 1.6 Hz, 1H), 7.24 (dd, J = 8.6, 2.0 Hz, 1H), 6.22 (dd, J = 17.6, 10.6 Hz, 1H), 5.32 (d, J = 2.0 Hz, 1H), 5.29 (d, J = 8.6 Hz, 1H), 1.73 (s, 6H); <sup>13</sup>C NMR (100 MHz, MeOD) 210.2, 188.7, 159.0, 147.5, 137.1, 130.1, 126.9, 124.2, 123.8, 113.5, 112.7, 41.4, 30.8, 29.5 δ. Exact mass calcd for C<sub>14</sub>H<sub>14</sub>ClNONa[M+Na]<sup>+</sup>, 270.0656. Found 270.0656.

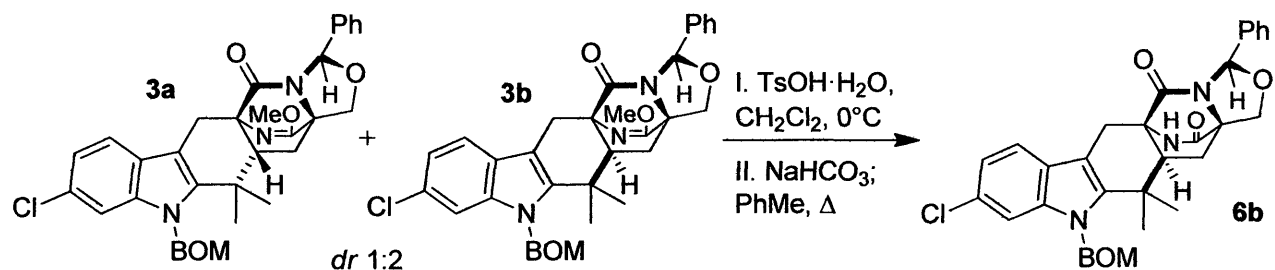
To a dry flask was added NaH (57–63% disp. on oil, 71.2 mg, ca. 1.75 mmol) and DMF (1.6 mL). The reaction vessel was cooled to 0 °C and 1-((benzyloxy)methyl)-6-chloro-2-(2-methylbut-3-en-

2-yl)-1H-indole-3-carbaldehyde (141.0 mg, 0.569 mmol) was added as a solid in three portions (gas evolution). The reaction mixture was stirred for 5 min, and then benzyl chloromethyl ether (tech grade 75%, 0.471 mL, 3.39 mmol) and tetrabutyl ammonium iodide (43.7 mg) were added. The mixture was brought to room temperature over 1 h while stirring. The reaction mixture was diluted with saturated aqueous  $\text{NH}_4\text{Cl}$  and extracted with EtOAc (4 x 10 mL). The combined organic portions were washed with brine, dried ( $\text{Na}_2\text{SO}_4$ ), and concentrated *in vacuo*. The resulting residue was purified by flash chromatography on silica gel (elution: 15% to 30% EtOAc in hexane gradient) to afford the protected indole **4** (185.2 mg, 88% yield) as a light yellow oil: TLC (20% EtOAc in hexane),  $R_f$ : 0.45 (CAM); IR (film) 1642, 1608, 1578, 1507, 1474, 1414, 1374, 1333, 1215, 1153, 1133  $\text{cm}^{-1}$ ;  $^1\text{H}$  NMR (400 MHz,  $\text{CDCl}_3$ ) 10.66 (s, 1H), 8.43 (d,  $J = 9.0$  Hz, 1H), 7.42–7.23 (m, 7H), 6.22 (dd,  $J = 17.2, 10.6$  Hz, 1H), 5.55 (s, 2H), 5.12 (d,  $J = 10.6$  Hz, 1H), 5.01 (d,  $J = 17.2$  Hz, 1H), 4.58 (s, 2H), 1.73 (s, 6H);  $^{13}\text{C}$  NMR (100 MHz,  $\text{CDCl}_3$ )  $\delta$  188.4, 154.0, 146.3, 138.0, 136.3, 129.9, 128.7, 128.5, 128.4, 128.1, 124.7, 123.8, 123.7, 117.4, 112.9, 110.2, 73.5, 70.5, 42.0, 30.7. Exact mass calcd for  $\text{C}_{22}\text{H}_{22}\text{ClNO}_2\text{Na}[\text{M}+\text{Na}]^+$ , 390.1231. Found 390.1232.



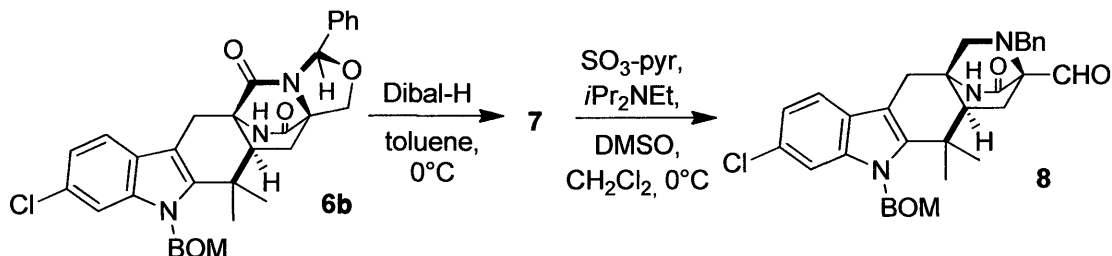
**Cycloadduct 3a, 3b.** To diketopiperazine **5** (0.3 mmol) in methanol (1.5 mL, degassed with nitrogen) at rt was added chloroindole **4** (0.4 mmol) and a freshly prepared solution of sodium methoxide (1 mmol, 0.5 mL, 2.0 M). The reaction mixture was heated to 65 °C for 22 h. After cooling to rt, the reaction mixture was diluted with sat. aqueous  $\text{NH}_4\text{Cl}$  (10 mL) and extracted with EtOAc (3 x 10 mL). The combined organic layers were washed with brine (10 mL), dried

(Na<sub>2</sub>SO<sub>4</sub>), filtered and concentrated *in vacuo*. The unpurified product was a 2:1 ratio of diastereomers as judged by <sup>1</sup>H NMR spectroscopy. The product was purified by flash chromatography on silica gel (elution: 0% to 45% EtOAc in hexanes) to afford products **3a** and **3b** (combined 255.1 mg, 85% yield) as a yellow oil: TLC (20% EtOAc in hexane) R<sub>f</sub> = 0.20 (CAM); [α]<sub>D</sub><sup>25</sup> = -8.8° (c = 0.77, CHCl<sub>3</sub>); IR (film) 1698, 1644, 1475, 1411, 1361, 1311, 1261, 1203, 1066, 885 cm<sup>-1</sup>; <sup>1</sup>H NMR (400MHz, CDCl<sub>3</sub>) 7.44 (d, J = 8.2 Hz, 0.5H), 7.40 (d, J = 8.2 Hz, 1H), 7.39–7.30 (m, 20H), 7.26–7.23 (m, 2H), 7.19 (d, J = 1.6 Hz, 1H), 7.17 (d, J = 1.8 Hz, 2H), 7.10 (dd, J = 8.2, 1.6 Hz, 2H), 7.06 (dd, J = 8.4, 1.6 Hz, 1H), 6.27 (s, 0.5H), 6.19 (s, 1H), 5.66–5.47 (m, 4H), 4.63–4.48 (m, 6.5H), 4.13 (d, J = 9.4 Hz, 0.5H), 4.12 (d, J = 9.8 Hz, 1H), 3.98 (d, J = 16.4 Hz, 1H), 3.86 (s, 3H), 3.76 (s, 1.5H), 3.28 (d, J = 17.2 Hz, 0.5H), 3.14 (d, J = 16.4 Hz, 1H), 2.54 (dd, J = 10.0, 3.7 Hz, 0.5H), 2.45 (dd, J = 10.0, 5.3 Hz, 1H), 2.38 (dd, J = 13.1, 10.0 Hz, 1H), 2.21 (dd, J = 13.1, 5.3 Hz, 1H), 2.17 (s, 1H), 2.07 (dd, J = 12.9, 10.2 Hz, 1H), 1.96 (dd, J = 12.9, 3.9 Hz, 1H), 1.59 (s, 1H), 1.48 (s, 3H), 1.44 (s, 1.5H), 1.32 (s, 3H), 1.27 (s, 1.5 H); <sup>13</sup>C NMR (100 MHz, CDCl<sub>3</sub>) δ 171.4, 169.0, 129.2, 129.1, 128.5, 128.5, 128.5, 128.3, 128.0, 128.0, 128.0, 128.0, 126.4, 126.4, 125.6, 120.5, 120.4, 119.5, 119.5, 109.3, 88.7, 88.5, 73.1, 69.8, 67.6, 67.5, 66.8, 63.4, 63.2, 54.7, 54.4, 48.6, 36.8, 31.0, 28.1, 27.8, 27.6, 25.7, 23.8, 21.5; Exact mass calcd for C<sub>35</sub>H<sub>34</sub>ClN<sub>3</sub>O<sub>4</sub>Na [M+Na]<sup>+</sup>, 618.2130. Found 618.2126.



**Diketopiperazine 6b.** To a solution of compounds **3a** and **3b** (200 mg, 0.34 mmol) in CH<sub>2</sub>Cl<sub>2</sub> (33.5 mL) was added TsOH·H<sub>2</sub>O (70 mg, 0.37 mmol) at 0°C. The reaction mixture was stirred at

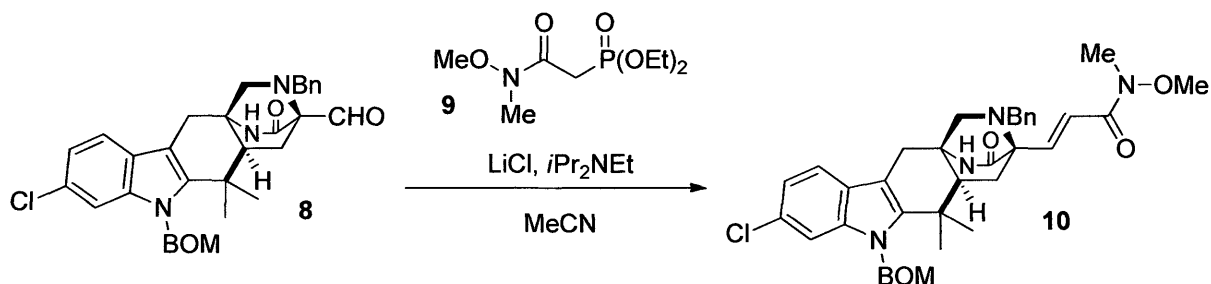
0°C for 1.5 h, and then sat. aqueous NaHCO<sub>3</sub> (2 mL) was added. The aqueous layer was separated and extracted with EtOAc (4 × 10 mL). The unpurified product was a 1:2 ratio of diastereomers as judged by <sup>1</sup>H NMR spectroscopy. The unpurified residue (223.7 mg) was dissolved in toluene (30 mL) and heated to 110°C. After 19 h, heat was removed, and the solution was concentrated *in vacuo*. The residue was purified by recrystallization from 25% EtOAc in hexane to afford product **6b** (127 mg, 65% yield) as a colorless amorphous solid: TLC (40% EtOAc in hexane) R<sub>f</sub> 0.20 (CAM); [α]<sub>D</sub><sup>25</sup> = -2.7 (c 0.48, MeOH); IR (KBr pellet) 1721, 1690, 1495, 1474, 1453, 1406, 1370, 1311, 1241, 1204, 1109, 1071, 929, 914, 881 cm<sup>-1</sup>; <sup>1</sup>H NMR (400 MHz, CDCl<sub>3</sub>) 7.38–7.31 (m, 11H), 7.18 (d, J = 1.6 Hz, 1H), 7.08 (dd, J = 8.2, 2.0 Hz, 1H), 6.42 (s, 1H), 6.22 (s, 1H), 5.55 (d, J = 10.9 Hz, 1H), 5.52 (d, J = 11.3 Hz, 1H), 4.77 (d, J = 9.4 Hz, 1H), 4.58 (d, J = 11.7 Hz, 1H), 4.51 (d, J = 11.7 Hz, 1H), 4.14 (d, J = 9.8 Hz, 1H), 3.78 (d, J = 15.6 Hz, 1H), 2.68 (t, J = 7.4 Hz, 1H), 2.66 (d, J = 15.6 Hz, 1H), 2.34 (m, J = 7.8 Hz, 2H), 1.49 (s, 3H), 1.32 (s, 3H); <sup>13</sup>C NMR (100 MHz, CDCl<sub>3</sub>) δ 171.5, 166.1, 140.5, 139.1, 136.3, 129.4, 128.6, 128.6, 128.2, 127.9, 126.5, 125.0, 120.8, 119.2, 109.6, 107.2, 89.3, 73.0, 70.0, 68.4, 65.1, 60.8, 50.6, 36.4, 29.9, 27.8, 25.0, 21.0; Exact mass calcd for C<sub>34</sub>H<sub>32</sub>ClN<sub>3</sub>O<sub>4</sub>Na [M + Na]<sup>+</sup>, 604.1973, found 604.1967.



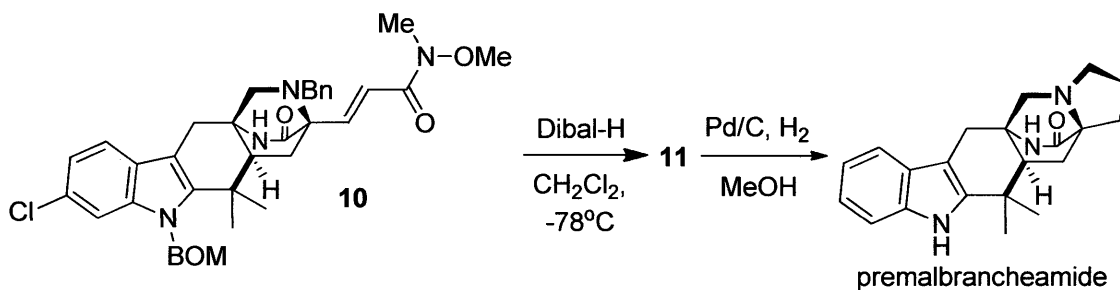
**Aldehyde 8.** To a solution of compound **6b** (63 mg, 0.11 mmol) in toluene (1 mL) at 0°C was added Dibal-H (2.10 mL, 1.0 M solution in toluene). The reaction was stirred for 0.5 h at 0°C, and then EtOAc (2 mL), potassium sodium tartrate tetrahydrate (100 mg), and water (2 mL) were successively added. The biphasic mixture was stirred rapidly for 1 h, and the organic layer was

removed. The aqueous layer was extracted with additional EtOAc (3 × 10 mL). The organic layers were combined, dried (Na<sub>2</sub>SO<sub>4</sub>), and concentrated in vacuo. The unpurified product was a single diastereomer as judged by <sup>1</sup>H NMR spectroscopy. The residue was purified by flash chromatography on silica gel (elution: 45–65% EtOAc in hexane) to afford the derived intermediate aminoalcohol **7** (49 mg, 80% yield) as a yellow oil. Spectral data were in agreement with published data.<sup>9</sup> To a portion of aminoalcohol **7** (43 mg, 0.08 mmol) in CH<sub>2</sub>Cl<sub>2</sub> (1.5 mL) at 0°C was added DMSO (55 μL) and *i*Pr<sub>2</sub>NEt (100 μL, 0.57 mmol). To this solution was added SO<sub>3</sub>·pyridine (0.5 M, 450 μL). The solution was stirred for 30 min at 0°C and extracted with EtOAc (3 × 10 mL). The organic layers were combined, washed with brine, dried (Na<sub>2</sub>SO<sub>4</sub>), and concentrated *in vacuo*. The residue was purified by flash chromatography on silica gel (elution: 35–100% EtOAc in hexane) to afford product **8** (39 mg, 92% yield) as a yellow oil: TLC (50% EtOAc in hexane) R<sub>f</sub> 0.25 (CAM); [α]<sub>D</sub><sup>25</sup> = +20.9 (c 1.0, CH<sub>2</sub>Cl<sub>2</sub>); IR (film) 1733, 1669, 1475, 1454, 1360, 1318, 1266, 1240, 1202, 1132, 1065, 882, 805, 738 cm<sup>-1</sup>; <sup>1</sup>H NMR (400 MHz, CDCl<sub>3</sub>) 10.23 (s, 1H), 7.43–7.18 (m, 11H), 7.06 (d, J = 8.2 Hz, 2H), 6.44 (s, 1H), 5.53 (s, 2H), 4.57 (s, 2H), 4.28 (d, J = 12.9 Hz, 1H), 3.31 (d, J = 12.9 Hz, 1H), 3.23 (d, J = 10.9 Hz, 1H), 2.88 (d, J = 15.6 Hz, 1H), 2.80 (d, J = 15.2 Hz, 1H), 2.29–2.01 (m, 4H), 1.54 (s, 3H), 1.45 (s, 3H) <sup>13</sup>C NMR (100 MHz, CDCl<sub>3</sub>) δ 198.9, 171.7, 141.2, 138.8, 137.7, 136.7, 128.6, 128.4, 128.4, 128.3, 128.2, 127.9, 127.3, 125.0, 120.8, 118.8, 109.7, 106.6, 77.2, 73.0, 70.1, 66.5, 59.4, 59.2, 55.1, 47.3, 35.2, 30.1, 29.5, 28.8, 22.5; Exact mass calcd for C<sub>34</sub>H<sub>34</sub>ClN<sub>3</sub>O<sub>3</sub>Na [M + Na]<sup>+</sup>, 590.2181, found 590.2184.

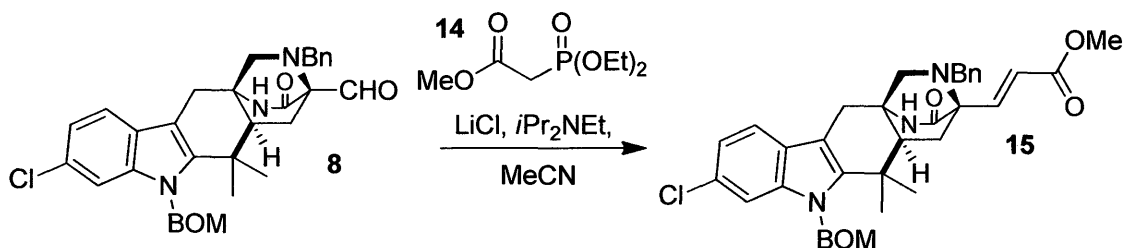




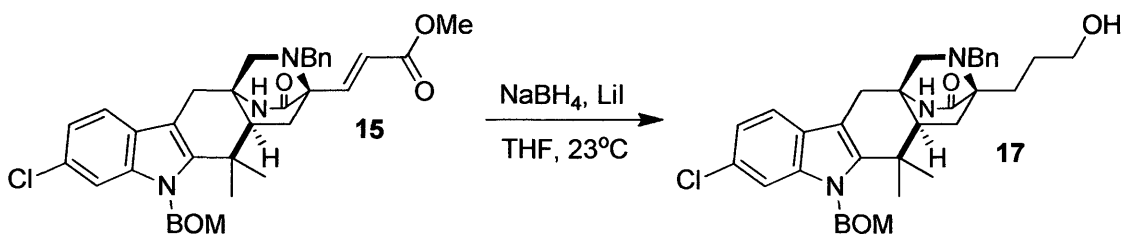
**Weinreb Amide 10.** To a solution of compound **8** (39 mg, 0.069 mmol) in acetonitrile (3.8 mL) was added phosphoramidite **9** (34 mg, 0.14 mmol), LiCl (23 mg, 0.54 mmol), and DBU (0.026 mL, 0.17 mmol). The solution was stirred at rt for 1 h, and then H<sub>2</sub>O (2 mL) was added. The aqueous layer was separated and extracted with EtOAc (3 × 10 mL). The organic layers were combined, washed with brine, dried (Na<sub>2</sub>SO<sub>4</sub>), and concentrated *in vacuo*. The residue was purified by flash chromatography on silica gel (elution: 60–80% EtOAc in hexane) to afford product **10** (27 mg, 60% yield) as a yellow oil: TLC (60% EtOAc in hexane) *R<sub>f</sub>* 0.20 (CAM); [ $\alpha$ ]<sub>D</sub><sup>25</sup> = +8.9 (*c* = 0.09, CH<sub>2</sub>Cl<sub>2</sub>); IR (film) 1682, 1629, 1472, 1455, 1418, 1374, 1313, 1241, 1204, 1131, 1061, 999, 882, 800, 753 cm<sup>-1</sup>; <sup>1</sup>H NMR (400 MHz, CDCl<sub>3</sub>) 7.52–7.13 (m, 14H), 7.05 (dd, *J* = 8.4, 1.8 Hz, 1H), 6.33 (s, 1H), 5.55 (s, 2H), 4.57 (d, *J* = 0.8 Hz, 2H), 4.28 (d, *J* = 13.7 Hz, 1H), 3.68 (s, 3H), 3.27 (s, 3H), 3.27 (d, *J* = 10.9 Hz, 1H), 3.13 (d, *J* = 13.3 Hz, 1H), 2.83 (q, *J* = 15.2 Hz, 2H), 2.30–2.25 (m, 2H), 2.10–2.04 (m, 2H), 1.58 (s, 3H), 1.43 (s, 3H); <sup>13</sup>C NMR (100 MHz, CDCl<sub>3</sub>)  $\delta$  172.0, 143.2, 141.5, 138.9, 138.5, 136.8, 128.6, 128.4, 128.3, 128.2, 128.1, 128.0, 127.0, 125.1, 122.0, 120.8, 118.7, 109.8, 106.8, 73.1, 70.2, 62.0, 61.9, 60.1, 59.3, 54.9, 47.8, 35.1, 35.0, 30.3, 30.2, 22.5; Exact mass calcd for C<sub>38</sub>H<sub>41</sub>ClN<sub>4</sub>O<sub>4</sub>Na [M + Na]<sup>+</sup>, 675.2709, found 675.2702.



**Premalbrancheamide.** To a solution of compound **10** (26 mg, 0.39 mmol) in PhMe (1 mL) at -78°C was added a solution of Dibal-H (1.0 M in PhMe, 0.20 mL). The solution was stirred for 1 h, and then MeOH (1 mL), HCl (1 mL), EtOAc (1 mL), and potassium sodium tartrate·4H<sub>2</sub>O (50 mg) was added. After an additional 1 h of stirring, the aqueous layer was separated and extracted with EtOAc (3 × 10 mL). The organic layers were combined, dried (Na<sub>2</sub>SO<sub>4</sub>), and concentrated *in vacuo*. The residue was quickly purified by flash chromatography on silica gel (elution: 40–100% EtOAc in hexanes) to afford product **11** (15.5 mg, 67% yield) as a light yellow oil. Aldehyde **11** was unstable and prone to decomposition; accordingly, the product was used immediately in the following reduction sequence. To a solution of compound **11** (7.0 mg, 0.015 mmol) in MeOH (1.0 mL) was added Pd/C (17 mg) at rt. The solution was sparged with H<sub>2</sub>. After 5 min, the H<sub>2</sub> was stopped and Ar was bubbled through the solution. The suspension was filtered through Celite and concentrated *in vacuo* to afford a mixture containing predominantly premalbrancheamide (4.0 mg, 65% yield): TLC (80% EtOAc in hexane) R<sub>f</sub> 0.25 (CAM). Spectral data for premalbrancheamide were in agreement with published data.<sup>10,11</sup>

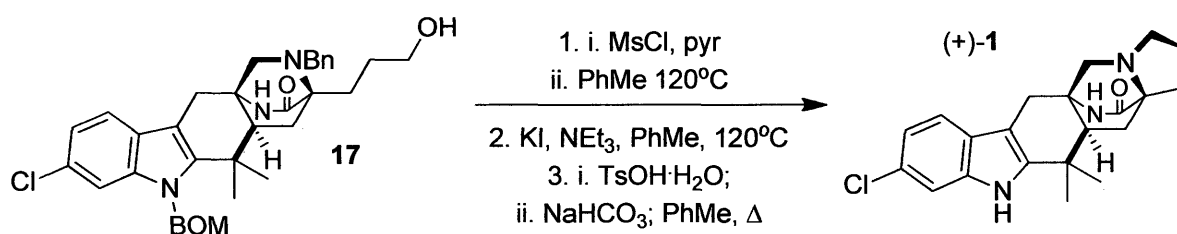


**Methyl Ester 15.** To a solution of compound **8** (110 mg, 0.19 mmol) in acetonitrile (10 mL) was added trimethyl phosphonoacetate **14** (0.065 mL, 0.40 mmol), LiCl (67 mg, 1.60 mmol), and DBU (0.075 mL, 0.50 mmol). The solution was stirred at rt for 1 h, and then H<sub>2</sub>O (2 mL) was added. The aqueous layer was separated and extracted with EtOAc (3 × 10 mL). The organic layers were combined, washed with brine, dried (Na<sub>2</sub>SO<sub>4</sub>), and concentrated *in vacuo* to give a 3:1 mixture of *E* and *Z* isomers of **15** as shown by <sup>1</sup>H NMR spectroscopy. The residue was purified by flash chromatography on silica gel (elution: 40–100% EtOAc in hexane) to afford product **15** (110 mg, 91% yield) as a yellow oil: TLC (40% EtOAc in hexane) R<sub>f</sub> 0.40 (CAM); [α]<sub>D</sub><sup>25</sup> = +7.9 (c 2.4, CH<sub>2</sub>Cl<sub>2</sub>); IR (film) 1724, 1685, 1608, 1562, 1495, 1475, 1454, 1359, 1308, 1241, 1202, 1174, 1131, 1062, 882, 803, 740 cm<sup>-1</sup>; <sup>1</sup>H NMR (400 MHz, CDCl<sub>3</sub>) 7.51 (d, J = 16.4 Hz, 1H), 7.38–7.18 (m, 12H), 7.05 (d, J = 8.2, 1H), 6.63 (d, J = 16.4 Hz, 1H), 5.55 (s, 2H), 4.60–4.54 (m, 2H), 4.25 (d, J = 12.9 Hz, 1H), 3.78 (s, 3H), 3.71 (s, 1H), 3.26 (d, J = 10.9 Hz, 1H), 3.13 (d, J = 13.3 Hz, 1H), 2.89–2.81 (m, 2H), 2.25–2.05 (m, 4H), 1.58 (s, 3H), 1.43 (s, 3H); <sup>13</sup>C NMR (100 MHz, CDCl<sub>3</sub>) δ 171.9, 166.8, 145.2, 141.3, 138.8, 138.3, 136.8, 128.6, 128.4, 128.3, 128.3, 128.2, 128.1, 128.0, 127.9, 127.1, 125.0, 124.1, 120.8, 120.7, 118.8, 109.7, 106.8, 77.2, 73.0, 70.1, 61.6, 59.8, 59.3, 54.9, 51.7, 47.8, 35.1, 34.6, 30.3, 30.0, 24.3, 22.4; Exact mass calcd for C<sub>37</sub>H<sub>38</sub>ClN<sub>3</sub>O<sub>4</sub>Na [M + Na]<sup>+</sup>, 646.2443, found 646.2436.



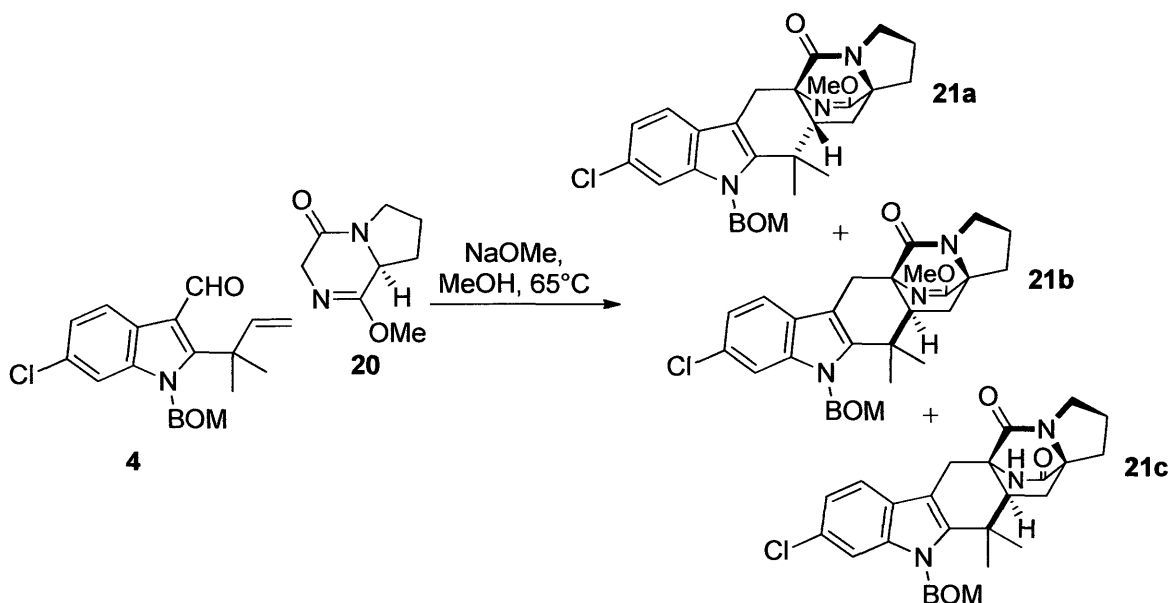
**Saturated Alcohol 17.** To a solution of compound **15** (36 mg, 0.059 mmol) in THF (1.0 mL) at 0°C was added NaBH<sub>4</sub> (24 mg, 0.64 mmol) and Lil (76 mg, 0.57 mmol). The solution was warmed to rt, and additional NaBH<sub>4</sub> and Lil (10 equivalents each) were added in three portions after successive 12 h increments. After 48 h, sat. aqueous NH<sub>4</sub>Cl (1 mL) was added. The aqueous layer was separated and extracted with EtOAc (3 × 10 mL). The organic layers were combined, washed with brine, dried (Na<sub>2</sub>SO<sub>4</sub>), and concentrated *in vacuo* to give a 1:3 mixture of alcohols **16** and **17** as shown by <sup>1</sup>H NMR spectroscopy. The residue was purified by flash chromatography on silica gel (elution: 50–100% EtOAc in hexanes) to afford product **17** (20 mg, 58% yield) as a white solid: mp 92.7–94.2°C; TLC (60% EtOAc in hexane), R<sub>f</sub> 0.15 (CAM); [α]<sub>D</sub><sup>25</sup> = +1.4 (c 0.85, CH<sub>2</sub>Cl<sub>2</sub>); IR (film) 1740, 1672, 1473, 1453, 1359, 1318, 1240, 1205, 1059, 882, 802, 746 cm<sup>-1</sup>; <sup>1</sup>H NMR (400 MHz, CDCl<sub>3</sub>) 7.40–7.13 (m, 12H), 7.04 (d, J = 8.2 Hz, 1H), 6.56 (s, 1H), 5.54 (s, 2H), 4.56 (s, 2H), 4.27 (d, J = 12.9 Hz, 1H), 3.78–3.72 (m, 2H), 3.11 (d, J = 10.9 Hz, 1H), 3.06 (d, J = 12.5 Hz, 1H), 2.81 (d, J = 15.6 Hz, 1H), 2.76 (d, J = 15.2 Hz, 1H), 2.48 (s, 1H), 2.27 (dd, J<sub>1</sub> = 13.3, J<sub>2</sub> = 4.3 Hz, 1H), 2.20 (d, J = 11.3 Hz, 1H), 2.07–1.98 (m, 2H), 1.93 (d, J = 11.7 Hz, 2H), 1.88–1.83 (m, 2H), 1.52 (s, 3H), 1.44 (s, 3H); <sup>13</sup>C NMR (100 MHz, CDCl<sub>3</sub>) δ 174.4, 141.6, 138.8, 138.5, 136.8, 128.6, 128.4, 128.3, 128.2, 127.9, 127.0, 125.1, 120.8, 118.7, 109.7, 106.8, 77.2, 73.1, 70.1, 62.7, 60.2, 59.6, 57.3, 54.5, 47.3, 35.1, 30.4, 30.2, 30.1, 26.9, 26.4, 22.3; Exact mass calcd for C<sub>36</sub>H<sub>40</sub>ClN<sub>3</sub>O<sub>3</sub> Na [M + Na]<sup>+</sup>, 620.2650, found 620.2643. Alcohol **17** can also be prepared from **16** as follows. To a solution of compound **16** (6.0 mg, 0.0092 mmol) in EtOH (0.4 mL) at rt was added 4-methylbenzene sulfonhydrazide (2 mg, 0.010 mmol) and NaOAc (1mg, 0.010 mmol). The

solution was heated to reflux, and additional portions (0.010 mmol) of sulfonylhydrazide and NaOAc were added after 2 h. After 6.5 h at reflux, heat was removed, and the solution was concentrated *in vacuo*. Sat. aqueous Na<sub>2</sub>CO<sub>3</sub> (2 mL) and EtOAc (2 mL) were added to the residue, and the aqueous layer was separated and extracted with additional EtOAc (3 × 5 mL). The organic layers were combined, washed with brine, dried (Na<sub>2</sub>SO<sub>4</sub>), and concentrated *in vacuo*. The residue was purified by flash chromatography according to the above procedure to afford **17** (3.3 mg, 60% yield) as a white solid.



**Malbrancheamide B (1).** To a solution of compound **17** (24 mg, 0.040 mmol) in CH<sub>2</sub>Cl<sub>2</sub> (0.4 mL) at 0°C was added pyridine (6.3 μL, 0.079 mmol) and MsCl (3.4 μL, 0.043 mmol). The solution was allowed to warm to rt with stirring, and additional portions of MsCl (3.4 μL, 0.043 mmol) were added every 3 h. After a total of 12 h, sat. aq. NaHCO<sub>3</sub> (2 mL) was added. The aqueous layer was separated and extracted with EtOAc (3 × 10 mL). The organic layers were combined, washed with brine, dried (Na<sub>2</sub>SO<sub>4</sub>), and concentrated *in vacuo*. The resulting residue (22 mg) was dissolved in toluene (2 mL) and heated to 125°C in a sealed tube with stirring. After 10 h, heat was removed, and the solution was concentrated *in vacuo*. To a solution of the unpurified residue (18 mg) in toluene (1.5 mL) was added KI (6.0 mg, 0.035 mmol) and NEt<sub>3</sub> (0.15 mL) in a sealed tube. The solution was heated to 125°C and stirred for 20 h. After 20 h, heat was removed, and the solution was concentrated *in vacuo*. To a solution of the unpurified residue (13 mg) in CH<sub>2</sub>Cl<sub>2</sub> (2.6 mL) was added TsOH·H<sub>2</sub>O (15.8 mg, 0.083 mmol) at 0°C. The solution was allowed to warm to rt with stirring, and an additional portion of TsOH·H<sub>2</sub>O (14 mg, 0.072 mmol)

was added after 2 h. After a total of 4 h, NaHCO<sub>3</sub> (2 mL) was added. The aqueous layer was separated and extracted with EtOAc (4 × 10 mL). The organic layers were combined, washed with brine, dried (Na<sub>2</sub>SO<sub>4</sub>), and concentrated *in vacuo*. The product was purified by flash chromatography on silica gel (elution: 0–10% MeOH in CHCl<sub>3</sub>) to afford product **1** (6.0 mg, 40% yield) as an amorphous colorless solid: TLC (5% MeOH in CHCl<sub>3</sub>), R<sub>f</sub> 0.50 (CAM); [α]<sub>D</sub><sup>25</sup> = +25 (c 0.4, MeOH), Lit.<sup>12</sup> [α]<sub>D</sub> = +50 (c 1, MeOH), Lit.<sup>6,13</sup> (–)-**1**, [α]<sub>D</sub> = –36 (c 0.81, MeOH), Lit.<sup>14</sup> [α]<sub>D</sub> = +28 (c 0.5, MeOH); HPLC trace and UV signature identical for both synthetic and an authentic natural sample of **1**; Mobile phase, gradient mixture of H<sub>2</sub>O + 0.1% TFA/MeCN, 1.0 mL/min; 0–10 min 20% MeCN, 10.01–20 min 20–50% MeCN; Phenomenex C18 Luna (250 mm × 4.6 mm × 5 μm), retention time 15.17 min; UV λ 230, 283 nm; IR (film) 1653, 1465, 1361, 1319, 1291, 1253, 1227, 1198, 1131, 1099, 1059, 1024, 904, 797 cm<sup>–1</sup>; Exact mass calcd for C<sub>21</sub>H<sub>24</sub>ClN<sub>3</sub>O[M+H]<sup>+</sup>, 370.1681, found 370.1677. <sup>1</sup>H and <sup>13</sup>C NMR spectral data for synthetic material both match the data for the authentic sample and are in agreement with published data.<sup>15a,6,12b</sup>



**Cycloadducts 21a, 21b, 21c.** To diketopiperazine **20** (18 mg, 0.11 mmol) in MeOH (0.1 mL, degassed with nitrogen) at rt in a sealed tube was added **4** (20 mg, 0.05 mmol) and a freshly prepared solution of NaOMe in MeOH (5 equiv, 0.3 mL, 5.0 M). The reaction vessel was heated to 90°C (bath temperature) for 68 h. After cooling to rt, the reaction mixture was diluted with sat. aqueous NH<sub>4</sub>Cl (1 mL) and extracted with EtOAc (4 × 5 mL). The combined organic layers were washed with brine (5 mL), dried (Na<sub>2</sub>SO<sub>4</sub>), filtered and concentrated *in vacuo* to give a 1.7:1.0:2.9 mixture of cycloadducts **21a**, **21b**, and **21c** as determined by <sup>1</sup>H NMR spectroscopy on the unpurified mixture of products. The residue was purified by flash chromatography on silica gel (elution: 0–5% MeOH in CHCl<sub>3</sub>) to afford products **21a** (8.0 mg, 29% yield), **21b** (6.0 mg, 22% yield), and **21c** (13.0 mg, 48% yield).

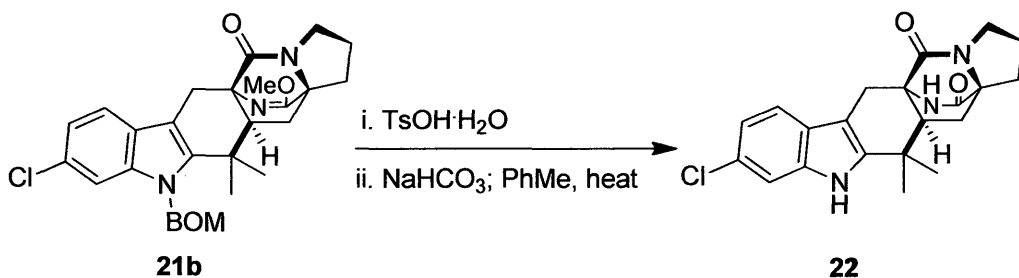
**21a:** (light yellow oil) TLC (5% MeOH in CHCl<sub>3</sub>), R<sub>f</sub> 0.55 (CAM); IR (film) 1685, 1633, 1476, 1419, 1354, 1324, 1260, 1205, 1179, 1092, 1077, 1055, 1001, 920, 886, 838, 799, 740, 702 cm<sup>-1</sup>; <sup>1</sup>H NMR (400 MHz, CDCl<sub>3</sub>) 7.50 (d, J = 8.2 Hz, 1H), 7.38–7.30 (m, 5H), 7.19 (s, 1H), 7.10 (dd, J = 8.2, 1.6 Hz, 1H), 5.59 (d, J = 11.3 Hz, 1H), 5.53 (d, J = 11.3 Hz, 1H), 4.56 (d, J = 11.7 Hz, 1H), 4.50 (d, J =

11.7 Hz, 1H), 3.91 (d, J = 17.6 Hz, 1H), 3.71 (s, 3H), 3.54–3.43 (m, 2H), 3.28 (d, J = 17.2 Hz, 1H), 2.71–2.64 (m, 1H), 2.41 (dd, J = 9.6, 4.1 Hz, 1H), 2.09–1.84 (m, 5H), 1.39 (s, 3H), 1.23 (s, 3H);  $^{13}\text{C}$  NMR (100 MHz,  $\text{CDCl}_3$ )  $\delta$  172.2, 170.9, 141.3, 139.3, 137.3, 128.8, 128.2, 128.1, 126.4, 120.6, 120.0, 109.5, 109.4, 73.3, 70.0, 66.8, 64.4, 54.6, 47.6, 43.8, 36.9, 34.5, 29.3, 27.9, 26.4, 24.9, 24.1; Exact mass calcd for  $\text{C}_{30}\text{H}_{32}\text{ClN}_3\text{O}_3\text{Na}$   $[\text{M} + \text{Na}]^+$ , 540.2024, found 540.2017.

**21b:** (light yellow oil) TLC (5% MeOH in  $\text{CHCl}_3$ ),  $R_f$  0.52 (CAM); IR (film) 1678, 1638, 1475, 1419, 1356, 1310, 1265, 1200, 1060, 882, 800, 736, 699  $\text{cm}^{-1}$ ;  $^1\text{H}$  NMR (400 MHz,  $\text{CDCl}_3$ ) 7.46 (d, J = 8.2 Hz, 1H), 7.39–7.30 (m, 5H), 7.18 (d, J = 1.6 Hz, 1H), 7.09 (dd, J = 8.2, 2.0 Hz, 1H), 5.55 (d, J = 5.1 Hz, 2H), 4.56 (d, J = 12.1 Hz, 1H), 4.48 (d, J = 12.1 Hz, 1H), 3.99 (d, J = 16.4 Hz, 1H), 3.80 (s, 3H), 3.51–3.33 (m, 2H), 3.08 (d, J = 16.4 Hz, 1H), 2.68–2.66 (m, 1H), 2.34 (dd, J = 10.4, 5.1 Hz, 1H), 2.04–1.92 (m, 4H), 1.83 (dd, J = 12.9, 5.1 Hz, 1H), 1.42 (s, 3H), 1.18 (s, 3H);  $^{13}\text{C}$  NMR (100 MHz,  $\text{CDCl}_3$ )  $\delta$  172.9, 171.3, 140.7, 139.1, 137.1, 128.5, 128.0, 127.9, 125.7, 120.4, 119.6, 109.9, 109.2, 73.1, 69.7, 65.5, 64.3, 54.5, 54.5, 48.8, 43.4, 36.7, 32.8, 29.3, 27.8, 24.8, 21.4; Exact mass calcd for  $\text{C}_{30}\text{H}_{32}\text{ClN}_3\text{O}_3\text{Na}$   $[\text{M} + \text{Na}]^+$ , 540.2024, found 540.2017.

**21c:** (colorless solid) mp 224.2–225.6°C; TLC (5% MeOH in  $\text{CHCl}_3$ ),  $R_f$  0.50 (CAM); IR (KBr pellet) 3199, 1691, 1475, 1455, 1199, 1098, 1058, 883, 811, 733, 697  $\text{cm}^{-1}$ ;  $^1\text{H}$  NMR (400 MHz, DMSO) 8.76 (s, 1H), 7.57 (s, 1H), 7.44 (d, J = 8.6 Hz, 1H), 7.37–7.28 (m, 5H), 7.10 (dd, J = 8.6, 2.0 Hz, 1H), 5.69 (d, J = 10.9 Hz, 1H), 5.64 (d, J = 10.9 Hz, 1H), 4.59 (s, 2H), 3.44 (d, J = 15.6 Hz, 1H), 3.35 (s, 1H), 3.33–3.23 (m, 1H), 2.72 (d, J = 16.0 Hz, 1H), 2.55–2.50 (m, 2H), 2.12–1.81 (m, 5H), 1.36 (s, 3H), 1.09 (s, 3H);  $^{13}\text{C}$  NMR (100 MHz, DMSO)  $\delta$  173.0, 168.2, 141.5, 138.6, 137.5, 128.3, 127.7, 127.7, 126.8, 125.0, 120.0, 119.1, 109.8, 107.2, 73.1, 69.0, 66.1, 58.9, 50.2, 43.6, 35.8, 30.5, 28.6, 27.1, 24.0, 23.6, 20.3; Exact mass calcd for  $\text{C}_{29}\text{H}_{30}\text{ClN}_3\text{O}_3\text{Na}$   $[\text{M} + \text{Na}]^+$ , 526.1868, found 526.1862.





**Oxomalbrancheamide B (22).** To a solution of compound **21b** (6 mg, 0.012 mmol) in  $\text{CH}_2\text{Cl}_2$  (0.5 mL) at  $0^\circ\text{C}$  was added  $\text{TsOH}\cdot\text{H}_2\text{O}$  (6 mg, 0.029 mmol). The solution was allowed to warm to rt with stirring, and an additional portion of  $\text{TsOH}\cdot\text{H}_2\text{O}$  (6 mg, 0.029 mmol) was added after 2 h. After a total of 4 h, sat. aqueous  $\text{NaHCO}_3$  (2 mL) was added. The aqueous layer was separated and extracted with EtOAc ( $4 \times 10$  mL). The organic layers were combined, washed with brine, dried ( $\text{Na}_2\text{SO}_4$ ), and concentrated *in vacuo*. The unpurified residue (4 mg) was dissolved in toluene (1 mL) and heated to  $125^\circ\text{C}$  in a sealed tube with stirring. After 22 h, heat was removed, and the solution was concentrated *in vacuo*. The residue was purified by flash chromatography on silica gel (elution: 5% MeOH in  $\text{CHCl}_3$ ) to afford product **22** (3.0 mg, 61% yield). **22** was also prepared from **21c** as follows: to a solution of compound **21c** (11 mg, 0.021 mmol) in  $\text{CH}_2\text{Cl}_2$  (0.5 mL) at  $0^\circ\text{C}$  was added  $\text{TsOH}\cdot\text{H}_2\text{O}$  (10 mg, 0.053 mmol). The solution was allowed to warm to rt with stirring, and an additional portion of  $\text{TsOH}\cdot\text{H}_2\text{O}$  (10 mg, 0.053 mmol) was added after 2 h. After a total of 4 h, sat. aqueous  $\text{NaHCO}_3$  (2 mL) was added. The aqueous layer was separated and extracted with EtOAc ( $4 \times 10$  mL). The organic layers were combined, washed with brine, dried ( $\text{Na}_2\text{SO}_4$ ), and concentrated *in vacuo*. The unpurified residue (12.4 mg) was dissolved in toluene (1 mL) and heated to  $125^\circ\text{C}$  in a sealed tube with stirring. After 17 h, heat was removed, and the solution was concentrated *in vacuo*. The residue was purified by flash chromatography on silica gel (elution: 5% MeOH in  $\text{CHCl}_3$ ) to afford product **22** (7.0 mg, 87% yield). Spectral data were in agreement with published data.<sup>15a</sup>

## REFERENCES

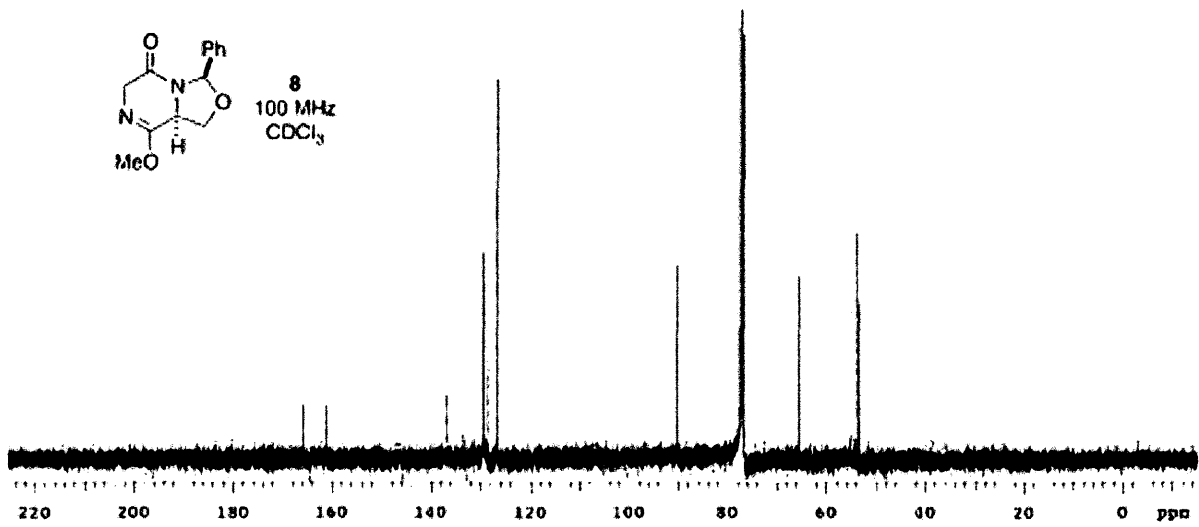
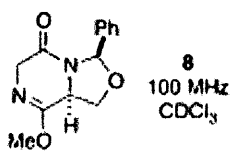
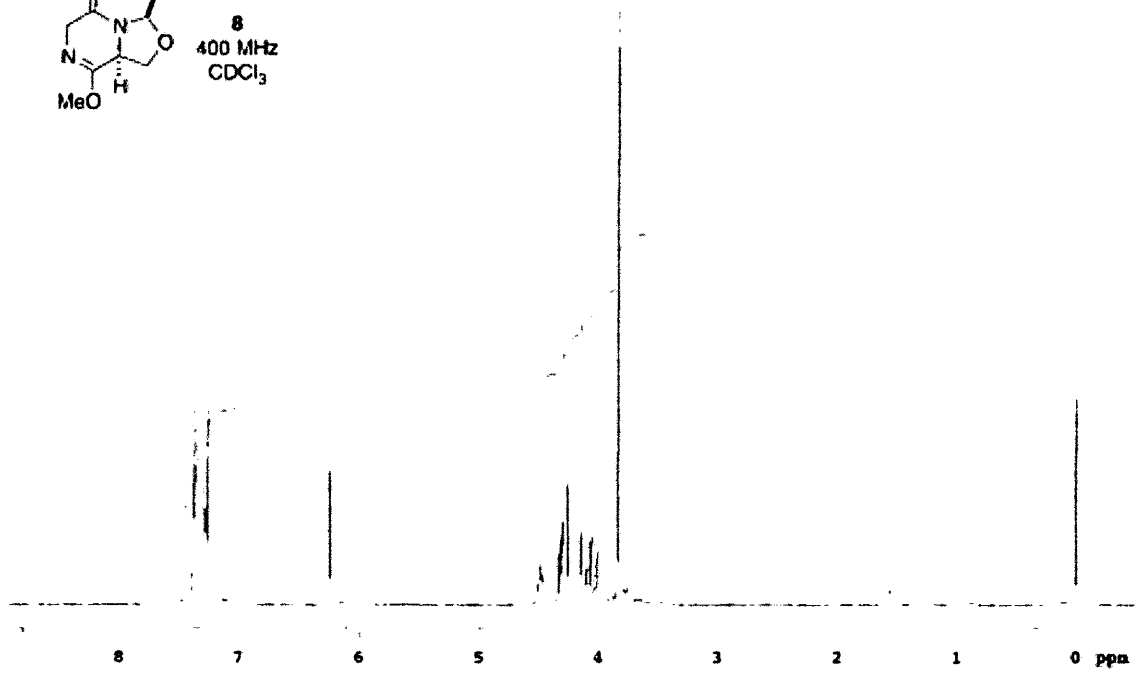
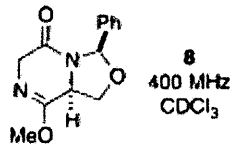
1. Marinez-Luis, S.; Rodrigues, R.; Acevedo, L. Gonzales, M. C.; Lira-Rocha, A.; Mata, R. *Tetrahedron* **2006**, *62*, 1817-1822.
2. Figueroa, M.; Gonzales, M.; Mata, R. *Planta Med.* **2008**, *74*, PB92.
3. Watts, K. R.; Loveridge, S. T.; Tenney, K.; Media, J.; Valeriote, F. A.; Crews, P. *J. Org. Chem.* **2011**, *76*, 6201-6208.
4. Ding, Y.; Greshock, T. J.; Miller, K. A.; Sherman, D. H.; Williams, R. M. *Org. Lett.* **2008**, *10*, 4863-4866.
5. Miller, K. A.; Welch, T. R.; Greshock, T. J.; Ding, Y.; Sherman, D. H.; Williams, R. M. *J. Org. Chem.* **2008**, *73*, 3116-3119.
6. Frebault, F.; Simpkins, N. S.; Fenwick, A. *J. Am. Chem. Soc.* **2009**, *131*, 4215.
7. Pichowicz, M.; Simpkins, N. S.; Blake, A. J.; Wilson, C. *Tetrahedron* **2008**, *64*, 3713.
8. Blanchette, M. A.; Choy, W.; Davis, J. T.; Essensfeld, A. P.; Masamune, S.; Roush, W. R.; Sakai, T. *Tetrahedron Lett.* **1984**, *25*, 2183-2186.
9. Margrey, K. A.; Chinn, A. J.; Laws, S. W.; Pike, R. D.; Scheerer, J. R. *Org. Lett.* **2012**, *43*, 2458-2461.
10. Miller, K. A.; Figueroa, M.; Valente, M. W. N.; Greshock, T. J.; Mata, R.; Williams, R. M. *Bioorg. Med. Chem. Lett.* **2008**, *18*, 6479-6481.
11. (a) Ding, Y. S.; Greshock, T. J.; Miller, K. A.; Sherman, D. H.; Williams, R. M. *Org. Lett.* **2008**, *10*, 4863-4866. (b) Ding, Y. S.; Williams, R. M.; Sherman, D. H. *J. Biol. Chem.* **2008**, *283*, 16068-16076.
12. (a) Martinez-Luis, S.; Rodriguez, R.; Acevedo, L.; Gonzalez, M. C.; Lira-Rocha, A.; Mata, R. *Tetrahedron* **2006**, *62*, 1817-1822. (b) Figueroa, M.; Gonzalez, M. D. C.; Mata, R. *Nat. Prod. Res.* **2008**, *22*, 709-714.
13. Frebault, F. C.; Simpkins, N. S. *Tetrahedron* **2010**, *66*, 6585-6596.
14. Watts, K. R.; Loveridge, S. T.; Tenney, K.; Media, J.; Valeriote, F. A.; Crews, P. *J. Org. Chem.* **2011**, *76*, 6201-6208.
15. (a) Miller, K. A.; Welch, T. R.; Greshock, T. J.; Ding, Y. S.; Sherman, D. H.; Williams, R. M. *J. Org. Chem.* **2008**, *73*, 3116-3119. (b) Valente, M. W. N.; Williams, R. M. *Heterocycles* **2006**, *70*, 249-259.

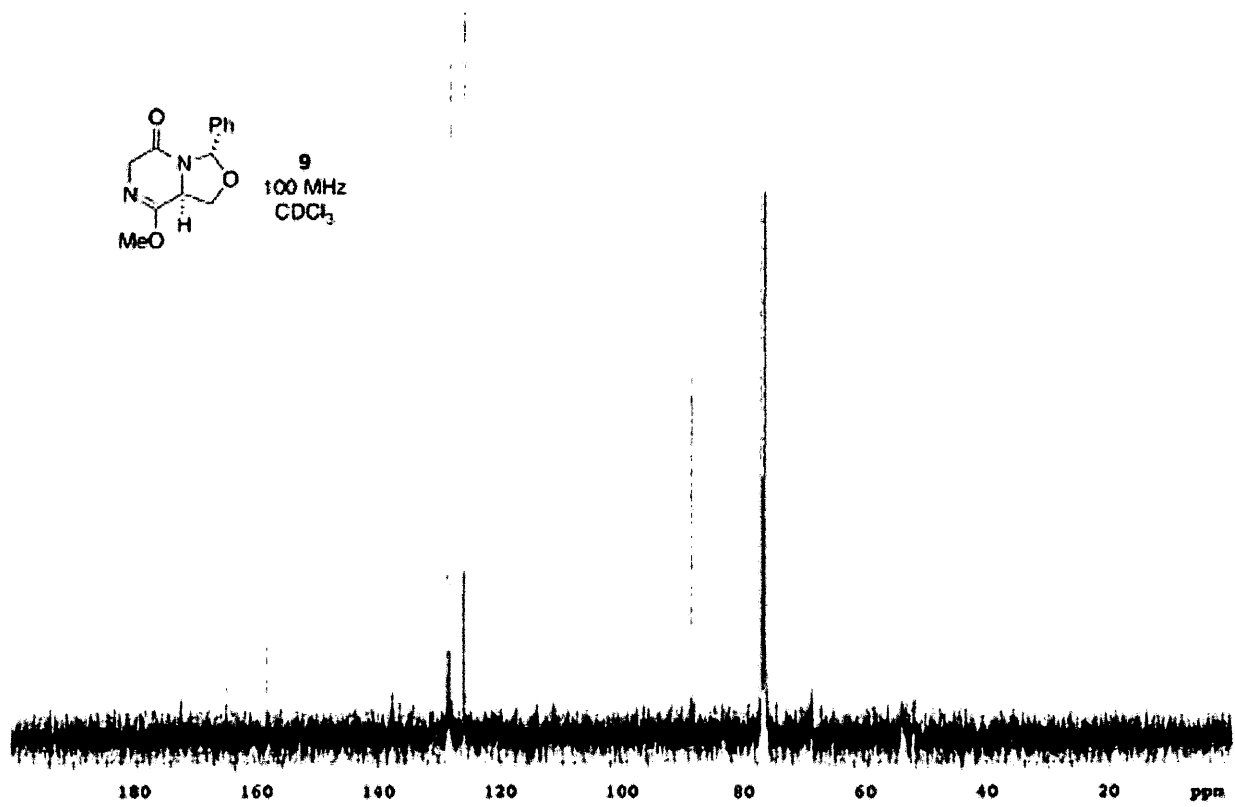
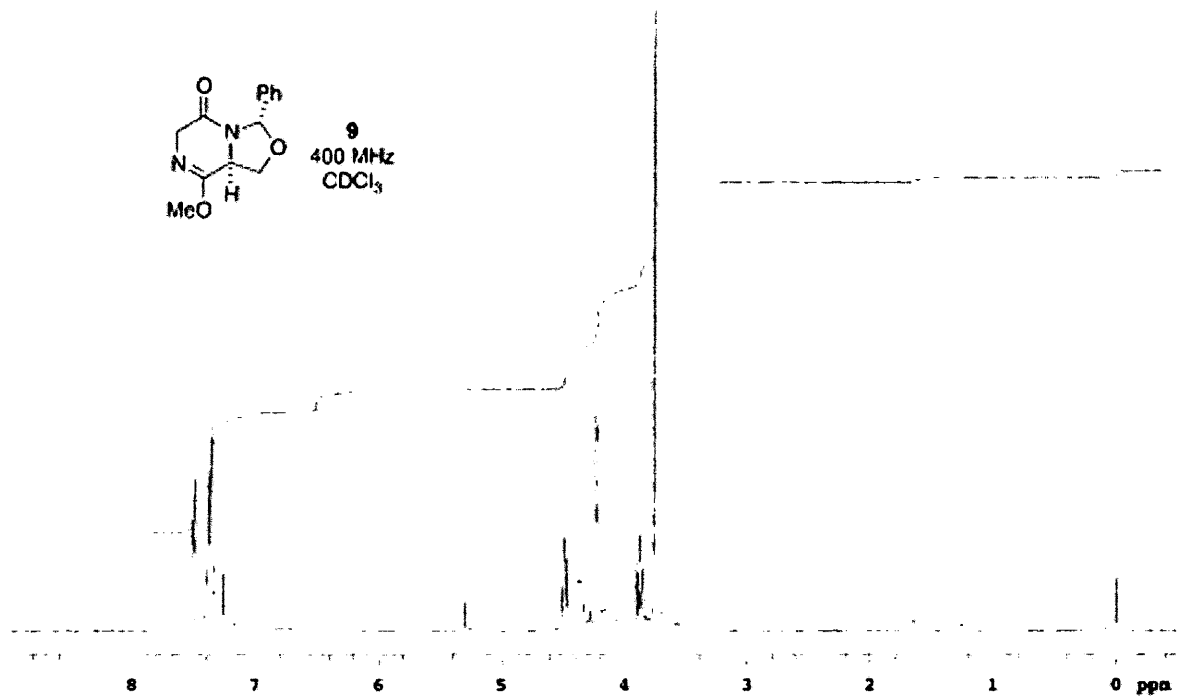
## APPENDIX

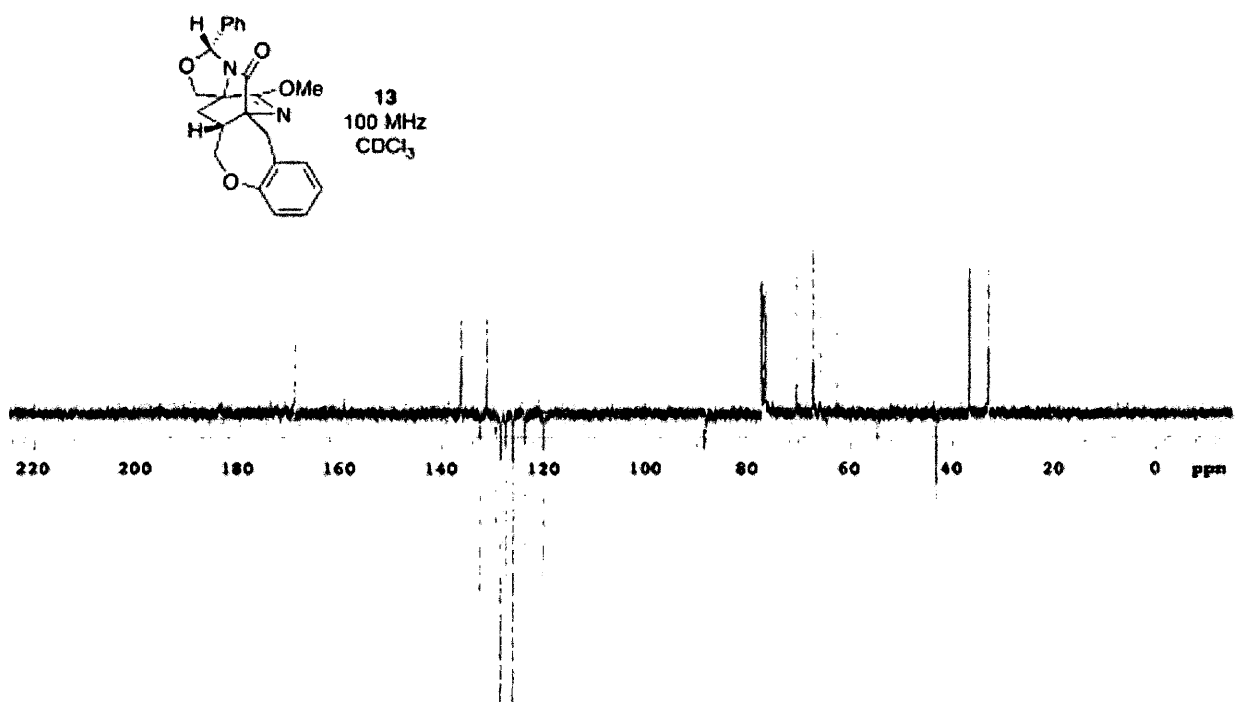
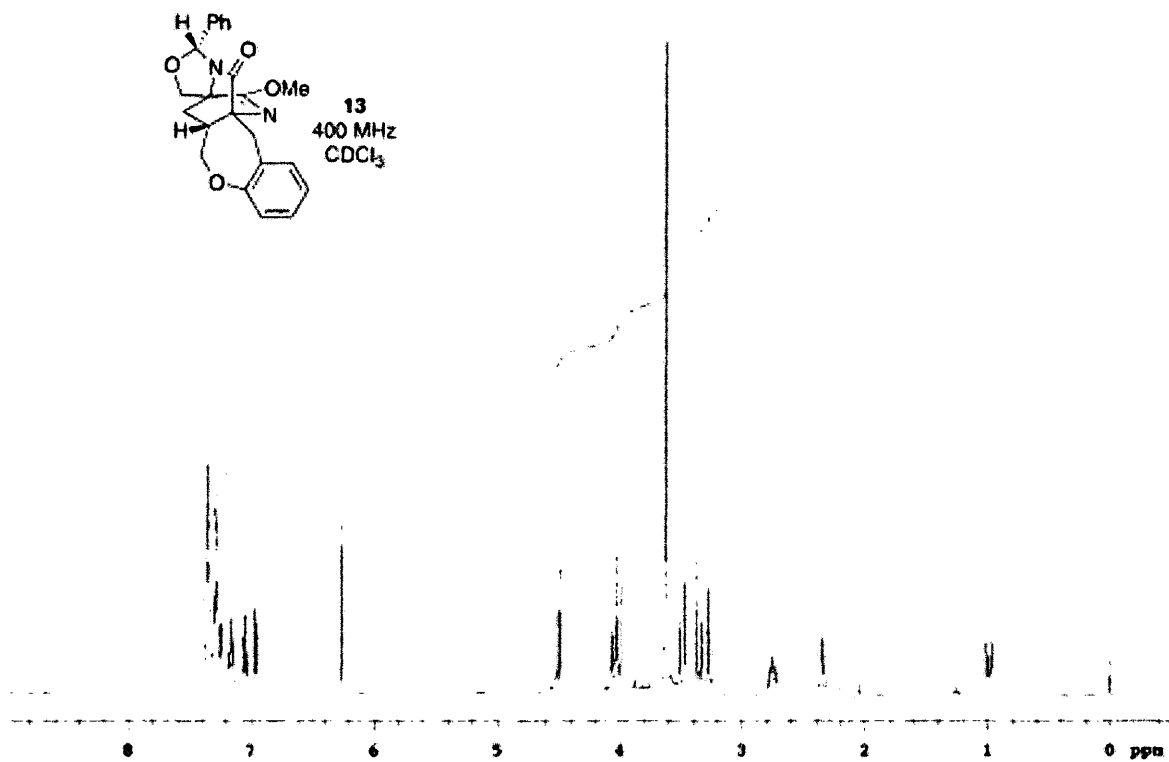
### SUPPORTING INFORMATION FOR:

#### CHAPTER II:

**General Information.** All reactions were carried out under an atmosphere of nitrogen in flame-dried or oven-dried glassware with magnetic stirring unless otherwise indicated. Acetonitrile, THF, toluene, and Et<sub>2</sub>O were degassed with argon and purified by passage through a column of molecular sieves and a bed of activated alumina.<sup>1</sup> Dichloromethane was distilled from CaH<sub>2</sub> prior to use. All reagents were used as received unless otherwise noted. Flash column chromatography<sup>2</sup> was performed using SiliCycle siliaflash P60 silica gel (230–400 mesh). Analytical thin layer chromatography was performed on SiliCycle 60Å glass plates. Visualization was accomplished with UV light, anisaldehyde, ceric ammonium molybdate, potassium permanganate, or ninhydrin, followed by heating. Film (or KBr pellet) infrared spectra were recorded using a Digilab FTS 7000 FTIR spectrophotometer. Optical rotations were determined on either a Perkin-Elmer 341 polarimeter at 25 °C. <sup>1</sup>H NMR spectra were recorded on a Varian Mercury 400 (400 MHz) spectrometer and are reported in ppm using solvent as an internal standard (CDCl<sub>3</sub> at 7.26 ppm) or tetramethylsilane (0.00 ppm). Proton-decoupled <sup>13</sup>C NMR spectra were recorded on a Mercury 400 (100 MHz) spectrometer and are reported in ppm using solvent as an internal standard (CDCl<sub>3</sub> at 77.00 ppm). All compounds were judged to be homogeneous (>95% purity) by <sup>1</sup>H and <sup>13</sup>C NMR spectroscopy. Mass spectra data analysis was obtained through positive electrospray ionization (w/ NaCl) on a Bruker 12 Tesla APEX–Qe FTICR-MS with an Apollo II ion source. HPLC was performed on a Shimadzu Prominence with LC20AT pumps and photodiode array detector.



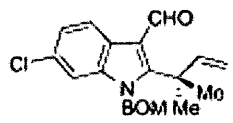




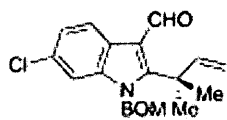
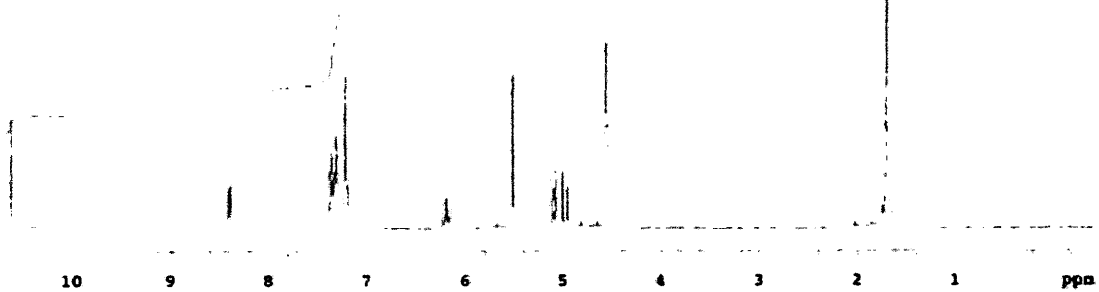
## SUPPORTING INFORMATION FOR:

### CHAPTER III:

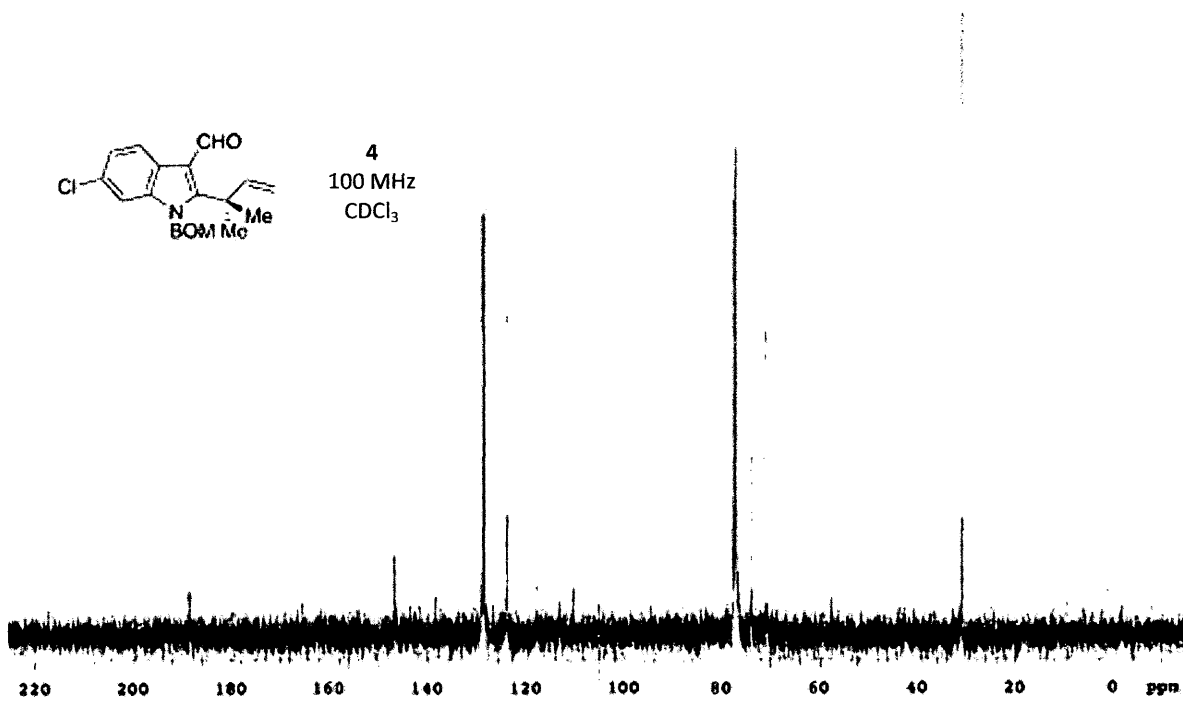
**General Information.** All reactions were carried out under an atmosphere of nitrogen in flame-dried or oven-dried glassware with magnetic stirring unless otherwise indicated. Acetonitrile, THF, toluene, and Et<sub>2</sub>O were degassed with argon and purified by passage through a column of molecular sieves and a bed of activated alumina.<sup>1</sup> Dichloromethane was distilled from CaH<sub>2</sub> prior to use. All reagents were used as received unless otherwise noted. Flash column chromatography<sup>2</sup> was performed using SiliCycle siliaflash P60 silica gel (230–400 mesh). Analytical thin layer chromatography was performed on SiliCycle 60Å glass plates. Visualization was accomplished with UV light, anisaldehyde, ceric ammonium molybdate, potassium permanganate, or ninhydrin, followed by heating. Film (or KBr pellet) infrared spectra were recorded using a Digilab FTS 7000 FTIR spectrophotometer. Optical rotations were determined on either a Perkin-Elmer 341 polarimeter at 25 °C. <sup>1</sup>H NMR spectra were recorded on a Varian Mercury 400 (400 MHz) spectrometer and are reported in ppm using solvent as an internal standard (CDCl<sub>3</sub> at 7.26 ppm) or tetramethylsilane (0.00 ppm). Proton-decoupled <sup>13</sup>C NMR spectra were recorded on a Mercury 400 (100 MHz) spectrometer and are reported in ppm using solvent as an internal standard (CDCl<sub>3</sub> at 77.00 ppm). All compounds were judged to be homogeneous (>95% purity) by <sup>1</sup>H and <sup>13</sup>C NMR spectroscopy. Mass spectra data analysis was obtained through positive electrospray ionization (w/ NaCl) on a Bruker 12 Tesla APEX–Qe FTICR-MS with an Apollo II ion source. HPLC was performed on a Shimadzu Prominence with LC20AT pumps and photodiode array detector.



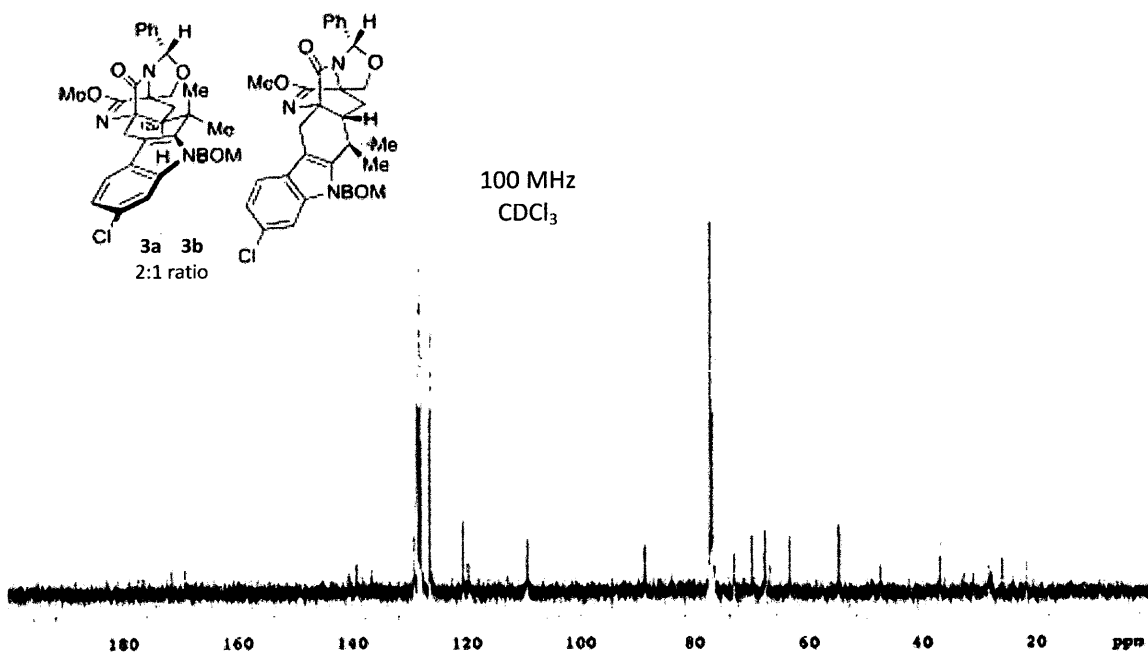
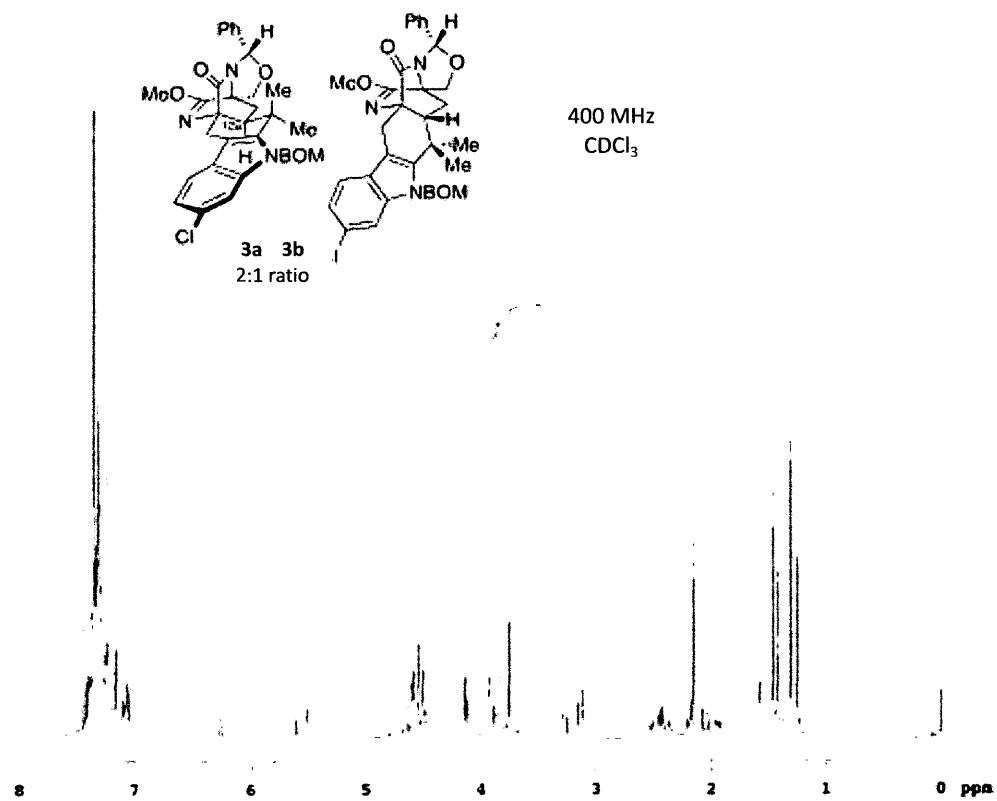
4  
400 MHz  
CDCl<sub>3</sub>

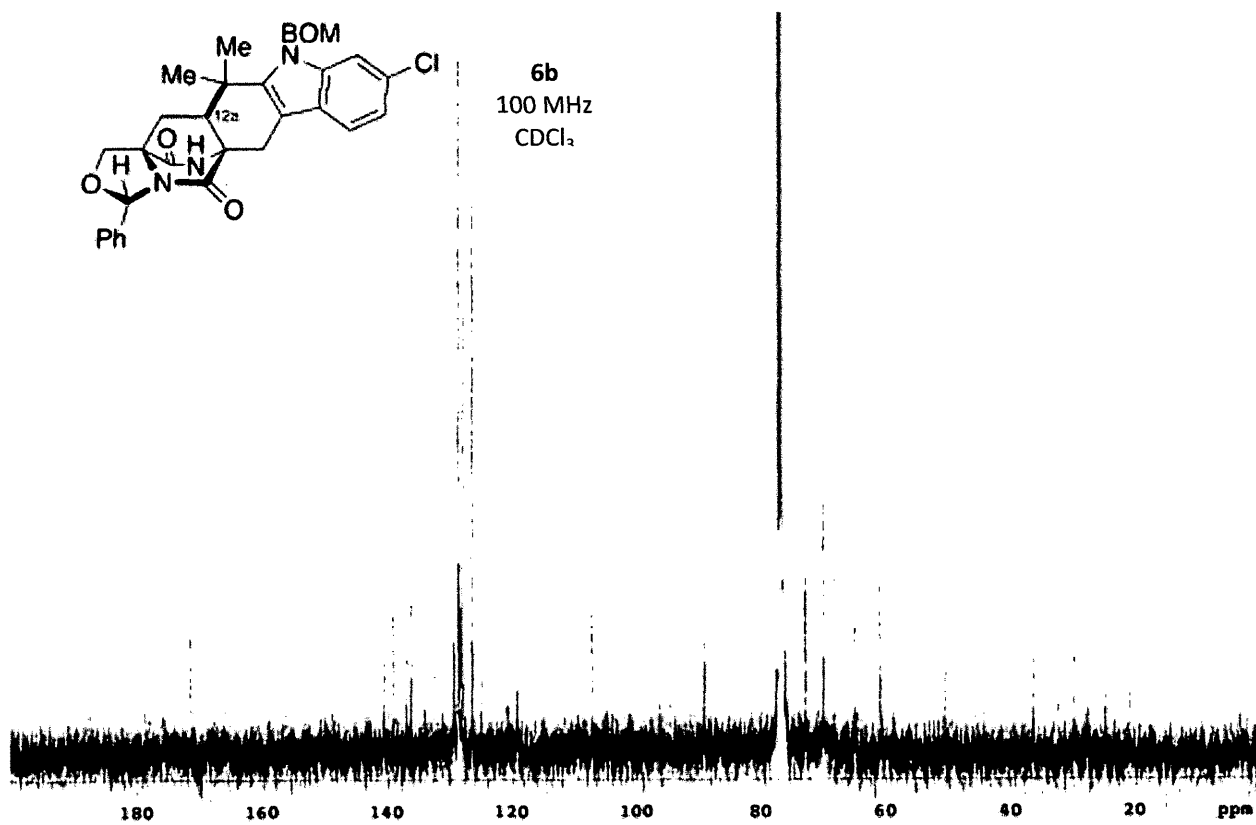
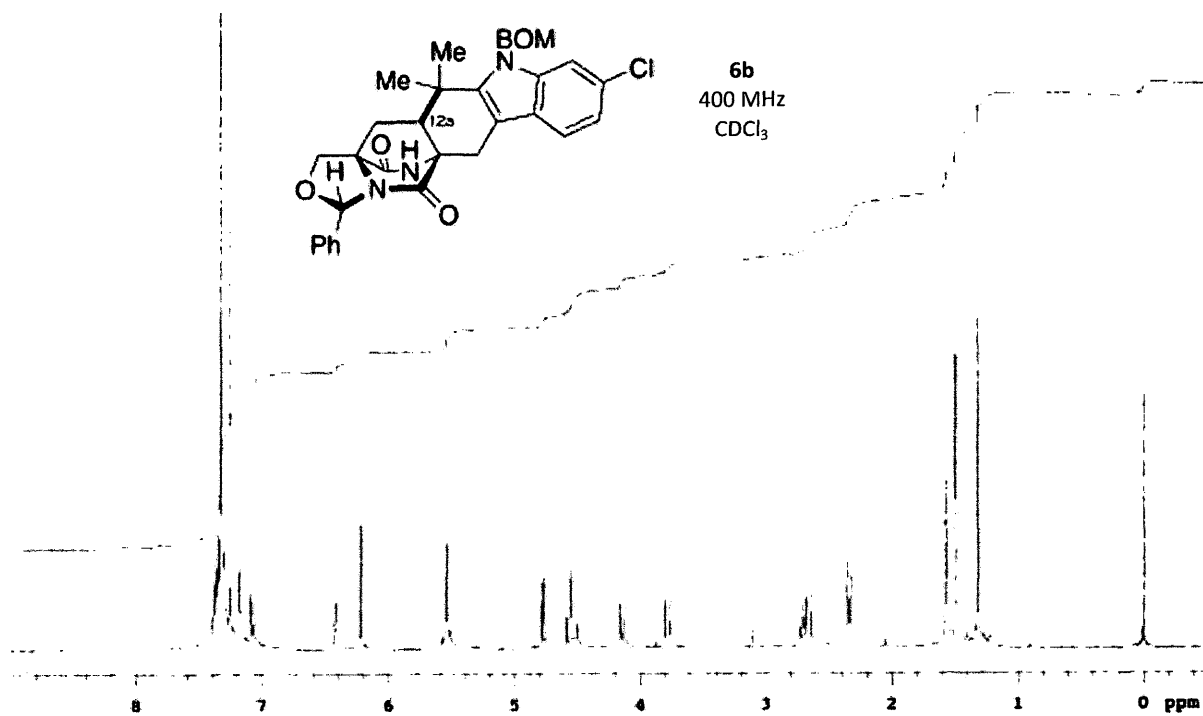


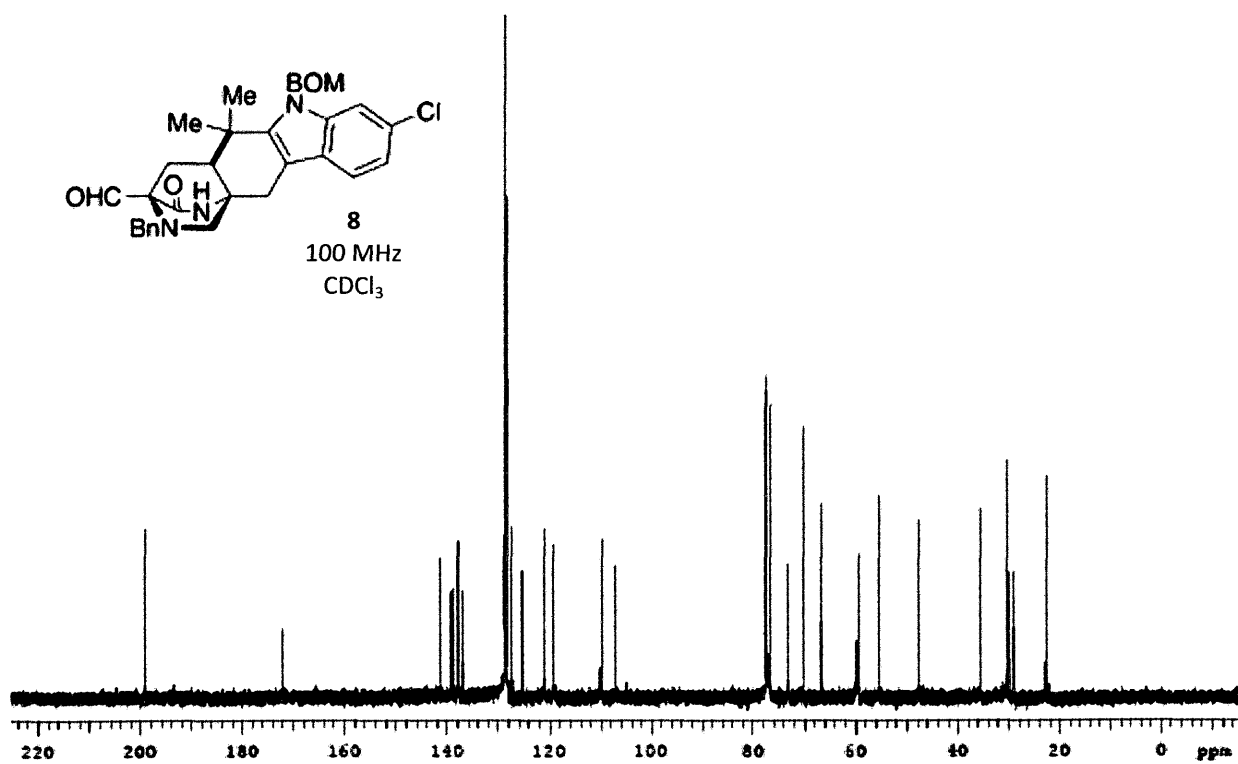
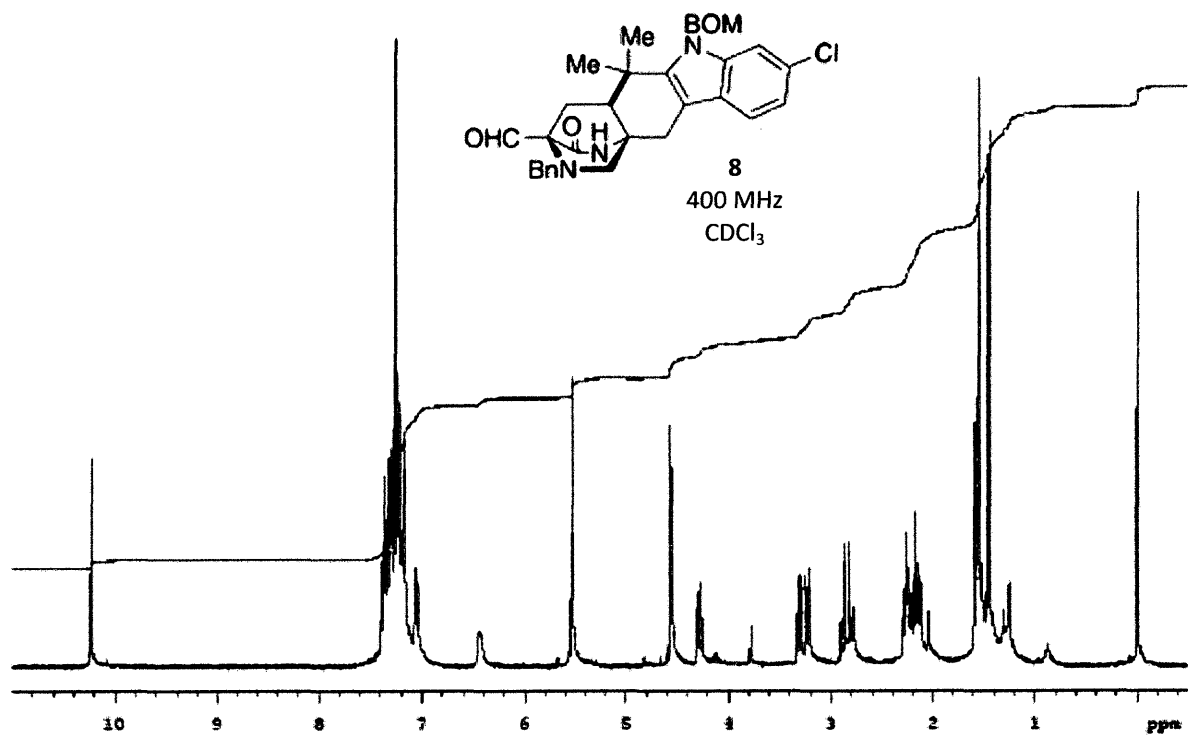
4  
100 MHz  
CDCl<sub>3</sub>

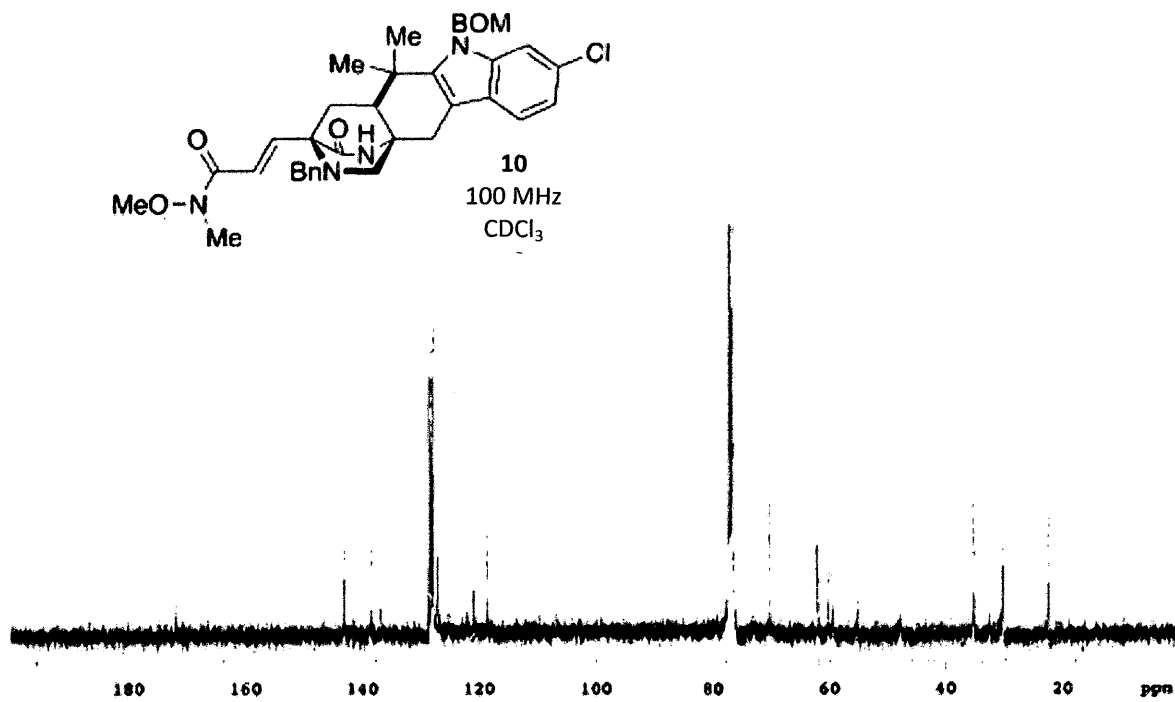
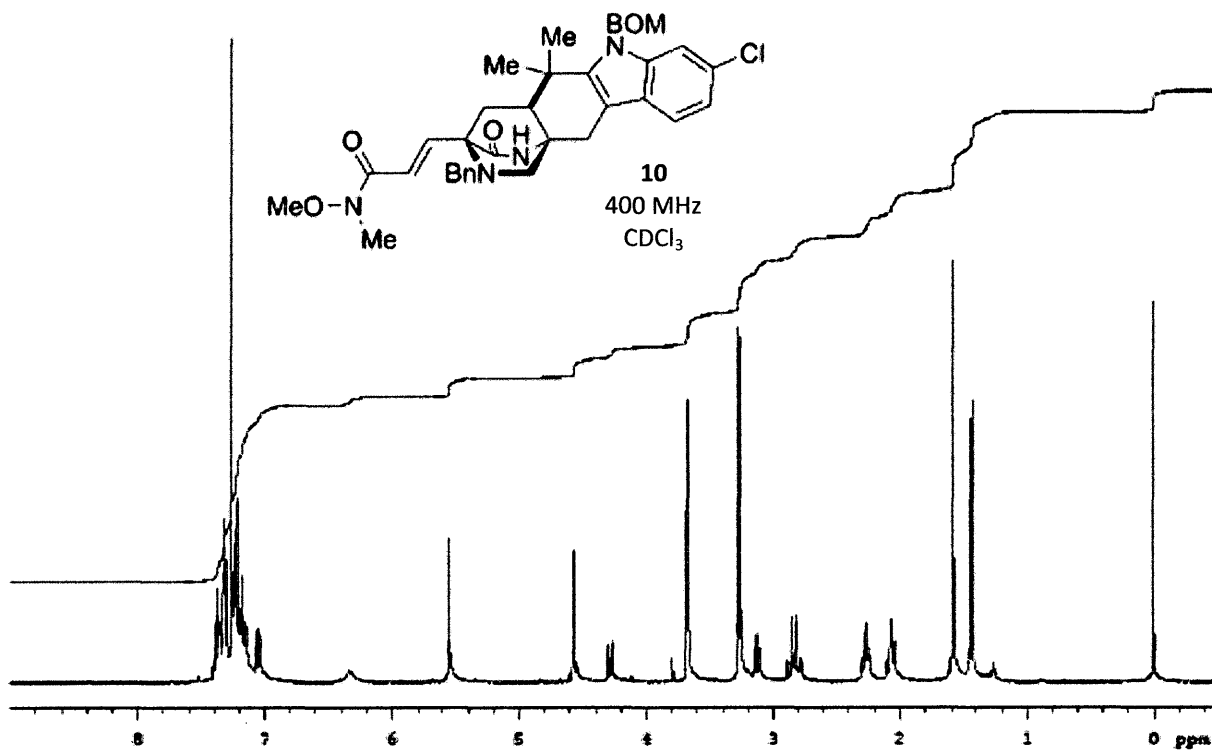


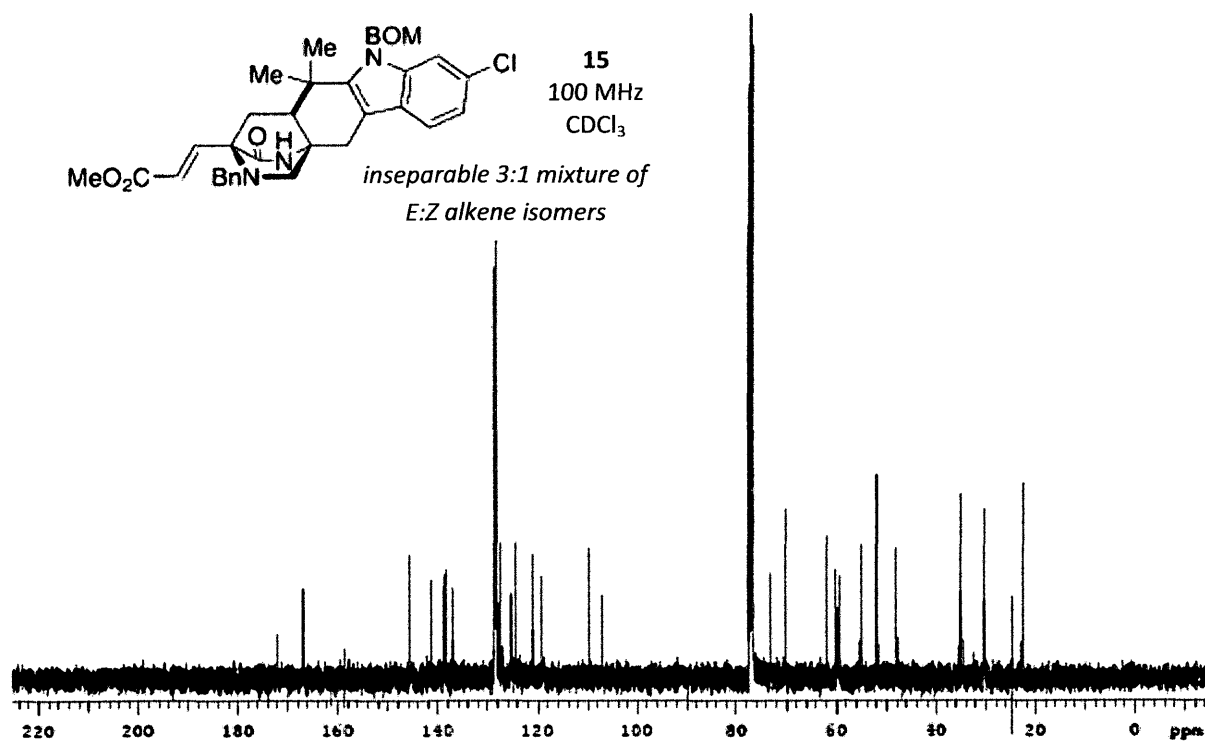
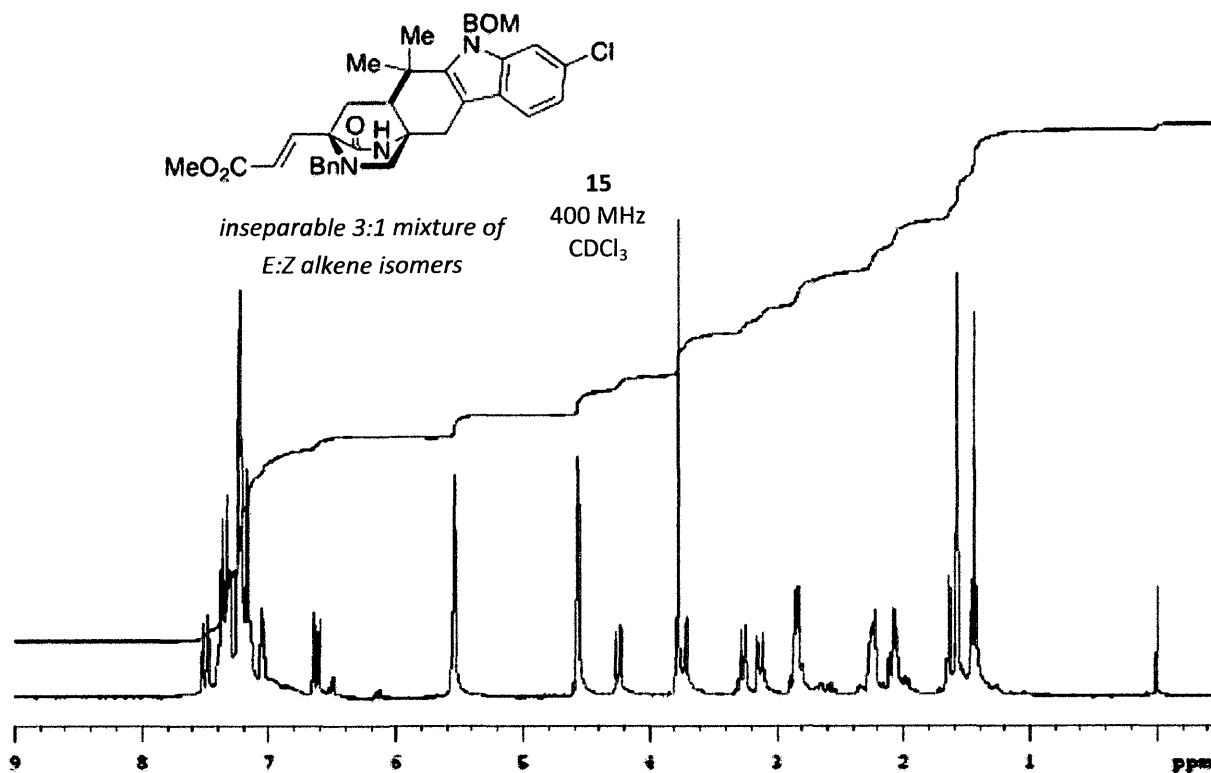


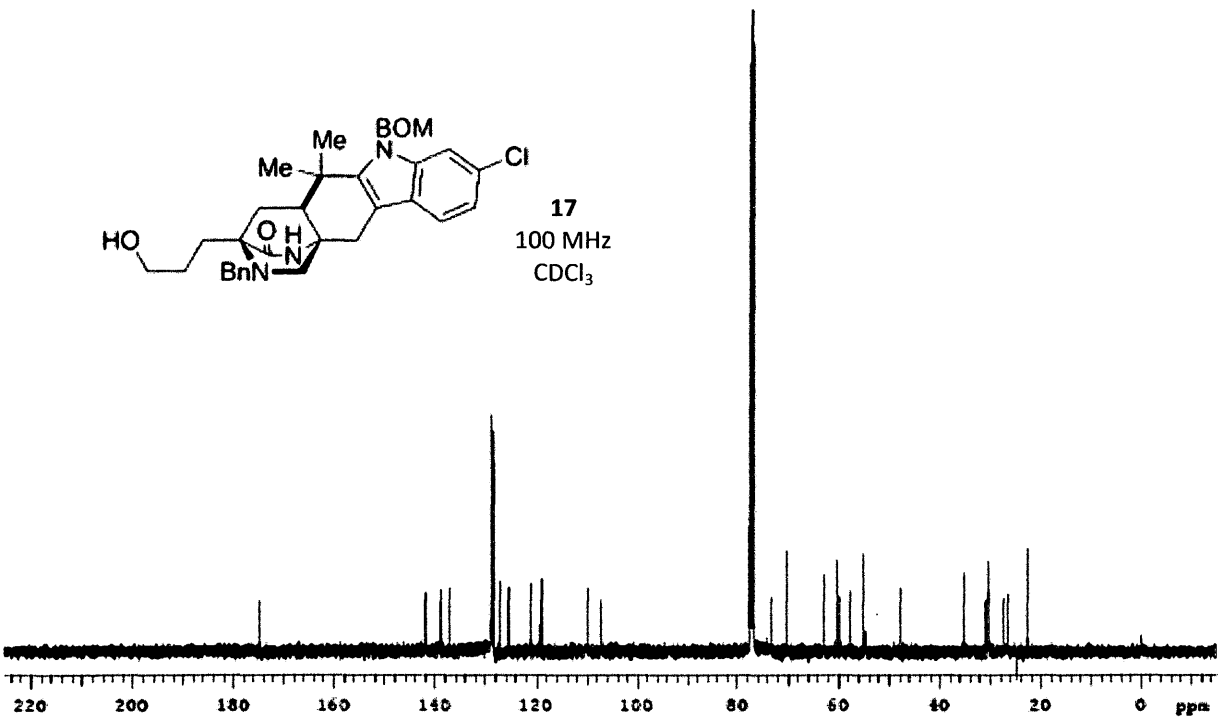
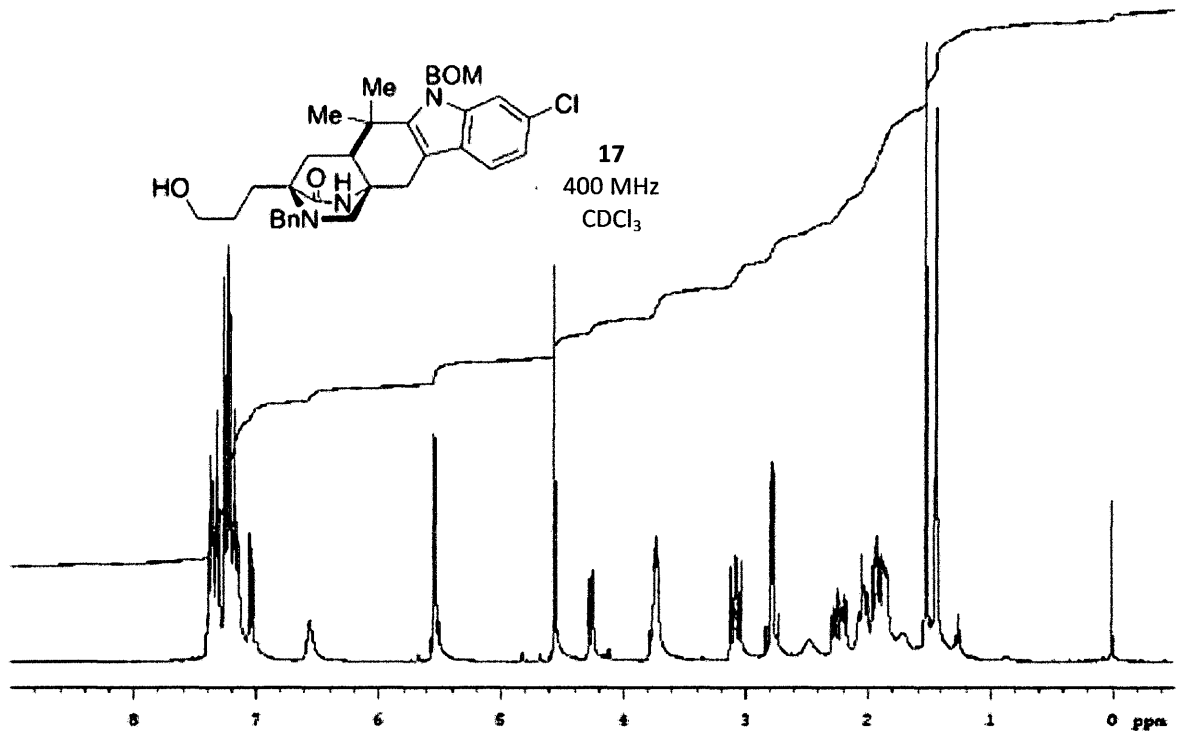


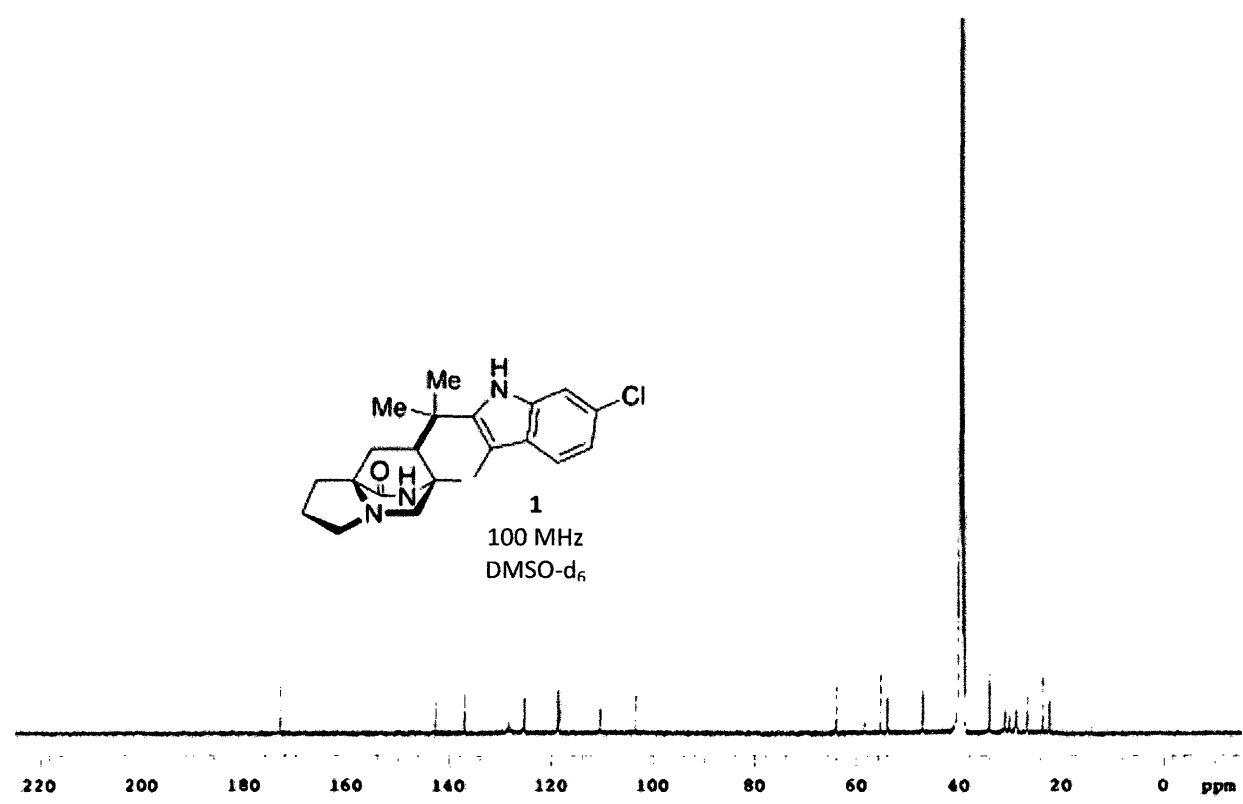
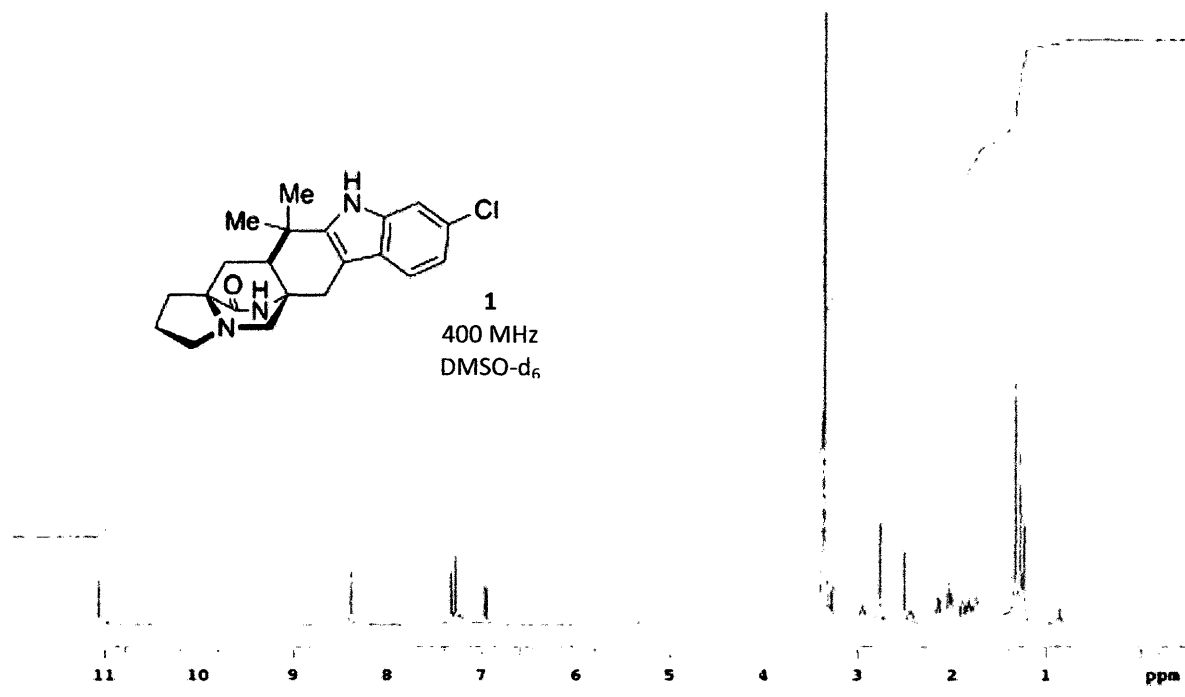


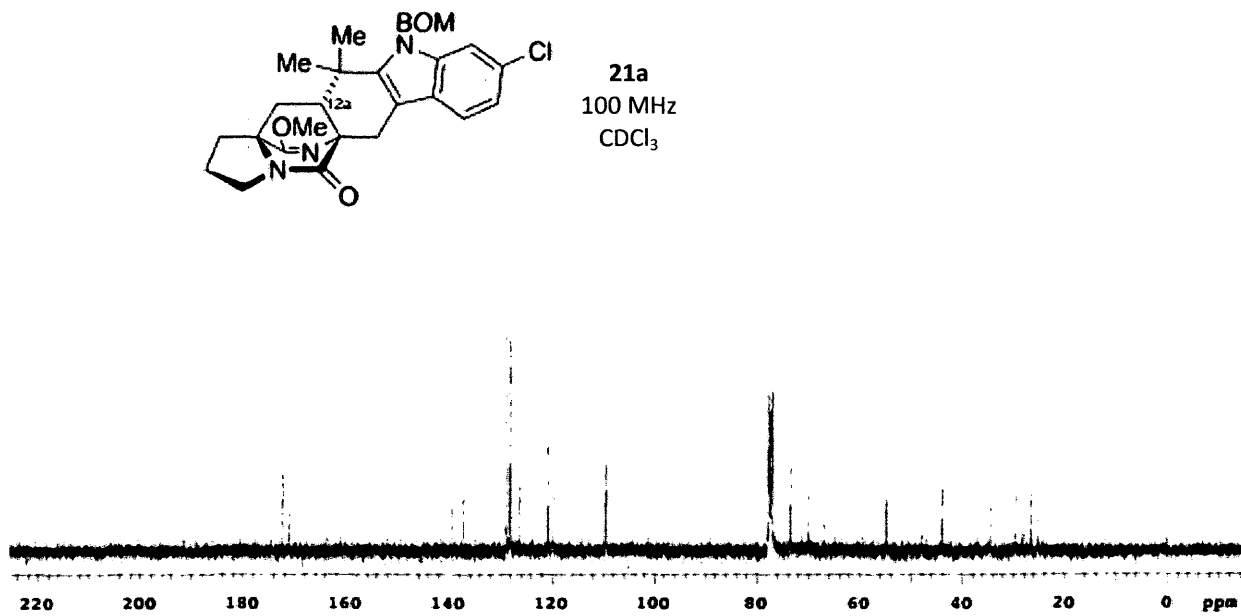
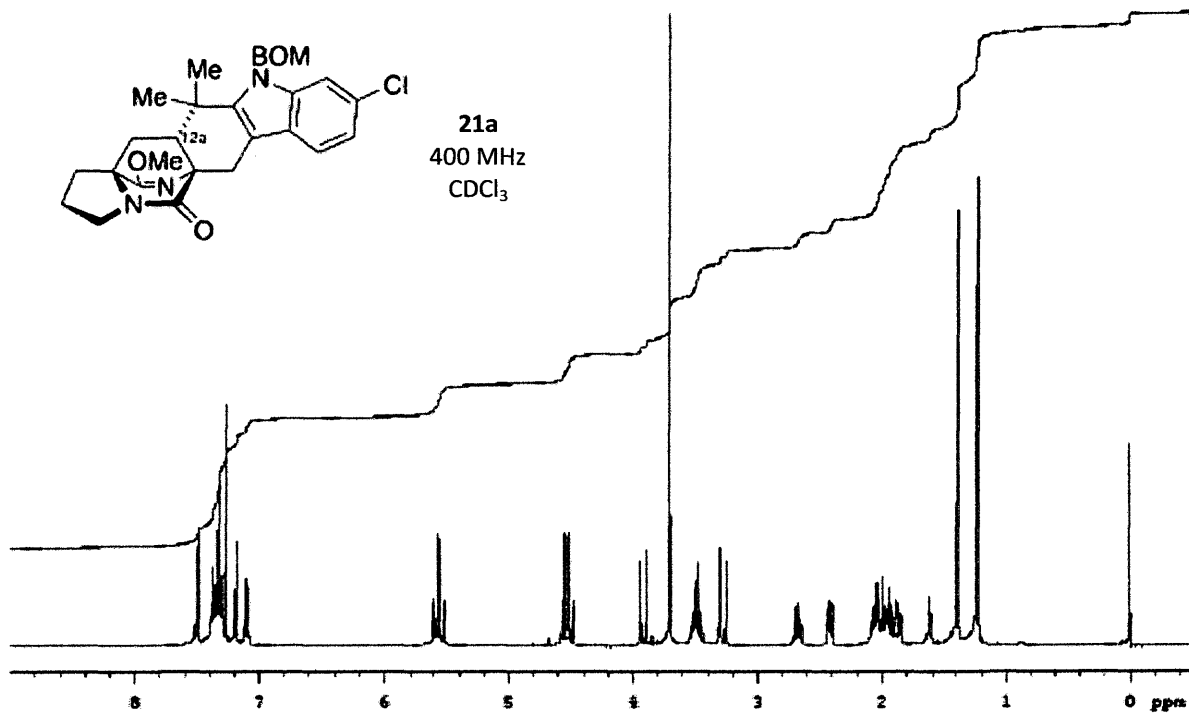




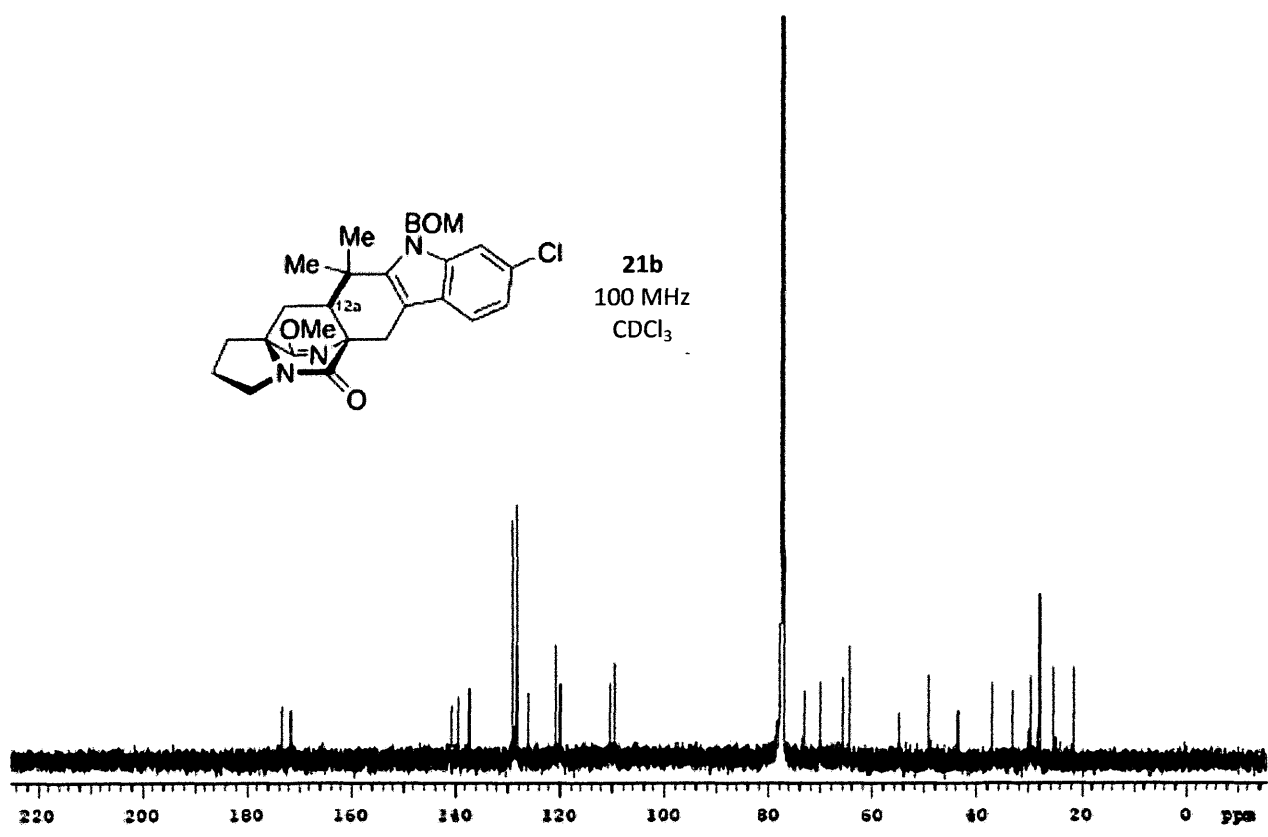
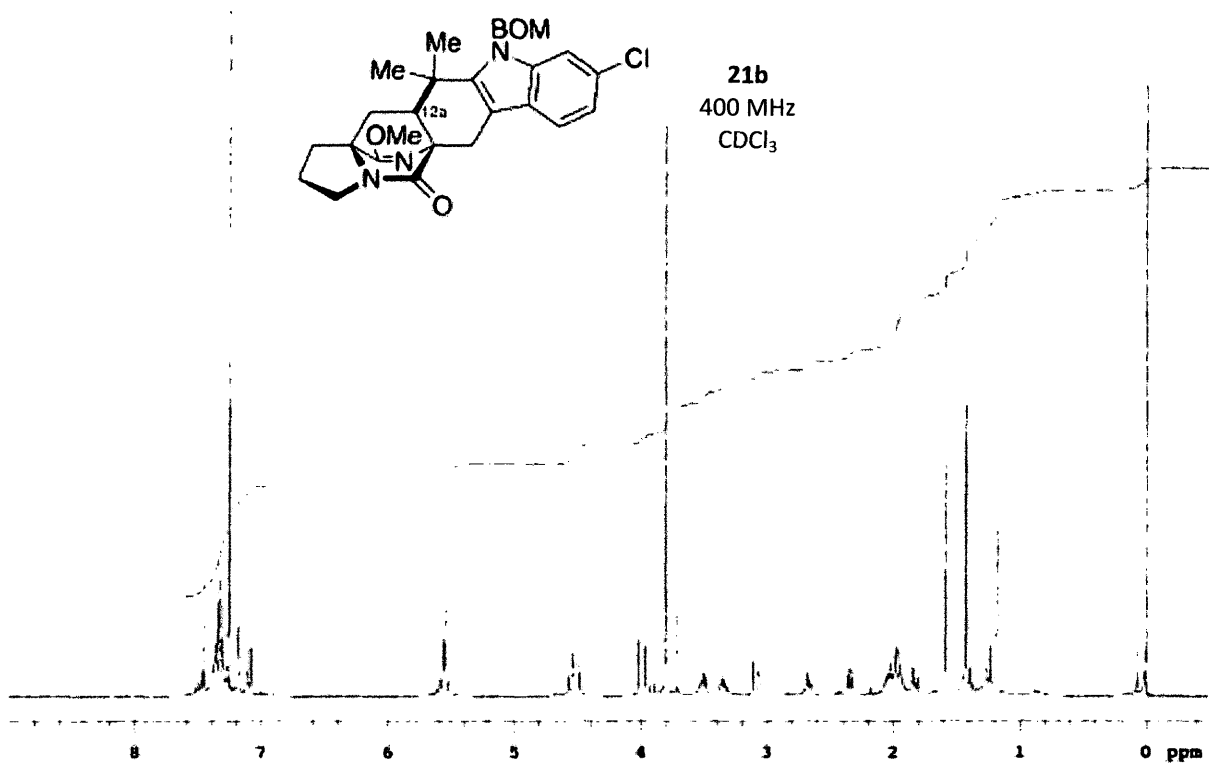


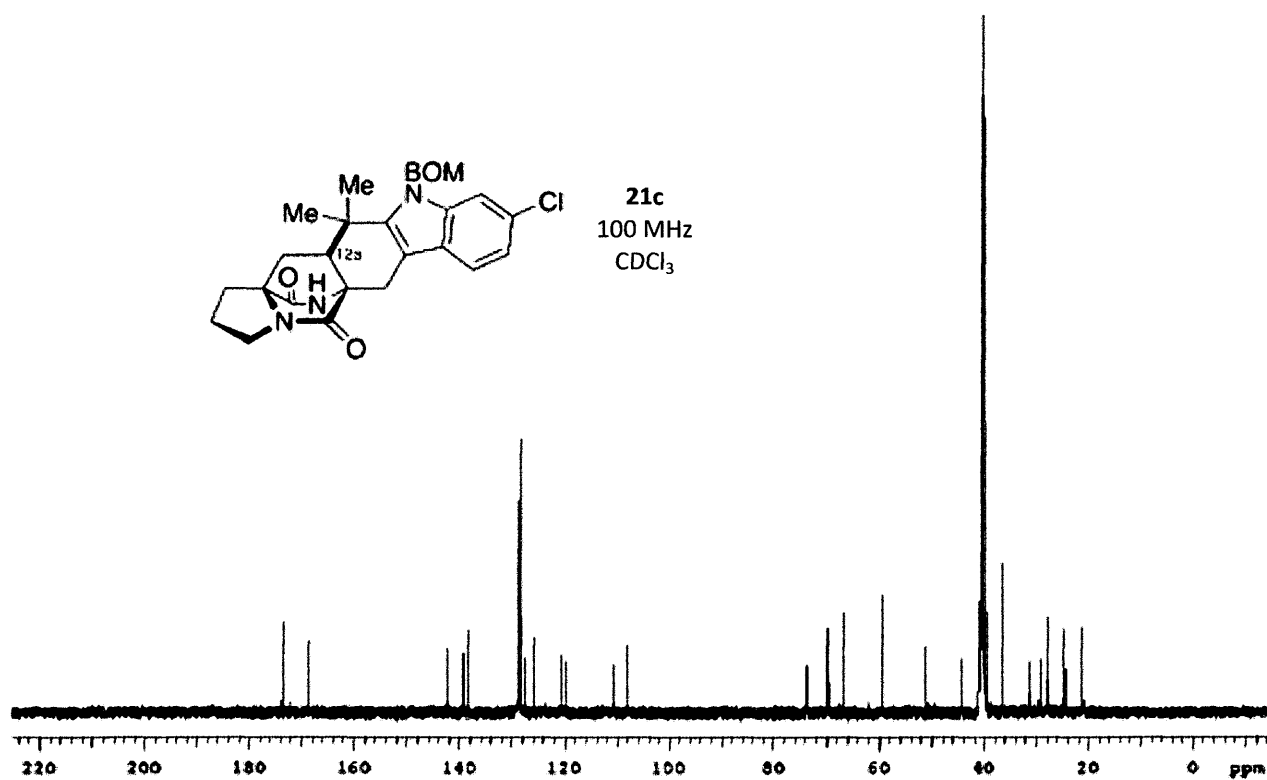
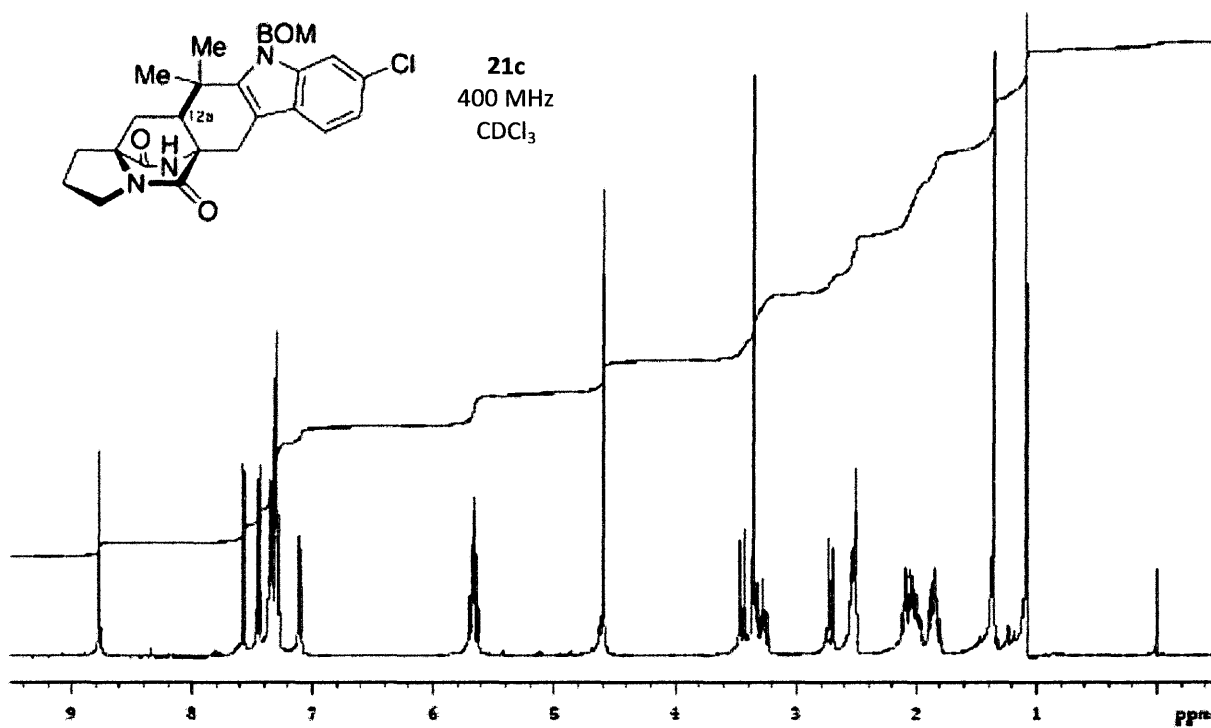












#### REFERENCES

1. Pangborn, A. B.; Giardello, M. A.; Grubbs, R. H.; Rosen, R. K.; Timmers, F. J. *Organometal.* **1996**, *15*, 1518-1520.
2. Still, W. C.; Kahn, M.; Mitra, A. *J. Org. Chem.* **1978**, *43*, 2923-2925

## VITA

### Stephen W. P. Laws

Stephen William Parkinson Laws was born on November 29<sup>th</sup>, 1989 in Oakville, Ontario, Canada to W. John and Lori Laws. He graduated from the Maggie L. Walker Governor's School in Richmond, Virginia in 2007 and received a B.S. from the College of William and Mary of Williamsburg, Virginia in 2011. In 2011 he began working toward a Master of Science through the chemistry department of the College of William and Mary, conducting research in the lab of Dr. Jonathan Scheerer. Upon the completion of this degree, he will continue his graduate studies in organic chemistry at the University of California, Davis in pursuit of a Ph.D.